NASA CONTRACTOR REPORT

NASA CR-1241

THE BOSSLER COUPLING

by R. J. Mayerjak and R. B. Bossler, Jr.

Prepared by
KAMAN CORPORATION
Bloomfield, Conn.
for

NATIONAL AERONAUTICS AND SPACE ADMINISTRATION • WASHINGTON, D. C. • JANUARY 1969

THE BOSSLER COUPLING

By R. J. Mayerjak and R. B. Bossler, Jr.

Issued by Originator as Kaman Report No. R-741

Prepared under Contract No. NASw-1554 by
KAMAN CORPORATION
Bloomfield, Conn.

for

NATIONAL AERONAUTICS AND SPACE ADMINISTRATION

For sale by the Clearinghouse for Federal Scientific and Technical Information
Springfield, Virginia 22151 – CFSTI price $3.00

ABSTRACT

The Bossler coupling is a new, flexible, drive-shaft coupling which is suitable for any level of power transmission. This report presents the results of an investigation of the mechanical characteristics of Bossler couplings. The investigation included analyses and tests. Simplified coupling analysis methods, parameter studies, and design guidelines were developed. The test areas included torsion, stiffness, strain, fatigue, constancy of velocity, critical speed, and balancing. The tests substantiated the analyses for predicting internal forces and moments, steady and alternating stress, bending and change-of-length stiffness, critical speeds, and the effects of unbalance. Experience is limited for fatigue (two tests), and for ultimate torque (six tests).

Important characteristics of the Bossler coupling were established. Velocity can be constant. The coupling has unusual capability for accommodating combined axial motion, misalignment, and torque. The coupling can survive shock-torque greatly in excess of ultimate continuous torque and transient misalignments over three times the design continuous operating angle. Configuration modification may improve performance further. Fail-safe design is accomplished easily. The coupling has unusual characteristics that are potentially useful. The coupling appears well suited for applications requiring very long life with high reliability, very low weight, no maintenance or lubrication, and survival in hostile environments.

TABLE OF CONTENTS

LIST OF SYMBOLS

BOSSLER COUPLING

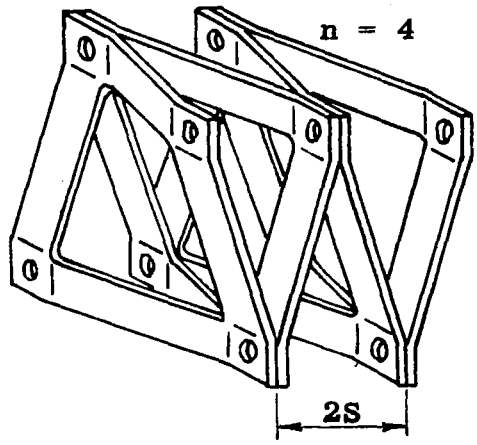

PLATE

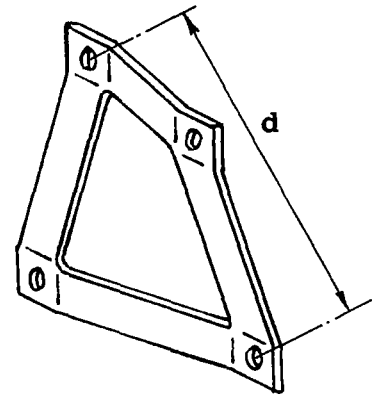

ELEMENT

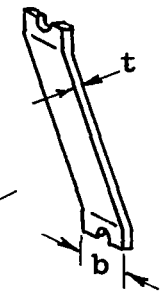

b	Width of an element
d	Diameter at the bolt circle
E	Modulus of elasticity
F	Ratio of variances
f_1	First critical speed, rpm
g	Acceleration of gravity
I	Flatwise moment of inertia of an element = $bt^3/12$
k	Spring constant for single degree of freedom idealization
L	Effective length of an element. Concept is required because joint details tend to stiffen the ends of the elements. L = .667 d is recommended
M_s	Mass of center shaft + mass of one coupling with fasteners
n	Number of plates in each coupling
p	Angular velocity of rotation, radians/second
P_a	Axial load applied to the compression helix

LIST OF SYMBOLS (Continued)

P_u	Axial load capacity of the compression helix, useful ultimate, see also definition of α
S	Offset distance by which a plate is out of plane
t	Thickness of an element
T	Torque applied to coupling
T_u	Torque applied to coupling, useful ultimate, usually taken as lowest critical buckling torque
w	Weight per unit volume
W	Total weight of plates in a coupling
$(EI)_c$	Flexural stiffness, the moment which causes one radian of flexural angle change per unit length of coupling
$(JG)_c$	Torsional stiffness, the torque which causes one radian of torsional rotation per unit length of coupling
$(Ka)_c$	Axial stiffness, the force which causes a coupling to change its length one unit
α	Fixity parameter which relates the axial load capacity of the compression path to the Euler column load calculated using the center-to-center distance between fasteners as the column length. $P_u = \alpha\pi^2 EI/(.707\ d)^2$ From experiments, $\alpha = 5.0\ n^{-.9}$ for $n \leq 5$. Thus, $P_u = 8.22\ Ebt^3/d^2 n.9$
β	Equivalent angle change at each coupling when assembly is subjected to parallel offset misalignment, degrees, see sketch Page 21
θ	Total uniform angle change, degrees, see sketch Page 19
σ	Stress
σ_c	Characteristic limiting stress for the material σ_c = yield stress for static performance σ_c = endurance limit stress for fatigue performance

LIST OF FIGURES

LIST OF FIGURES (Continued)

LIST OF TABLES

INTRODUCTION

Background.- Drive-shaft couplings accommodate the inevitable misalignments between rotating shafts in a drive train. The misalignments are caused by imperfect parts, temperature changes, and deflections of the supporting structures. The couplings accommodate these misalignments by either moving contact or flexing.

Coupling parts with moving contact require lubrication and maintenance. The rubbing parts absorb power. The lubricant and the seals limit coupling environment and coupling life. The parts wear out. The coupling may develop a large resistance to movement as the parts deteriorate. The coupling may not have constant velocity. The location of parts will be inexact because of the internal clearances required to allow motion. However, in spite of these drawbacks, many very successful applications of couplings with moving contact are known. These couplings are in wide use. Coupling behavior usually is predictable from past experience.

Couplings which accommodate misalignments by flexing avoid all the drawbacks that come with moving contact. Flexible coupling behavior, however, is not without design problems. Any flexible coupling can be proportioned with strong, thick, stiff members that easily transmit a design torque and that easily provide the stiffness to operate at a design speed. However, misalignment requires flexing of these members. The flexing produces alternating stresses that can limit coupling life. The greater the strength and stiffness of a member, the higher the alternating stress from a given misalignment. Therefore, strength and stiffness provisions to transmit torque at speed will be detrimental to misalignment capability. The problem of design is to proportion the flexible coupling to accomplish torque transmission and misalignment for the lowest system cost.

Bossler Coupling*.- This is a new flexible coupling. It transmits torque through axially-loaded straight elements. It is structurally very efficient. Deformations resulting from shaft misalignments and changes in length are distributed among the many slender, straight, elements that comprise the coupling. The coupling geometry is illustrated in the List of Symbols and throughout the text. The Bossler coupling can have various configurations, depending on use and method of manufacture. The configuration investigated in this program is made from metal plates of square planform with a square concentric hole. The plates are attached at the corners to adjacent similar plates. The individual slender elements are rectangular in cross-section.

* U. S. Patent No. 3,177,684

Purpose.- The purpose of this program was to provide the National Aeronautics and Space Administration with an initial investigation of the mechanical characteristics of the Bossler coupling.

Program.- This investigation started with the identification of possible failure modes and of other design considerations. For each topic identified, importance was evaluated, appropriate analysis methods were developed where conventional methods were not available, and tests were performed as required to substantiate the analyses and refine the analyses by inclusion of empirical adjustments.

The modes of failure considered were failure from torque, fatigue, and critical speed. The other design considerations included constancy of velocity, coupling stiffness as it affects critical speed and also supporting structure, and response to unbalance.

Each chapter in this report is a semi-independent topic, which contains its own introduction and conclusion. Appropriate cross-references and comparisons are made. Simplified analysis, parameter studies and design guidelines are presented first to establish the framework for understanding the test results as they appear and for later comparisons of test results with theory. In addition, a discussion is presented for a configuration modification which follows the design guidelines in the direction of improved coupling capability. A concept was explored for a fail-safe feature with a warning signal that a failure has occurred. Also discussed are some unusual characteristics and possible uses of the coupling.

SIMPLIFIED ANALYSIS

Introduction.- This Section presents simple formulas for the analysis of Bossler couplings. The formulas relate the structural behavior (e.g. internal loads, stiffness, stresses) to the coupling dimensions, material properties, and loadings.

Torque.-

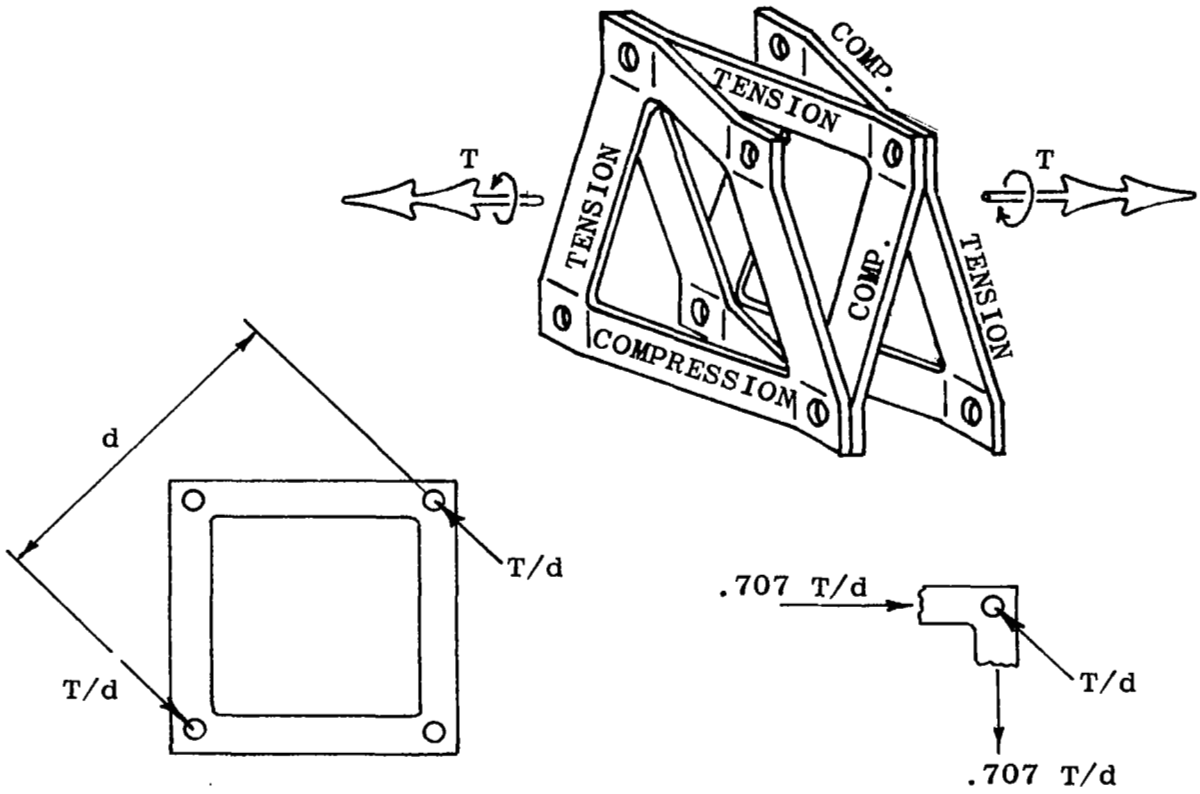

The torque T causes in each element an axial force P_a. For typical proportions the effect of plate offset S can be ignored, thus:

$$P_a = .707\ T/d \qquad (1)$$

The sketch shows that the compression elements and the tension elements form helical paths which transmit torque across the coupling. The stability of the compression load path limits the torque capacity. Tests to failure have shown that the useful ultimate torque for a Bossler coupling can be predicted with the following equation.

$$T_u = 11.62 \frac{Ebt^3}{dn \cdot 9}, \text{ for } n \leq 5 \qquad (2)$$

Equation (2) assumes that the instability occurs in the elastic range. This assumption will be correct for the great majority of applications since the axial stress is typically less than 40 ksi at ultimate torque. This fact can be shown as follows:

$$\sigma = P_u/bt = 8.22 \frac{E}{n \cdot 9} \left(\frac{t}{d}\right)^2$$

For a typical power transmission application, E = 27000 ksi (nickel maraging steel), n = 3, $t/d \cong 1/50$. Substituting these values into the equation shows σ to be approximately 33 ksi at ultimate torque. The corresponding steady stress at normal operating torque is then typically only 11 ksi; the corresponding alternating stress from typical torque variation is only 2 ksi. These values are quite low. It can be concluded that the stresses from torque transmission have only a secondary effect upon the endurance of the coupling. The primary source of fatigue damage is the alternating stress resulting from shaft misalignments.

The theoretical torsional stiffness of a Bossler coupling can be derived by considering a single element, as follows.

External work = internal work

$$\frac{T\phi}{2} = \frac{1}{2} \int \frac{P_a^2}{AE} \, ds = \frac{1}{2btE} \left(.707 \frac{T}{d}\right)^2 \frac{4d}{1.414}$$

$$\frac{T}{\phi} = \frac{btdE}{1.414}, \text{ for a single plate}$$

Since there are 1/S plates per unit length of coupling, the torsional stiffness per unit length becomes:

$$(JG)_c = .707 \text{ btdES, theoretical}$$

In tests, the observed torsional stiffness approached the theoretical value initially but gradually decreased with increasing torque. At normal operating torque, the tangent stiffness was approximately 40% less than the theoretical stiffness; Equation (3) includes a 40% reduction.

$$(JG)_c = .425 \text{ btdES} \qquad (3)$$

Misalignment.- The flexural stiffness can be derived by considering a single, flat Bossler plate. The following sketch shows one plate subjected to a moment M' which causes an angle change "a" radians about a diagonal.

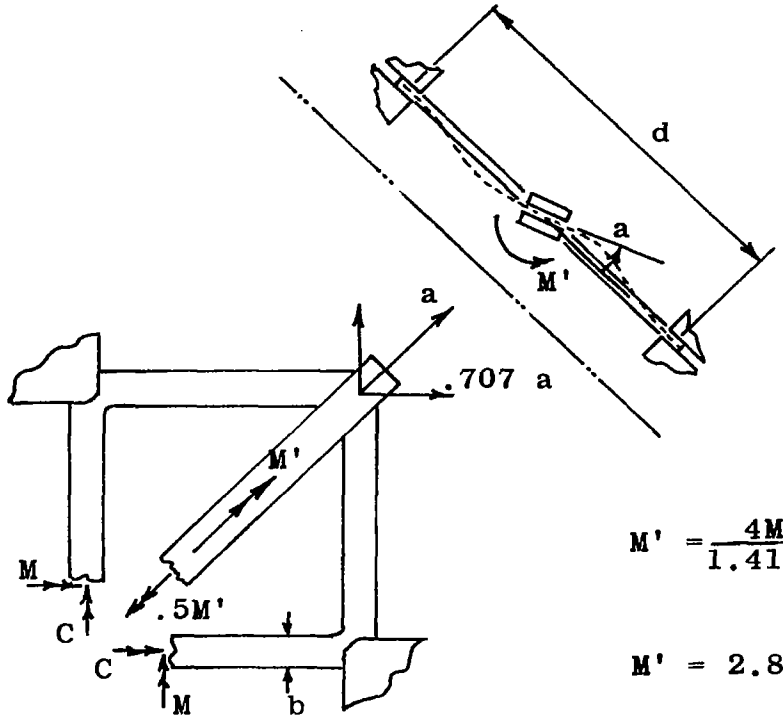

$$M' = \frac{4M}{1.414} + \frac{4C}{1.414}$$

$$M' = 2.828\ (M + C) \qquad (4)$$

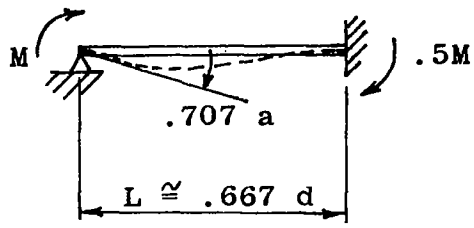

$$M = \frac{4\ EI}{L}\ \frac{a}{1.414} \qquad (5)$$

$$M = .2357\ \frac{bt^3Ea}{L} \qquad (6)$$

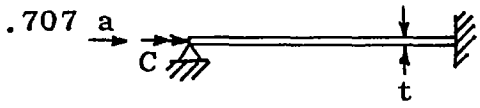

$$C = \frac{\beta'\ bt^3G}{L}\ \frac{a}{1.414}$$

β' is a function of b/t (Reference 1).

b/t	=	1	1.5	2	2.5	3	4	6	10	∞
α	=	.208	.231	.246	.256	.267	.282	.299	.312	.333
β'	=	.141	.196	.229	.249	.263	.281	.299	.312	.333

For typical Bossler couplings, b/t = 6; use $\beta' = .30$. For steel, G/E = .367.

Therefore, $$C = .0779 \frac{bt^3Ea}{L} \quad (7)$$

Divide Eq. (7) by Eq. (6) $$C = .33\ M \quad (8)$$

Subst. Eq. (8) into Eq. (4) $$M' = 3.76\ M \quad (9)$$

$$\frac{M'}{a} = \frac{3.76\ M}{a}, \text{ for one plate}$$

There are 1/S plates per unit length of coupling.

Therefore, $$(EI)_c = 3.76\ MS/a$$

or, $$(EI)_c = 10.64\ EIS/L \quad (10)$$

or, $$(EI)_c = .886\ Ebt^3S/L \quad (11)$$

By symmetry it is apparent that Equation (11) also applies to a moment M' rotated 90 degrees to that used in the derivation. Thus, the coupling has constant flexural stiffness for any direction of bending.

Equation (11) is particularly useful because it permits a Bossler coupling to be idealized as just another beam segment. Conventional methods for calculating beam deflections then can be used to analyze the shaft-coupling system for support displacements, angular misalignments, critical speeds, and the effects of unbalance, and also to determine support reactions. Conventional beam analyses provide the internal moments M'. Equation (9) can be used to find the internal moment M which exists on a coupling element, and stress can be found using Mc/I.

In a typical installation the shaft rotates and thus the moment M' rotates. During each revolution the end moment, m, on each element will vary between $\pm$.297 M', as shown in the following derivation.

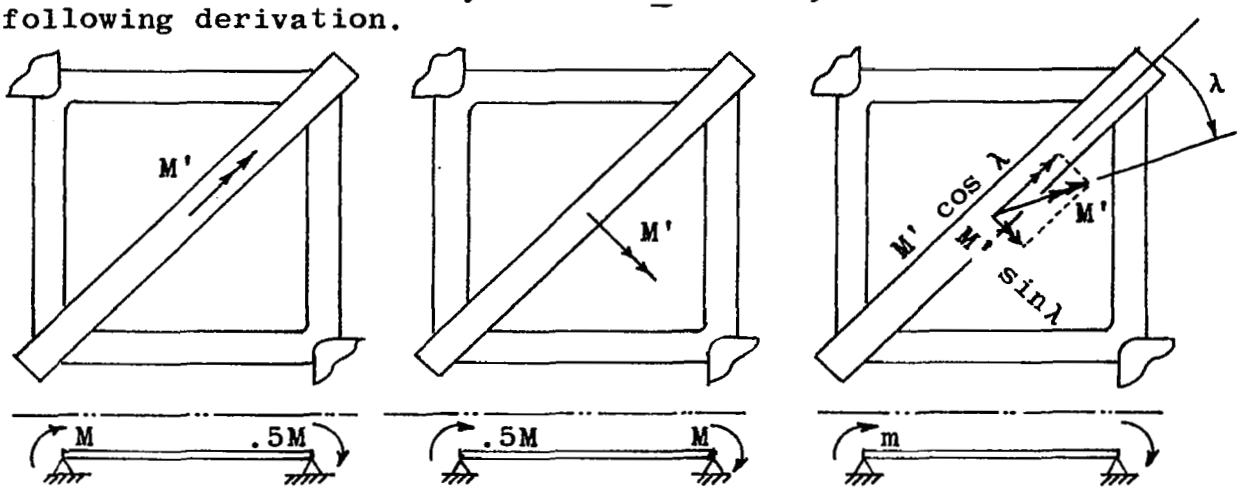

$$m = M \cos \lambda + .5M \sin \lambda$$

At m maximum, $\frac{dm}{d\lambda} = -M \sin \lambda + .5\, M \cos \lambda = 0$

$$\lambda = 26^{o}\ 34'$$

Therefore, $m_{max} = \pm\ 1.118\ M$ (12)

or, from Eq. (9), $m_{max} = \pm\ .297\ M'$ (13)

The maximum flatwise bending stress produced when a single Bossler plate is misaligned at an angle "a" and then rotated can be found from Equations (12) and (5), thus:

$$\sigma_{\substack{max \\ flatwise}} = \frac{t}{2I} (\pm\ 1.118)\ \frac{4\ EIa}{1.414\ L} = \pm 1.581\ \frac{Eta}{L}$$

or

$$\sigma_{\substack{max \\ flatwise}} = \pm\ .0276\ \frac{Et}{L}\ , \begin{array}{l}\text{per degree of} \\ \text{misalignment} \\ \text{in one plate}\end{array} \quad (14)$$

The angle "a" also causes a twisting of the element. This twisting has little significance upon the endurance of the coupling, as shown below.

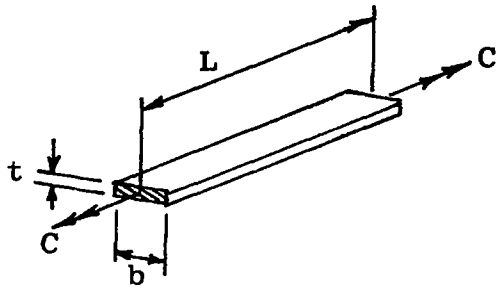

λ = twist angle per unit length, radians
s = maximum shear stress

$$\lambda = \frac{C}{\beta' Gbt^3}$$

$$s = \frac{C}{\alpha bt^2}$$

$$s = \frac{\beta'}{\alpha} Gt\lambda \cong Gt\lambda \text{ , for broad rectangular elements}$$

$$s = .0174 \frac{Gt}{L} \text{ , per degree of twist over total length}$$

Using G = .367E and the fact that one degree of misalignment causes .707 degrees of twist,

$$s = \pm .00452 \frac{Et}{L} \text{ , per degree of misalignment} \qquad (15)$$

Equations (14) and (15) show that the torsional stress is quite small in comparison to the flatwise bending stress. The torsion causes less than a 3% increase in the maximum principal stress, it will be ignored.

Extension and Compression.- When a Bossler coupling is subjected to an axial load the end plates act differently from the interior plates because the end plates are bolted to end fittings which typically are sufficiently rigid to restrain radial displacement. This restraint induces edgewise moments in the end plates which are not present in the interior plates.

The structural behavior can be understood by considering a single Bossler plate subjected to an axial load P which causes a displacement δ, as shown in the following sketch.

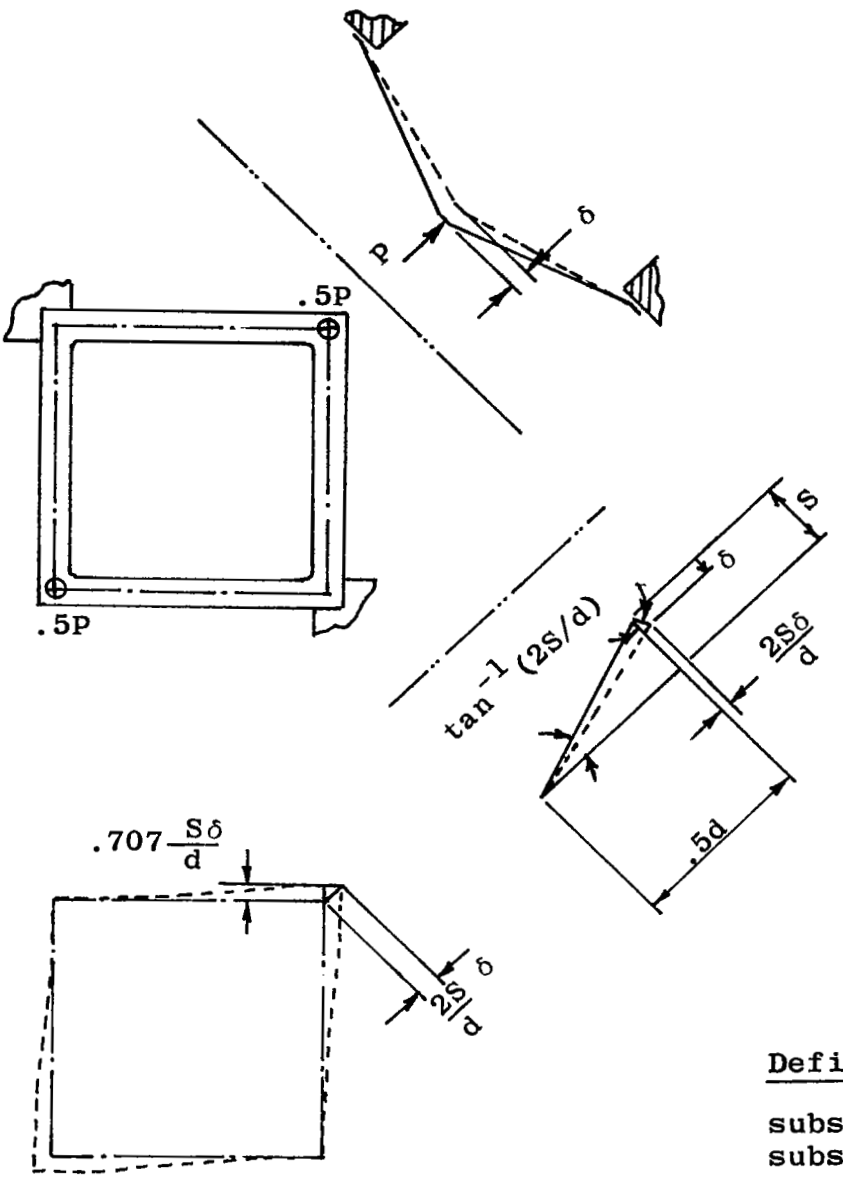

Definitions:

subscript e = edgewise
subscript f = flatwise
a = effective length in bending

Moment Diagrams.-

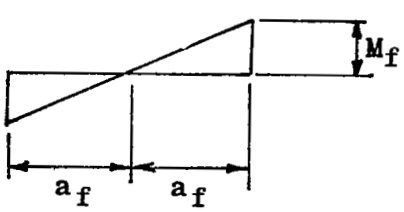

$$M_f = \frac{1.5\ EI\delta}{a_f^2} \qquad (16)$$

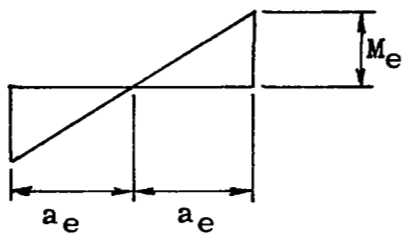

$$M_e = \frac{2.121\ EI_e}{a_e^2}\ \frac{S\delta}{d} \qquad (17)$$

External work = internal work

$$\frac{P\delta}{2} = \left[\frac{1}{2}\int \frac{m^2 ds}{EI}\right]_{\text{edgewise}} + \left[\frac{1}{2}\int \frac{m^2 ds}{EI}\right]_{\text{flatwise}}$$

$$P\delta = 8\left[\frac{1.5\ EI_e}{a_e^3}\left(\frac{S}{d}\right)^2 \delta^2 + \frac{.75\ EI\delta^2}{a_f^3}\right]$$

$$\frac{P}{\delta} = \frac{6\ EI}{a_f^3}\left[2\left(\frac{Sb}{dt}\right)^2 \left(\frac{a_f}{a_e}\right)^3 + 1\right]$$

It was concluded from test data that the effective length for edgewise bending $2a_e = .707d$, and that the effective length for flatwise bending $2a_f = .667d = L$. The reduction in effective length for flatwise bending is attributed to clamp-up in the joints.

The axial spring rate, k_a, for a single Bossler plate located at the end of a coupling becomes:

$$k_{a\ \text{end}} = \frac{48\ EI}{L^3}\left[1.679\left(\frac{Sb}{dt}\right)^2 + 1\right] \qquad (18)$$

For an interior plate no edgewise moments are induced, thus:

$$k_{a\ \text{interior}} = 48\ \frac{EI}{L^3} \tag{19}$$

The effective axial spring rate, $(K_a)_c$ for a coupling with n plates becomes:

$$\frac{1}{(Ka)_c} = \frac{2}{k_{a\ \text{end}}} + \frac{n-2}{k_{a\ \text{interior}}}$$

$$(Ka)_c = \frac{48\ EI}{L^3}\left[\frac{1}{n-2+\left\{\frac{2}{1.679\ (Sb/dt)^2+1}\right\}}\right], \text{ for } n>1 \tag{20}$$

The location of the maximum stress produced by an axial load is not obvious. For a given axial load, the flatwise bending moments are larger in the interior plates than in the end plates; however, the end plates experience edgewise bending moments not present in the interior plates. The location of the maximum stress can be found using Equations (16) through (19) as follows. Assume that the stress in the end plate is the addition of the flatwise stress plus 1.6 times the edgewise stress. The factor 1.6 is a stress concentration factor for edgewise bending in a typical corner fillet radius. The stress concentration factor does not vary greatly in the range of interest for Bossler plates, as can be seen from the values shown below (Reference 2).

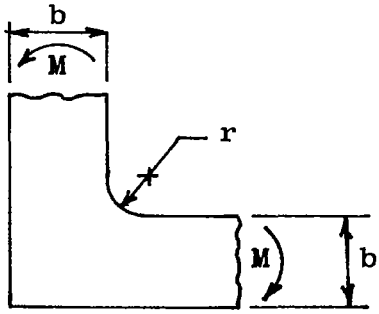

r/b	stress conc. factor
.10	1.79
.20	1.66
.30	1.53
.40	1.42

For any given axial load,

$$\frac{\sigma_{f\ end}}{\sigma_{f\ interior}} = \frac{k_{a\ interior}}{k_{a\ end}}$$

$$\frac{\sigma_{f\ end}}{\sigma_{f\ interior}} = \frac{1}{1.679\left(\frac{Sb}{dt}\right)^2 + 1} \qquad (21)$$

From Equations (16) and (17) for an end plate:

$$\frac{M_e}{M_{f\ end}} = .707\ \frac{S}{d}\ \frac{Ie}{I}\left(\frac{a_f}{a_e}\right)^2$$

$$\frac{M_e}{M_{f\ end}} = 1.259\ \frac{S}{d}\ \left(\frac{b}{t}\right)^2$$

Using $\sigma = Mc/I$, and introducing the notch factor =1.6, get:

$$\frac{\sigma_e}{\sigma_{f\ end}} = 2.014\ \frac{bS}{td} \qquad (22)$$

Combining Equations (21) and (22),

$$\frac{\sigma_{end}}{\sigma_{interior}} = \frac{(\sigma_e + \sigma_f)_{end}}{\sigma_{f\ interior}} = \frac{1 + 2.014\ (bS/td)}{1 + 1.679\ (bS/td)^2} \qquad (23)$$

Equation (23) states the ratio of maximum combined bending stress in the end plate to the maximum bending stress in an interior plate for any axial load. A plot of Equation (23) is shown in Figure 1.

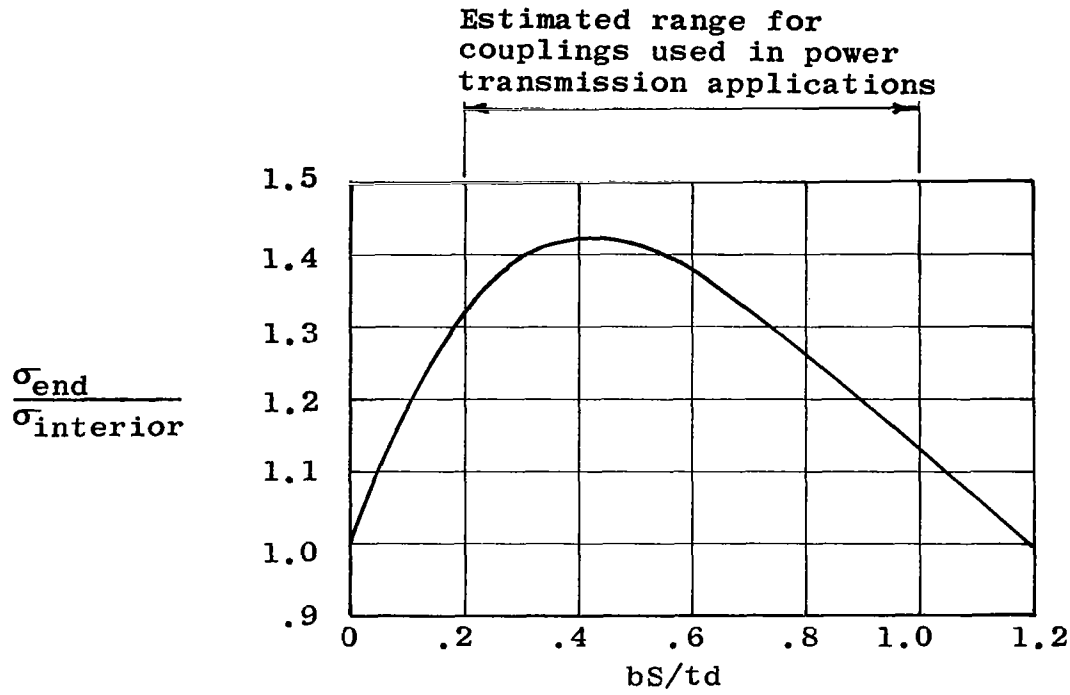

Figure 1. Ratio of Stresses for Axial Loading

It is concluded that the bending stress induced by extension or compression of the coupling is typically higher in an end plate than in an interior plate.

Having Figure 1, the calculation of stress from an axial load or deflection in any coupling is very simple. First, find the axial load P on the coupling. The axial load for any deflection can be found using the spring constant $(Ka)_c$ given by Equation (20). Next, calculate the stress in an interior plate using,

$$\sigma_{interior} = \frac{PL}{8} \frac{6}{bt^2} = \frac{Pd}{2bt^2}$$

Then, multiply the σ interior by the appropriate factor from Figure 1 to find the stress in the end plate.

Centrifugal Loads.- Rotation produces inertia forces which cause both an axial load and an edgewise bending moment in the elements. The internal loads and the stresses which result can be derived from the fixed-ended beam idealization shown below.

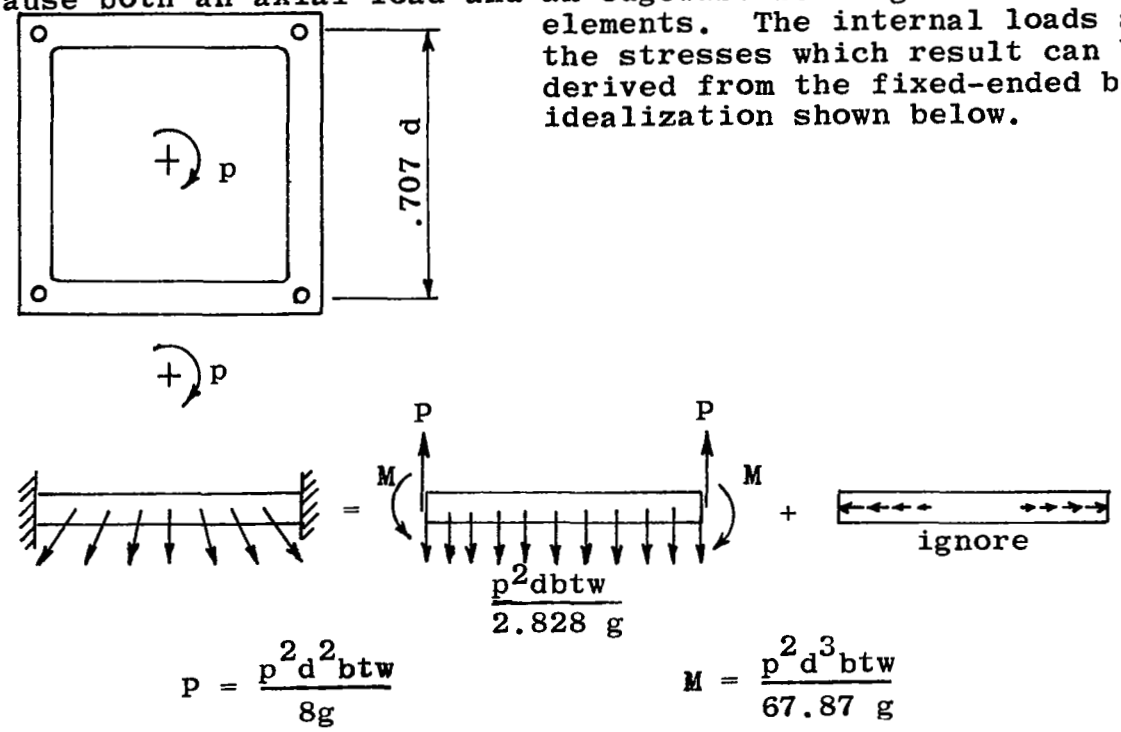

$$P = \frac{p^2d^2btw}{8g} \qquad M = \frac{p^2d^3btw}{67.87\ g}$$

Using a stress concentration factor = 1.6 on edgewise bending, the stress in the fillet becomes $P/A + (1.6)(6M)/tb^2$

$$\sigma = \frac{p^2d^2w}{8g}\left[1 + 1.131\ \frac{d}{b}\right] \qquad (24)$$

Equation (24) is shown graphically in Figure 2. Figure 2 was prepared using a unit weight corresponding to nickel maraging steel. For a titanium coupling, the stresses would be only 56% of the values shown.

The dotted lines in Figure 2 demonstrate the use of the curves. For the example shown, at 6300 rpm, with d = 8 inches, and d/b = 8, the maximum stress from centrifugal loads is 26 ksi. Such a steady stress would cause less than a 9% reduction in the allowable alternating stress in a nickel maraging steel coupling with an ultimate strength in the 300 ksi range. This result is typical. Except for high speed applications, the centrifugal forces will have only a secondary effect upon the endurance.

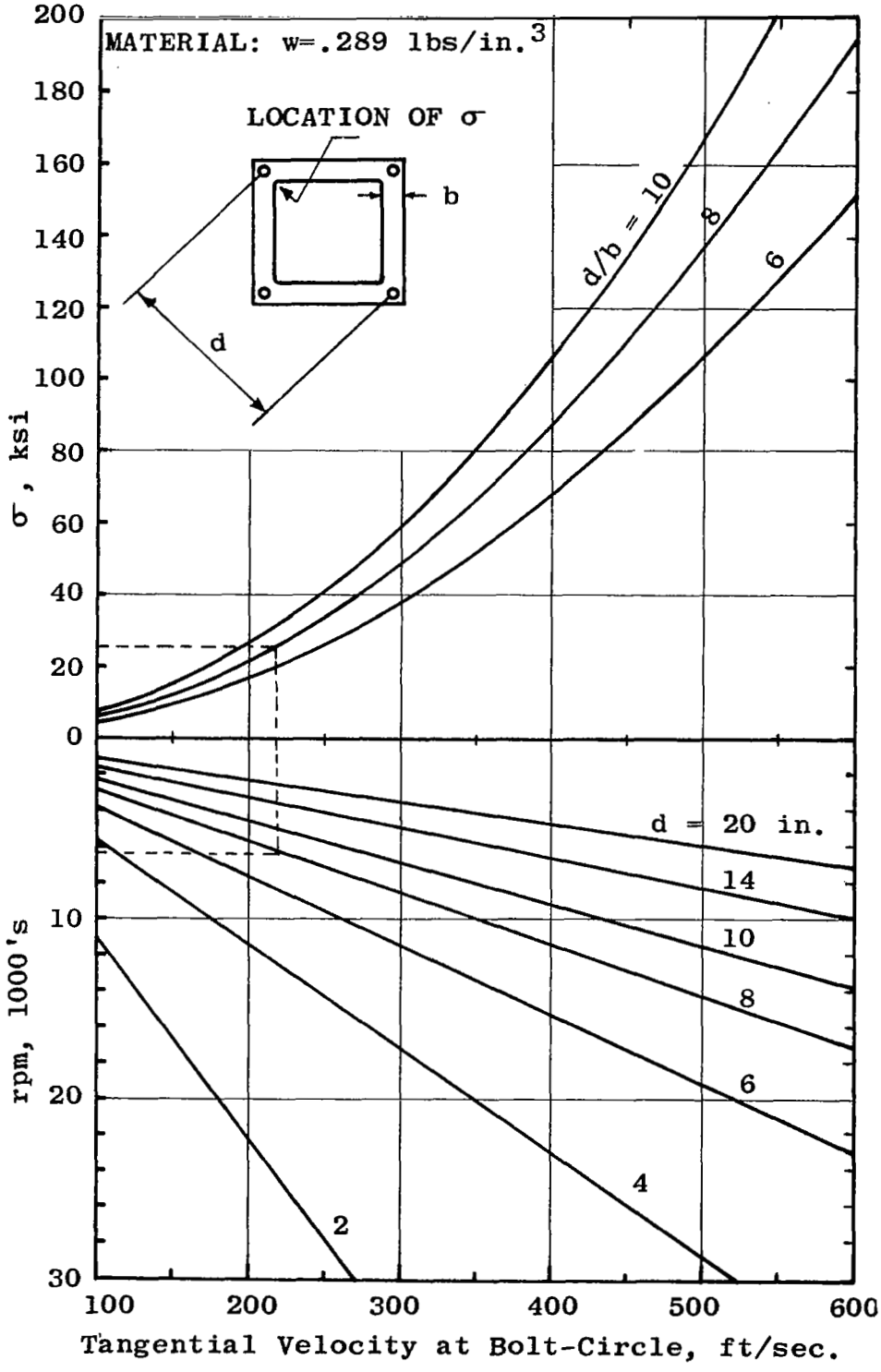

Figure 2. Maximum Stress From Centrifugal Loads

Critical Speed.- The very simple idealization shown here provides a preliminary estimate of the fundamental critical speed. An example using a more general approach suitable for final analysis is described in a separate section beginning on Page 88.

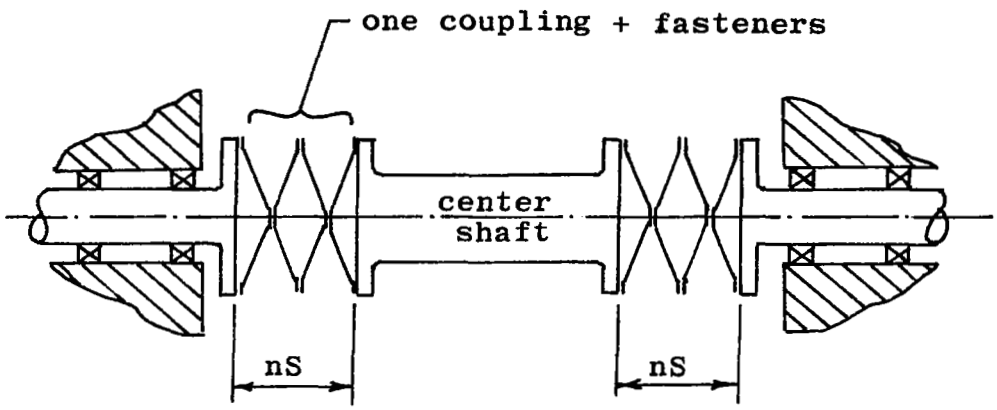

Idealization.-

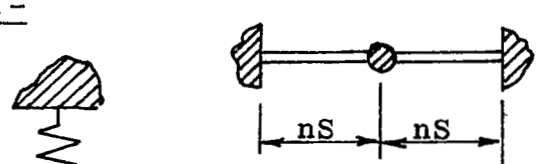

$$k = \frac{24\,(EI)c}{(nS)^3} \tag{25}$$

M_S = mass of center shaft + one coupling + fasteners

$$f_1 = \frac{60}{2\pi}\left(\frac{k}{M_S}\right)^{.5} \text{rpm} \tag{26}$$

From Equations (25) and (26), it is apparent that the critical speed is inversely proportional to the offset distance S. Thus, in computing the critical speed, it is important to use a value for S which includes any axial extensions of the coupling that may be encountered in service.

DESIGN GUIDELINES

Introduction.- Using the previously derived analysis formulas, design formulas are developed here. Their primary purpose is to show the performance that can be obtained if the coupling is proportioned efficiently. Fortunately, the formulas are simple; many of the effects of changes in the design parameters are readily apparent by inspection. Other less obvious characteristics are described using graphs.

Plate Thickness.- An optimum design for misalignment capability uses the minimum thickness that provides the required torque strength. From Equation (2), this thickness is:

$$t = .4415 \left(\frac{dT_u}{bE}\right)^{\frac{1}{3}} n^{.3} \qquad (27)$$

In the following evaluations it is assumed that the thickness will be chosen in accordance with Equation (27).

Weight.- The weight of any coupling using minimum thickness plates is:

$$W = 2.828\ wnbdt$$

$$W = 1.249\ w \left(\frac{T_u}{E}\right)^{\frac{1}{3}} d^{\frac{4}{3}} b^{\frac{2}{3}} n^{1.3} \qquad (28)$$

Figure 3 shows a plot of Equation (28) for a coupling using d/b = 7.5 made from nickel maraging steel. If titanium plates are used, the weight is 67% of the weight shown in Figure 3.

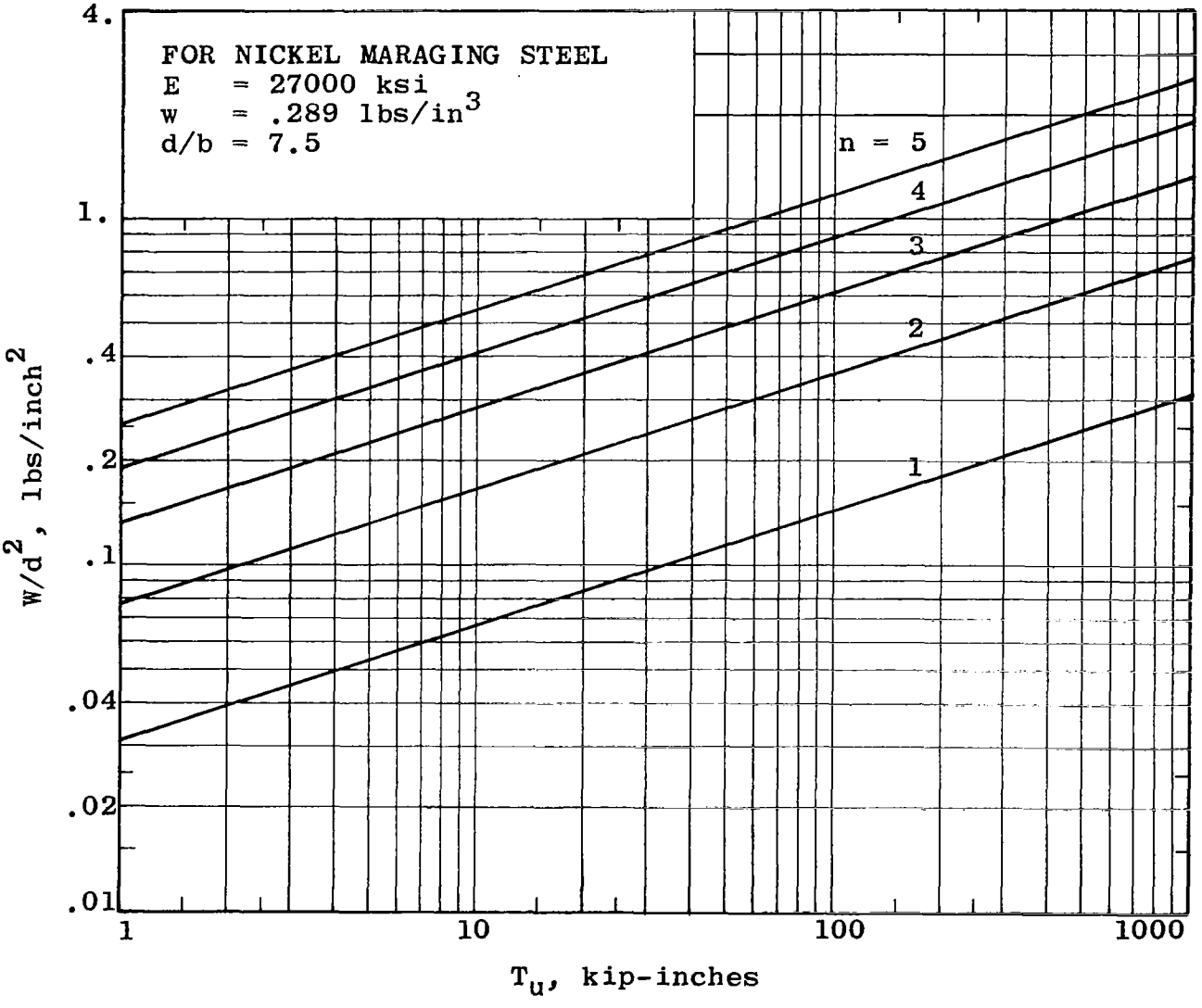

Figure 3. Total Weight of Plates

Uniform Angular Misalignment.- This is the simplest type of misalignment. It exists when the centerline of the input and output shafts intersect at the center of the coupling both before and after misalignment, as shown below. The misalignment is distributed equally to each plate.

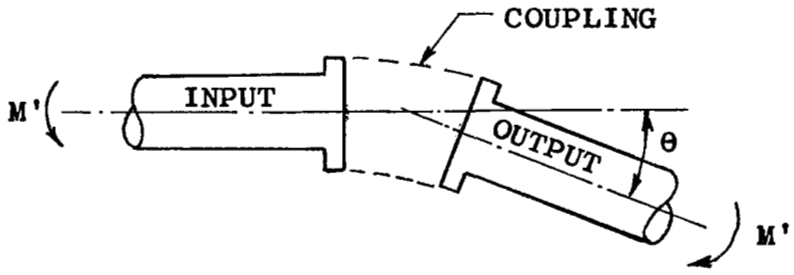

When the shaft is rotated, an alternating flatwise bending stress is induced in each element. From Equation (14),

$$\sigma = \pm .0276 \frac{Et}{L} \frac{\theta}{n}$$

Using L = .667d and t from Equation (27),

$$\sigma_{\substack{\text{uniform} \\ \text{angle}}} = \pm .01827 \frac{\theta E^{\frac{2}{3}} T^{\frac{1}{3}}}{d^{\frac{2}{3}} b^{\frac{1}{3}} n^{.7}} \qquad (29)$$

Assuming that the allowable angle change is governed primarily by the alternating flatwise bending stress,

$$\theta = 54.7 \frac{d^{\frac{2}{3}} b^{\frac{1}{3}} n^{.7}}{T_u^{\frac{1}{3}} E^{\frac{2}{3}}} \sigma_c^{\frac{2}{3}} \qquad (30)$$

Equation (30) is a performance equation. It states the maximum allowable uniform angular misalignment that can be obtained when the mean tensile stress is zero. A conservative adjustment for mean stress is to reduce the allowable angle by the percentage that the mean stress bears to the ultimate tensile strength. A primary contributor to mean stress is centrifugal loading.

If material properties and a ratio of b/d are introduced into Equation (30), the performance can be expressed in graphical form, as shown in Figure 4. These curves are based upon:

(1) An assumed ratio of endurance limit to modulus, $\sigma_c/E^{.667} = .389$ psi$^{.333}$. This corresponds to an endurance limit of 35 ksi in nickel maraging steel or 25 ksi in titanium. Such endurance limits are attainable with known surface properties and detail joint design.

(2) A ratio of d/b = 7.5. Substituting $\sigma_c/E^{.667} = .389$ and d/b = 7.5 into Equation (30) gives:

$$\theta/d = 10.87n^{.7}/T_u^{.333}$$, shown in Figure 4.

Use of the curves is shown by the following example. For a required ultimate torque = 50,000 in-lbs, the use of 3 plates gives $\theta/d = .637$. If a coupling with d = 8 inches is used, the allowable angle is .637 x 8 = 5.1 degrees.

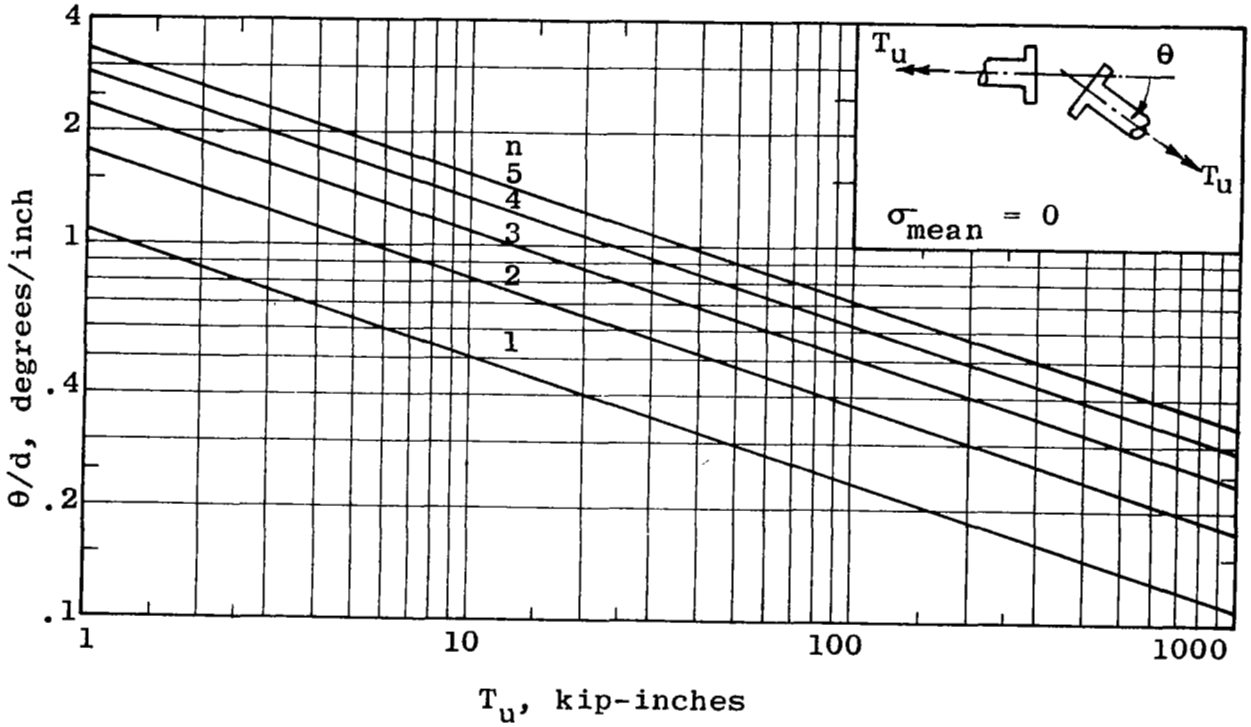

Figure 4. Allowable Uniform Angular Misalignment, Infinite Life

Parallel Offset Misalignment.- This condition is most often used to specify coupling performance. It exists when the input and output shafts remain parallel but are displaced laterally, as shown below. In this case the coupling plates do not share the misalignment uniformly. The plates attached to the input and output shafts have the greatest misalignment, as shown by the moment diagram.

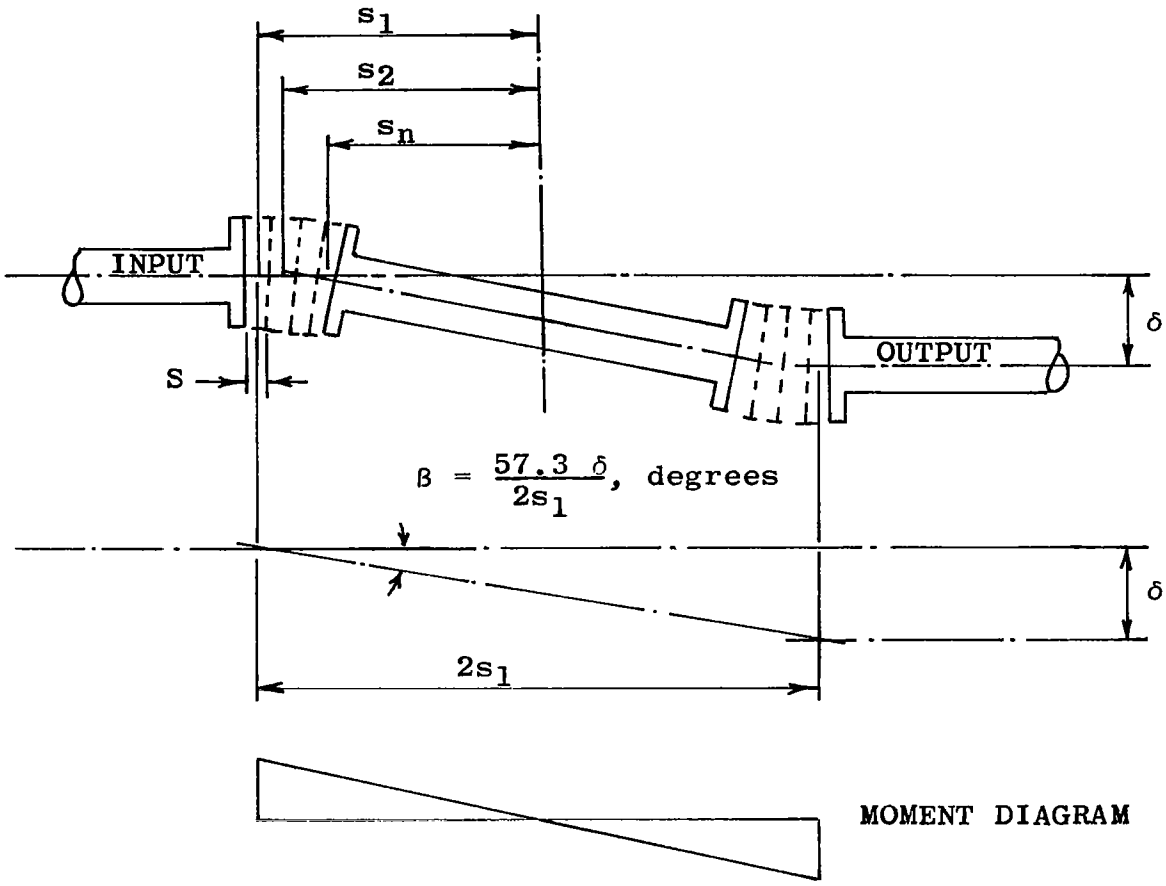

The evaluations which follow are made using the parameter β. The sketch shows β to be a fictitious concentrated angle which is equivalent to the actual distributed angle.

Let:

θ_i = angle change in plate i, degrees

for 1 plate at each end, $\delta = \frac{2\theta_1 s_1}{57.3}$

for n plates at each end, $\theta_i = \frac{s_i}{s_1}\theta_1$

$$\delta = \frac{2s_1\theta_1}{57.3} + \frac{2s_2s_2\theta_1}{57.3\ s_1} + \ \ldots \ + \frac{2s_ns_n\theta_1}{57.3\ s_1}$$

$$\delta = \frac{2\theta_1 s_1}{57.3} \sum_{m=1}^{m=n} \left(\frac{s_m}{s_1}\right)^2 = \frac{2\theta_1 s_1}{57.3} \sum_{m=1}^{m=n} \left[1 - (m-1)\ \frac{S}{s_1}\right]^2$$

$$\delta = \frac{2\theta_1 s_1 \alpha_2}{57.3}\ , \text{ where } \boxed{\alpha_2 = \sum_{m=1}^{m=n} \left[1 - (m-1)\ \frac{S}{s_1}\right]^2}$$

$$\beta = \frac{57.3\ \delta}{2s_1} = \theta_1 \alpha_2$$

$$\theta_1 = \frac{\beta}{\alpha_2}$$

Using L = .667d in Equation (14) shows the flatwise bending stress in plate 1 to be:

$$\sigma = \pm \frac{.0276\ Et\theta_1}{.667d}$$

$$\sigma_{\substack{\text{parallel} \\ \text{offset}}} = \frac{\pm\ .01827\ \beta\ E^{\frac{2}{3}}\ T_u^{\frac{1}{3}}\ n^{.3}}{d^{\frac{2}{3}}\ b^{\frac{1}{3}}\ \alpha_2} \qquad (31)$$

$$\beta = \frac{54.7\, d^{\frac{2}{3}}\, b^{\frac{1}{3}}}{T_u^{\frac{1}{3}}} \quad \frac{\sigma_c}{E^{\frac{2}{3}}} \quad \frac{\alpha_2}{n^{.3}} \tag{32}$$

Like Equation (30), Equation (32) is a performance equation. It also can be reduced to performance curves. Assuming, as before, that $\sigma_c/E^{.667} = .389\ psi^{.333}$ and d/b = 7.5, Equation (32) becomes:

$$\frac{\beta}{d} = \frac{10.87}{T^{\frac{1}{3}}} \quad \frac{\alpha_2}{n^{.3}} \tag{33}$$

Figure 5 shows Equation (33) for $S/s_1 = .05$ and .10. For $S/s_1 \rightarrow 0$, corresponding to a long center shaft, the curve shown in Figure 4 can be used with $\beta = 0$. The performance for other values of S/s_1 can be estimated by interpolation or calculated using Equation (33).

General.- From the preceding evaluations and by judgment, the following guidelines are recommended for least weight design. For final optimization, trade-off studies should be made.

(1) Size of plates - Use the largest d consistent with envelope and centrifugal force loading. Usually, centrifugal force will not be a problem below 300 ft/sec. tip speed.

(2) Number of plates - Use the least n consistent with the required performance.

(3) Thickness of plates - Use the smallest t consistent with the required ultimate torque.

(4) Joint details - Be conservative. Use high strength tension fasteners with high preload. Provide fretting protection. Make element centerlines and bolt centerlines intersect at a point.

(5) Offset distance - Use the smallest S consistent with clearance.

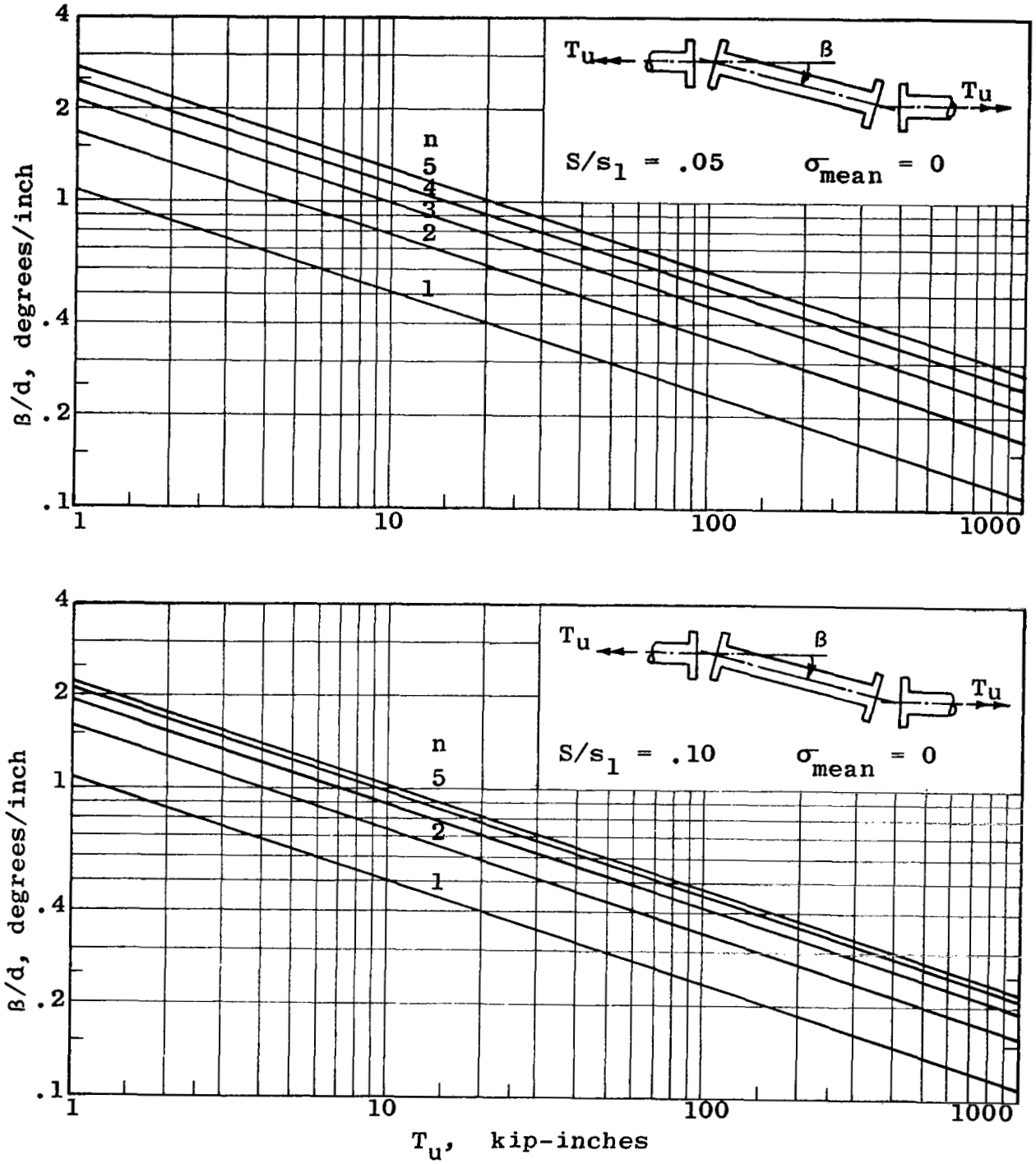

Figure 5. Allowable Angle for Parallel Offset Misalignment, Infinite Life

COMPUTER ANALYSIS

Introduction.- The simplified analysis presented in the preceding sections is based upon symmetry and engineering judgment regarding the final deflected positions. Fortunately, the simplified analysis is in good agreement with test results which are reported in later sections.

An alternative analysis is also possible. The coupling can be analyzed as a linear, redundant, elastic frame with no assumptions regarding symmetry or deflected position, but merely enforcing continuity. Such an analysis is both feasible and routine using the computer programming system called STRESS, Reference 3.

In this section, the application of STRESS to the analysis of Bossler couplings is described in detail. The description includes the idealization of the coupling for analysis and also examples of computer input and output. The examples chosen correspond to basic test conditions. Detailed comparisons of the computer results to test data are postponed to later sections which are devoted specifically to the tests.

In the later sections, it will be found that the computer results are good but not superior to the results from the simplified analysis. The principal value of the computer analysis approach is its ability to treat more complicated geometries which lack symmetry. Such geometries include couplings with non-square plates, unequal elements, and unusual end fittings.

Input Definitions.- Reference 3 is a short, 55 page, manual which states as concisely as possible the STRESS input language. For a full understanding of this section, acquaintance with Reference 3 is essential.

Identification numbers and coordinates were defined so as to simplify input preparation and output interpretations. The definitions shown on the following pages have these advantages:

1. repetitive regularity.

2. applicability to couplings with any number of plates, without destroying regularity.

3. simple definition of loading (at node number 1).

4. economy of input through use of symmetry.

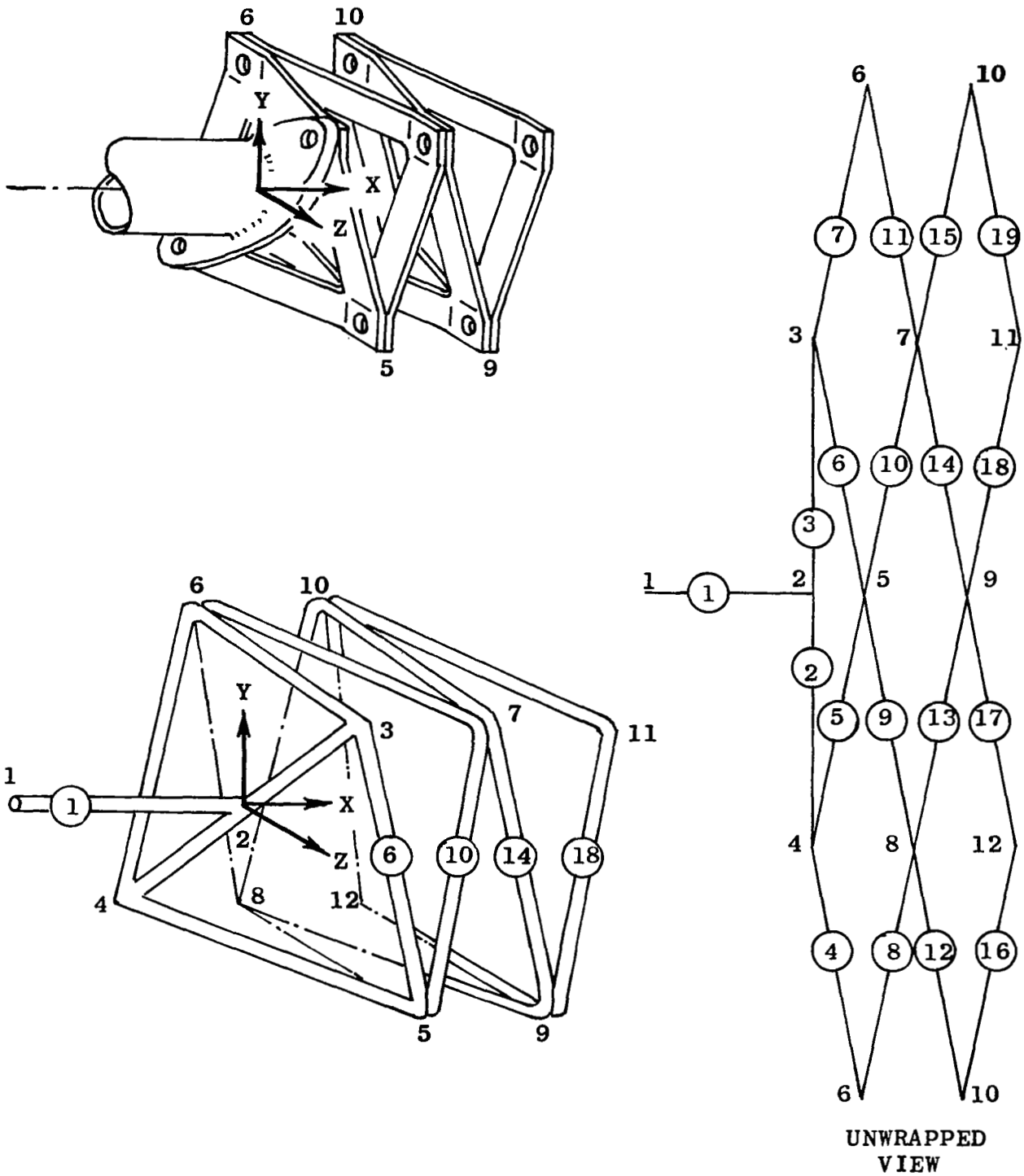

Figure 6. Global Coordinates and Numbering Convention

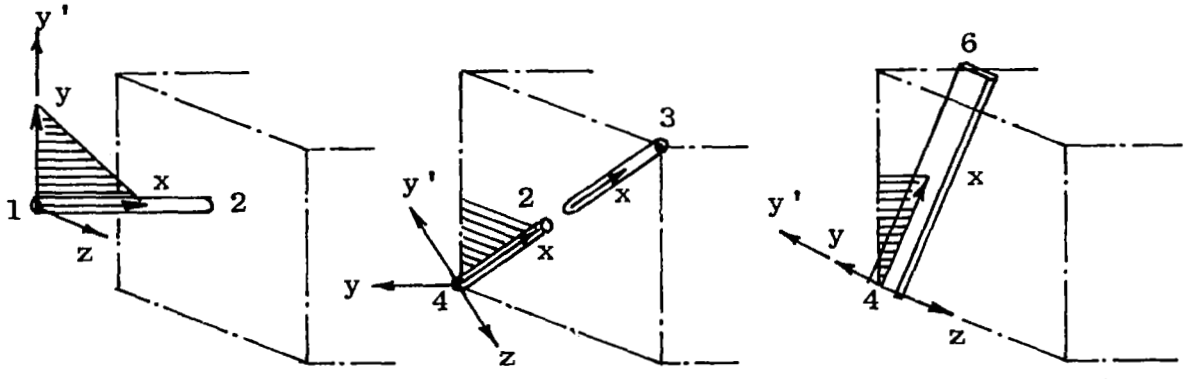

BETA = 0 BETA = 90 BETA = 0

MEMBERS 1 2,3 4,10,12,18

NOTES: PLANE-A SHOWN SHADED.
PLANE-A AND BETA DEFINED IN REF. 3

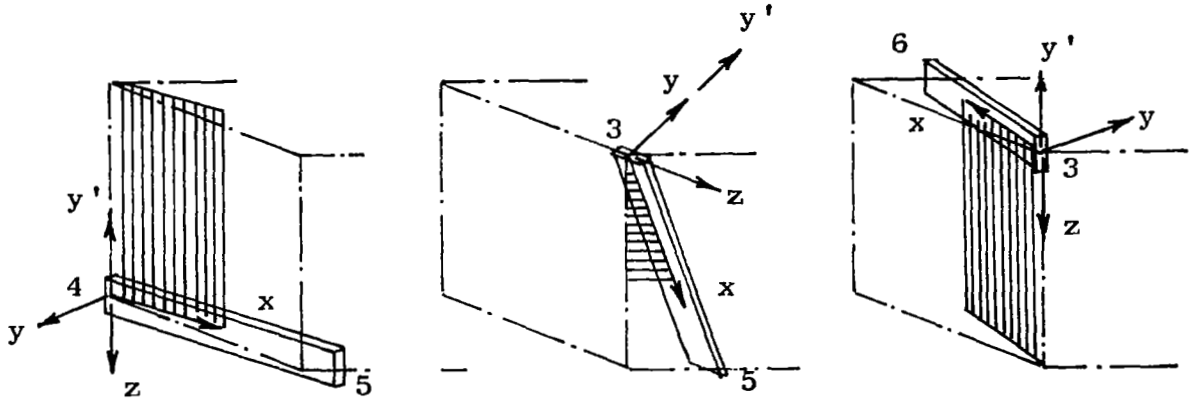

BETA = 90 BETA = 0 BETA = 90

MEMBERS 5,11,13,19 6,8,14,16 7,9,15,17

Figure 7. Local Coordinates

The identification system established here is used, not only for the computer analysis, but also for the discussion of results from stress tests reported in a later section.

Scale.- In the first attempt to use STRESS for the analysis of Bossler couplings, no scale factor was used. The attempt failed. No errors in input could be found; all was in agreement with Reference [3]. Fortunately, however, past experience enabled Mr. David Wang* to diagnose the difficulty. The elements had too small a moment of inertia (less than 10^{-5} inches^4) for the STRESS program. In all subsequent cases, good results have been obtained merely by scaling up all dimensions by a factor of 10. In order to preserve equal stress and scaled deflections, the applied forces also have been scaled up by 100 and moments, by 1000.

Results.- The total output from STRESS was very lengthy. Only the most significant results are evaluated in later discussions of strain and stiffness tests. Here, however, the entire input and output is presented for four basic loading conditions, three of which correspond to simple tests performed upon steel couplings. The test conditions are shown in the following sketch.

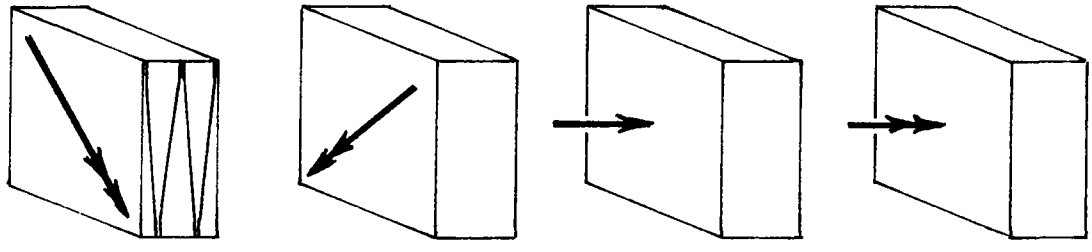

Loading	1	2	3	4
Test	5.2	6.2	4.6	None

One important feature to be noted in the input is the use of joint releases at joints 11 and 12 and member releases for members 2 and 3 at joints 3 and 4. These releases allow slippage to occur about the bolt axes at the end fittings. In the output, the locations of inflection points are seen to agree with those assumed in the simplified analysis.

* Project Analyst, Service Bureau Corporation, N.Y., N.Y.

```
STRUCTURE BOSSLER COUPLING  D8.0  STEEL (RIGID EARS, END SLIPPAGE)
* KAMAN CORP., BLOOMFIELD, CONN.  12 NOV 1967
NUMBER OF JOINTS  12
NUMBER OF SUPPORTS  2
NUMBER OF MEMBERS  19
NUMBER OF LOADINGS  4
TYPE SPACE FRAME
METHOD STIFFNESS
TABULATE ALL
JOINT COORDINATES
 1 X -40.5  Y   0.0   Z   0.0
 2 X   0.0  Y   0.0   Z   0.0
 3 X   0.0  Y  28.28  Z  28.28
 4 X   0.0  Y -28.28  Z -28.28
 5 X   7.5  Y -28.28  Z  28.28
 6 X   7.5  Y  28.28  Z -28.28
 7 X  15.0  Y  28.28  Z  28.28
 8 X  15.0  Y -28.28  Z -28.28
 9 X  22.5  Y -28.28  Z  28.28
10 X  22.5  Y  28.28  Z -28.28
11 X  30.0  Y  28.28  Z  28.28 S
12 X  30.0  Y -28.28  Z -28.28 S
JOINT RELEASES
11 MOMENT  X  0.0  0.0  0.0
12 MOMENT  X  0.0  0.0  0.0
MEMBER INCIDENCES
 1   1   2
 2   4   2
 3   2   3
 4   4   6
```

```
 5   4   5
 6   3   5
 7   3   6
 8   6   8
 9   5   8
10   5   7
11   6   7
12   8  10
13   8   9
14   7   9
15   7  10
16  10  12
17   9  12
18   9  11
19  10  11
MEMBER RELEASES
 2 START MOMENT Y
 3 END   MOMENT Y
MEMBER PROPERTIES  PRISMATIC  AX 17.65  AY 14.71  AZ 14.71   IX  14.410
$ IY  168.21 IZ 4.004  BETA 0.0
* CORRESPONDS TO ELEMENTS  1.65 X 10.695
 4
 6
 8
10
12
14
16
18
 5 BETA 90.
 7 BETA 90.
```

```
 9 BETA 90.
11 BETA 90.
13 BETA 90.
15 BETA 90.
17 BETA 90.
19 BETA 90.
MEMBER PROPERTIES PRISMATIC AX 999.  AY 999.  AZ 999.  IX 9999. IY 9999.
$ IZ 9999.  BETA 90.
 1
 2
 3
CONSTANTS  E  27000. ALL G 10400. ALL
* CORRESPONDS TO STATIC TEST NO. 5.2
LOADING  1
JOINT LOADS
2  MOMENT  Y -132.04  Z  132.04
* CORRESPONDS TO STATIC TEST NO. 6.2
LOADING   2
JOINT LOADS
2  MOMENT  Y -146.70  Z -146.70
* CORRESPONDS TO STATIC TEST NO. 4.6
LOADING   3
JOINT LOADS
3  FORCE   X   7.32
4  FORCE   X   7.32
LOADING   4
JOINT LOADS
2  MOMENT   X   2000.
SOLVE
```

STRUCTURE BOSSLER COUPLING D8.0 STEEL (RIGID EARS, END SLIPPAGE)

LOADING 1

MEMBER FORCES

MEMBER	JOINT	FORCES			MOMENTS		
		AXIAL	SHEAR Y	SHEAR Z	TORSIONAL	BENDING Y	BENDING Z
1	1	0.0000003	0.0020322	-0.0023184	0.0000000	0.0283240	0.0101115
1	2	-0.0000003	-0.0020322	0.0023184	-0.0000000	0.0655732	0.0721935
2	4	-0.0906046	2.5970365	0.0015026	-0.0085615	-0.0000000	10.5506353
2	2	0.0906046	-2.5970365	-0.0015026	0.0085615	-0.0600942	93.3151379
3	2	0.0675093	2.5972605	-0.0003101	0.0029966	0.0124005	93.3296175
3	3	-0.0675093	-2.5972605	0.0003101	-0.0029966	-0.	10.5451145
4	4	0.2754043	-1.2704525	-0.0557934	-16.9338212	0.9212305	-24.1342888
4	6	-0.2754043	1.2704525	0.0557934	16.9338212	2.2620669	-48.3514929
5	4	0.3057777	-1.2705918	0.0547930	16.9283988	-0.9220650	-24.1358099
5	5	-0.3057777	1.2705918	-0.0547930	-16.9283988	-2.2041532	-48.3579216
6	3	-0.2830168	-1.2704732	-0.0548288	16.9329469	0.9066278	-24.1357355
6	5	0.2830168	1.2704732	0.0548288	-16.9329469	2.2216330	-48.3512316
7	3	-0.2990112	-1.2707737	0.0547516	-16.9295344	-0.9069184	-24.1403437
7	6	0.2990112	1.2707737	-0.0547516	16.9295344	-2.2169369	-48.3637676
8	6	0.1689950	1.2665890	0.0544083	16.9036977	-2.2608208	48.2829757
8	8	-0.1689950	-1.2665890	-0.0544083	-16.9036977	-0.8434496	23.9823775
9	5	0.1451374	1.2724161	-0.0545885	-16.9887354	2.2814673	48.3898644
9	8	-0.1451374	-1.2724161	0.0545885	16.9887354	0.8330869	24.2079520
10	5	-0.1654518	1.2666927	0.0543013	-16.9036391	-2.2463665	48.2875957
10	7	0.1654518	-1.2666927	-0.0543013	16.9036391	-0.8517997	23.9836750
11	6	-0.1483150	1.2725221	-0.0533573	16.9886198	2.2570464	48.3914876
11	7	0.1483150	-1.2725221	0.0533573	-16.9886198	0.7872619	24.2123761
12	8	0.2757447	-1.2489123	-0.0564960	-16.6289744	1.0104585	-23.6803746
12	10	-0.2757447	1.2489123	0.0564960	16.6289744	2.2129261	-47.5764298
13	8	0.3017249	-1.2551584	0.0556203	16.7050598	-0.9969967	-23.9132271
13	9	-0.3017249	1.2551584	-0.0556203	-16.7050598	-2.1764234	-47.6999493
14	7	-0.2787777	-1.2490138	-0.0561480	16.6298077	0.9993970	-23.6842303
14	9	0.2787777	1.2490138	0.0561480	-16.6298077	2.2041314	-47.5783658
15	7	-0.2984555	-1.2551294	0.0554599	-16.7041552	-0.9938408	-23.9115229
15	10	0.2984555	1.2551294	-0.0554599	16.7041552	-2.1704296	-47.7000008
16	10	0.1670464	1.2452962	0.0558339	16.5965526	-2.2219394	47.5124307
16	12	-0.1670464	-1.2452962	-0.0558339	-16.5965526	-0.9636681	23.5380569
17	9	0.1444840	1.2570183	-0.0558832	-16.7599771	2.2464218	47.7301898
17	12	-0.1444840	-1.2570183	0.0558832	16.7599771	0.9419983	23.9891076
18	9	-0.1642655	1.2453598	0.0556416	-16.5967426	-2.2174391	47.5143995
18	11	0.1642655	-1.2453598	-0.0556416	16.5967426	-0.9571975	23.5397177
19	10	-0.1479961	1.2570505	-0.0556205	16.7597656	2.2378557	47.7309690
19	11	0.1479961	-1.2570505	0.0556205	-16.7597656	0.9355762	23.9901652

STRUCTURE BOSSLER COUPLING D8.0 STEEL (RIGID EARS, END SLIPPAGE)

LOADING 1

JOINT	X FORCE	Y FORCE	Z FORCE	X MOMENT	Y MOMENT	Z MOMENT
		SUPPORT REACTIONS				
11	2.5217431	-0.0564853	-0.0741714	0.0000040	-7.6632655	7.0483670
12	-2.5215520	-0.0539828	-0.0778411	0.0000007	-7.6632466	7.0473408
		APPLIED JOINT LOADS				
1	0.0000003	0.0023184	0.0020322	0.0000000	-0.0101115	0.0283240
2	-0.0002243	0.1107667	0.1084894	0.0476936	-132.0417900	132.0515137
3	0.0015564	0.0108478	0.0270251	0.0001604	0.0148687	-0.0179192
4	-0.0016446	-0.0139114	0.0173046	0.0001145	0.0035491	-0.0196206
5	-0.0001062	-0.0016803	-0.0035890	-0.0304295	-0.0061413	0.0063415
6	0.0002585	0.0010647	0.0010782	-0.0121895	0.0023050	-0.0046709
7	0.0001341	0.0008630	0.0001798	0.0485417	-0.0099964	-0.0097066
8	-0.0000151	0.0000043	-0.0001740	-0.0024378	-0.0004320	-0.0007573
9	-0.0001507	0.0001949	-0.0003170	0.0009334	0.0007872	-0.0003233
10	0.0000004	-0.0000000	-0.0000168	0.0000395	-0.0000134	-0.0000072

STRUCTURE BOSSLER COUPLING D8.0 STEEL (RIGID EARS, END SLIPPAGE)

LOADING 1

MEMBER DISTORTIONS

MEMBER	DISTORTIONS				ROTATIONS	
	AXIAL	SHEAR Y	SHEAR Z	TORSIONAL	BENDING Y	BENDING Z
1	-0.0000000	0.0000000	-0.	-0.0000000	0.0000000	0.0000000
2	0.0000001	0.0000613	-0.0000010	0.0000000	0.0000000	0.0000061
3	-0.0000001	-0.0001839	0.0000000	-0.0000000	-0.0000000	-0.0000061
4	-0.0000330	0.0000577	-0.0000293	0.0064469	0.0000084	-0.0063904
5	-0.0000366	0.0000407	0.0000226	-0.0064448	-0.0000080	-0.0063917
6	0.0000339	0.0000735	-0.0000283	-0.0064466	0.0000083	-0.0063900
7	0.0000358	0.0000570	0.0000277	0.0064453	-0.0000082	-0.0063921
8	-0.0000202	-0.3647379	-0.0004597	-0.0064354	0.0000089	-0.0064124
9	-0.0000174	-0.3646809	0.0004659	0.0064678	-0.0000091	-0.0063811
10	0.0000198	-0.3647778	-0.0004552	0.0064354	0.0000088	-0.0064133
11	0.0000178	-0.3646750	0.0004651	-0.0064678	-0.0000092	-0.0063804
12	-0.0000330	-0.0006166	-0.0000019	0.0063309	0.0000075	-0.0063057
13	-0.0000361	0.0011030	0.0000010	-0.0063598	-0.0000074	-0.0062768
14	0.0000334	-0.0005876	-0.0000036	-0.0063312	0.0000076	-0.0063052
15	0.0000357	0.0010856	0.0000011	0.0063595	-0.0000074	-0.0062773
16	-0.0000200	-0.3592257	-0.0004366	-0.0063185	0.0000079	-0.0063264
17	-0.0000173	-0.3591522	0.0004450	0.0063807	-0.0000082	-0.0062648
18	0.0000197	-0.3592372	-0.0004362	0.0063186	0.0000079	-0.0063264
19	0.0000177	-0.3591547	0.0004436	-0.0063806	-0.0000082	-0.0062647

STRUCTURE BOSSLER COUPLING D8.0 STEEL (RIGID EARS, END SLIPPAGE)

LOADING 1

JOINT DISPLACEMENTS

JOINT	X DISPLACEMENT	Y DISPLACEMENT	Z DISPLACEMENT	X ROTATION	Y ROTATION	Z ROTATION
		SUPPORT DISPLACEMENTS				
11	0.	0.	0.	-0.0000039	0.	0.
12	0.	0.	0.	0.0000039	0.	0.
		FREE JOINT DISPLACEMENTS				
1	-0.0000207	-1.4108076	-1.4032046	-0.0000000	-0.0253188	0.0254393
2	-0.0000207	-0.3805172	-0.3777921	-0.0000000	-0.0253188	0.0254393
3	-1.4352758	-0.3805163	-0.3777931	0.0000000	-0.0253145	0.0254349
4	1.4352345	-0.3805184	-0.3777911	-0.0000000	-0.0253145	0.0254349
5	0.0034014	-0.1897783	-0.1879633	-0.0008392	-0.0189228	0.0190449
6	-0.0034268	-0.1897815	-0.1879624	0.0008391	-0.0189224	0.0190445
7	-0.7121658	-0.0948723	-0.0939639	-0.0000020	-0.0125420	0.0126316
8	0.7121543	-0.0948732	-0.0939634	0.0000020	-0.0125416	0.0126320
9	0.0017009	-0.0002454	0.0002081	-0.0008267	-0.0062648	0.0063264
10	-0.0017077	-0.0002466	0.0002086	0.0008267	-0.0062647	0.0063264

STRUCTURE BOSSLER COUPLING D8.0 STEEL (RIGID EARS, END SLIPPAGE)

LOADING 2

MEMBER FORCES

MEMBER	JOINT	FORCES			MOMENTS		
		AXIAL	SHEAR Y	SHEAR Z	TORSIONAL	BENDING Y	BENDING Z
1	1	-0.0000003	0.0018390	0.0018390	-0.0000000	-0.0077512	0.0077512
1	2	0.0000003	-0.0018390	-0.0018390	0.0000000	-0.0667290	0.0667290
2	4	0.0036116	-0.0002865	0.0030060	103.6872263	0.0001402	-0.0135070
2	2	-0.0036116	0.0002865	-0.0030060	-103.6872263	-0.1203613	0.0020503
3	2	0.	-0.0006315	-0.0024077	-103.6987839	0.0962954	-0.0126286
3	3	-0.	0.0006315	0.0024077	103.6987839	-0.	-0.0126286
4	4	0.2631422	-1.4225138	0.0623124	-18.9613802	-2.5145898	-54.1672621
4	6	-0.2631422	1.4225138	-0.0623124	18.9613802	-1.0406491	-26.9943962
5	4	-0.2454142	1.4249164	0.0629132	-18.9943142	-2.5172147	54.2124791
5	5	0.2454142	-1.4249164	-0.0629132	18.9943142	-1.0723014	27.0862575
6	3	-0.2605363	-1.4225799	0.0613230	18.9630241	-2.5083511	-54.1680741
6	5	0.2605363	1.4225799	-0.0613230	-18.9630241	-0.9904371	-26.9973531
7	3	0.2432945	1.4250923	0.0624566	18.9957013	-2.5251457	54.2162418
7	6	-0.2432945	-1.4250923	-0.0624566	-18.9957013	-1.0383242	27.0925283
8	6	0.2395056	1.4226840	-0.0620797	18.9672115	1.0233600	26.9975381
8	8	-0.2395056	-1.4226840	0.0620797	-18.9672115	2.5186016	54.1738305
9	5	-0.2613607	-1.4254707	-0.0621988	18.9996507	1.0432607	-27.1003652
9	8	0.2613607	1.4254707	0.0621988	-18.9996507	2.5054961	-54.2299972
10	5	-0.2397913	1.4224061	-0.0629201	-18.9660349	1.0414475	26.9881973
10	7	0.2397913	-1.4224061	0.0629201	18.9660349	2.5484660	54.1673136
11	6	0.2606602	-1.4255872	-0.0617200	-18.9986191	1.0231309	-27.1020141
11	7	-0.2606602	1.4255872	0.0617200	18.9986191	2.4983097	-54.2349944
12	8	0.2634222	-1.4198290	0.0622676	-18.9204290	-2.5060382	-54.1259713
12	10	-0.2634222	1.4198290	-0.0622676	18.9204290	-1.0466465	-26.8825049
13	8	-0.2424816	1.4282941	0.0626813	-19.0443687	-2.5362315	54.2786269
13	9	0.2424816	-1.4282941	-0.0626813	19.0443687	-1.0400540	27.2128243
14	7	-0.2623565	-1.4195343	0.0619995	18.9203076	-2.5011765	-54.1167264
14	9	0.2623565	1.4195343	-0.0619995	-18.9203076	-1.0362108	-26.8749356
15	7	0.2425050	1.4285957	0.0622000	19.0445507	-2.5265086	54.2864566
15	10	-0.2425050	-1.4285957	-0.0622000	-19.0445507	-1.0223175	27.2222009
16	10	0.2389903	1.4199800	-0.0626259	18.9277198	1.0478242	26.8842907
16	12	-0.2389903	-1.4199800	0.0626259	-18.9277198	2.5253000	54.1327991
17	9	-0.2609496	-1.4289331	-0.0618013	19.0492685	1.0155171	-27.2265081
17	12	0.2609496	1.4289331	0.0618013	-19.0492685	2.5105641	-54.3014040
18	9	-0.2387973	1.4197792	-0.0619059	-18.9272366	1.0280232	26.8780718
18	11	0.2387973	-1.4197792	0.0619059	18.9272366	2.5040246	54.1275606
19	10	0.2623978	-1.4290459	-0.0625948	-19.0485895	1.0396776	-27.2293773
19	11	-0.2623978	1.4290459	0.0625948	19.0485895	2.5316746	-54.3049684

STRUCTURE BOSSLER COUPLING D8.0 STEEL (RIGID EARS, END SLIPPAGE)

LOADING 2

JOINT	X FORCE	Y FORCE	Z FORCE	X MOMENT	Y MOMENT	Z MOMENT
		SUPPORT REACTIONS				
11	-0.0122886	-0.0125023	-0.0103642	-0.0000079	73.3971224	73.3436489
12	0.0117621	-0.0115439	-0.0082235	0.0000186	73.3968344	73.3467855
		APPLIED JOINT LOADS				
1	-0.0000003	-0.0018390	0.0018390	-0.0000000	-0.0077512	-0.0077512
2	0.0003454	0.0031133	-0.0082209	0.0240660	-146.7033005	-146.7182579
3	-0.0004074	0.0071155	0.0091732	-0.0000725	-0.0094004	-0.0136933
4	0.0002351	0.0113818	0.0110150	-0.0013469	-0.0123806	-0.0192574
5	0.0002535	0.0031047	0.0034456	0.0914833	0.0178283	-0.0182636
6	-0.0001649	-0.0001028	0.0004624	-0.0061083	0.0014322	-0.0017478
7	0.0004764	0.0002920	0.0013084	-0.0059621	0.0000839	0.0013465
8	-0.0000035	0.0000300	0.0000098	-0.0023435	-0.0006032	-0.0005124
9	-0.0002070	0.0009107	-0.0004305	0.0237616	0.0057387	-0.0049462
10	-0.0000007	0.0000402	-0.0000144	-0.0000108	0.0001040	0.0000640

STRUCTURE BOSSLER COUPLING D8.0 STEEL (RIGID EARS, END SLIPPAGE)

LOADING 2

MEMBER DISTORTIONS

MEMBER	DISTORTIONS			ROTATIONS		
	AXIAL	SHEAR Y	SHEAR Z	TORSIONAL	BENDING Y	BENDING Z
1	0.0000000	0.0000000	0.0000000	0.0000000	-0.0000000	0.0000000
2	-0.0000000	0.0000000	0.0376188	-0.0000399	-0.0009406	0.0000000
3	-0.	0.0000000	0.0000002	0.0000399	-0.0009405	-0.
4	-0.0000315	0.4087414	-0.0004997	0.0072188	0.0000093	0.0071704
5	0.0000294	-0.4087351	-0.0004968	0.0072314	0.0000091	-0.0071581
6	0.0000312	0.4087347	-0.0005038	-0.0072195	0.0000095	0.0071698
7	-0.0000291	-0.4087415	-0.0005026	-0.0072319	0.0000093	-0.0071574
8	-0.0000287	0.0003665	-0.0000332	-0.0072211	0.0000094	0.0071713
9	0.0000313	0.0003847	-0.0000269	-0.0072334	0.0000092	-0.0071590
10	0.0000287	0.0004277	-0.0000321	0.0072206	0.0000095	0.0071720
11	-0.0000312	0.0003762	-0.0000310	0.0072330	0.0000093	-0.0071599
12	-0.0000315	0.4088875	-0.0004969	0.0072032	0.0000092	0.0071890
13	0.0000290	-0.4087652	-0.0005051	0.0072504	0.0000094	-0.0071421
14	0.0000314	0.4088326	-0.0004969	-0.0072032	0.0000092	0.0071886
15	-0.0000290	-0.4087968	-0.0005047	-0.0072505	0.0000094	-0.0071417
16	-0.0000286	0.0012983	-0.0000280	-0.0072060	0.0000093	0.0071903
17	0.0000312	0.0012938	-0.0000342	-0.0072523	0.0000094	-0.0071445
18	0.0000286	0.0013345	-0.0000304	0.0072058	0.0000093	0.0071906
19	-0.0000314	0.0013047	-0.0000307	0.0072520	0.0000094	-0.0071447

STRUCTURE BOSSLER COUPLING D8.0 STEEL (RIGID EARS, END SLIPPAGE)

LOADING 2

JOINT DISPLACEMENTS

JOINT	X DISPLACEMENT	Y DISPLACEMENT	Z DISPLACEMENT	X ROTATION	Y ROTATION	Z ROTATION
		SUPPORT DISPLACEMENTS				
11	-0.	-0.	-0.	0.0009410	-0.	-0.
12	-0.	-0.	-0.	-0.0009410	-0.	-0.
		FREE JOINT DISPLACEMENTS				
1	0.0000503	1.5954604	-1.5884496	0.0000000	-0.0286319	-0.0287492
2	0.0000503	0.4311178	-0.4288582	0.0000000	-0.0286319	-0.0287492
3	0.0033680	0.4311175	-0.4288579	0.0009405	-0.0286037	-0.0287210
4	-0.0032673	0.4311179	-0.4288583	-0.0009406	-0.0286037	-0.0287210
5	-1.2158998	0.2694080	-0.2680305	0.0000010	-0.0214456	-0.0215512
6	1.2159940	0.2694089	-0.2680312	-0.0000009	-0.0214463	-0.0215506
7	0.0026153	0.1078587	-0.1071655	0.0009407	-0.0142864	-0.0143792
8	-0.0025500	0.1078558	-0.1071687	-0.0009408	-0.0142866	-0.0143793
9	-0.4053810	0.0537257	-0.0537230	0.0000030	-0.0071445	-0.0071906
10	0.4054023	0.0537285	-0.0537257	-0.0000030	-0.0071447	-0.0071903

STRUCTURE BOSSLER COUPLING D8.0 STEEL (RIGID EARS, END SLIPPAGE)

LOADING 3

MEMBER FORCES

MEMBER	JOINT	FORCES			MOMENTS		
		AXIAL	SHEAR Y	SHEAR Z	TORSIONAL	BENDING Y	BENDING Z
1	1	-0.0099242	0.0000001	0.0000002	-0.0000000	-0.0000029	0.0000008
1	2	0.0099242	-0.0000001	-0.0000002	0.0000000	-0.0000067	0.0000047
2	4	-30.5089107	-0.0039179	0.0000003	-0.0050579	0.0000000	33.2978072
2	2	30.5089107	0.0039179	-0.0000003	0.0050579	-0.0000121	-33.4545012
3	2	-30.5089142	0.0045303	-0.0000003	0.0016334	0.0000120	33.4577103
3	3	30.5089142	-0.0045303	0.0000003	-0.0016334	-0.	-33.2765255
4	4	11.5697159	-2.1564377	10.3881646	1.3215768	-291.0295982	-60.5423198
4	6	-11.5697159	2.1564377	-10.3881646	-1.3215768	-301.6680870	-62.4934297
5	4	11.5687163	-2.1563703	-10.3877994	-1.3225512	291.0301971	-60.5381880
5	5	-11.5687163	2.1563703	10.3877994	1.3225512	301.6466522	-62.4937172
6	3	11.5683352	2.1561471	-10.3886689	1.3254576	291.0381851	60.5339532
6	5	-11.5683352	-2.1561471	10.3886689	-1.3254576	301.6882706	62.4852157
7	3	11.5679501	2.1563767	10.3882934	-1.3224204	-291.0387955	60.5411644
7	6	-11.5679501	-2.1563767	-10.3882934	1.3224204	-301.6662369	62.4911079
8	6	0.0857771	3.6792860	-0.3984390	1.3341174	6.0125535	103.9912872
8	8	-0.0857771	-3.6792860	0.3984390	-1.3341174	16.7204204	105.9307137
9	5	0.0856838	3.6790141	0.3984375	-1.3305268	-6.0142448	103.9845562
9	8	-0.0856838	-3.6790141	-0.3984375	1.3305268	-16.7186437	105.9219322
10	5	0.0858316	-3.6791093	0.3989512	1.3317402	-6.0222552	-103.9871426
10	7	-0.0858316	3.6791093	-0.3989512	-1.3317402	-16.7399402	-105.9247780
11	6	0.0858471	-3.6791118	-0.3979739	-1.3318016	6.0065777	-103.9856606
11	7	-0.0858471	3.6791118	0.3979739	1.3318016	16.6998620	-105.9264050
12	8	0.0853726	-3.6792508	0.3990339	-1.3325787	-16.7378635	-105.9309101
12	10	-0.0853726	3.6792508	-0.3990339	1.3325787	-6.0290496	-103.9890842
13	8	0.0858238	-3.6790828	-0.3988019	1.3302846	16.7324858	-105.9242191
13	9	-0.0858238	3.6790828	0.3988019	-1.3302846	6.0211909	-103.9861889
14	7	0.0851237	3.6791359	-0.3992557	-1.3310364	16.7413795	105.9241924
14	9	-0.0851237	-3.6791359	0.3992557	1.3310364	6.0381935	103.9892483
15	7	0.0848203	3.6794381	0.3990517	1.3351064	-16.7372317	105.9354668
15	10	-0.0848203	-3.6794381	-0.3990517	-1.3351064	-6.0307004	103.9952145
16	10	11.5757289	2.1555395	-10.3938588	-1.3316959	301.8652344	62.4597659
16	12	-11.5757289	-2.1555395	10.3938588	1.3316959	291.1573334	60.5247397
17	9	11.5756472	2.1552847	10.3938211	1.3350475	-301.8635254	62.4546309
17	12	-11.5756472	-2.1552847	-10.3938211	-1.3350475	-291.1568909	60.5153351
18	9	11.5761217	-2.1554750	10.3938346	-1.3325076	-301.8642693	-62.4618745
18	11	-11.5761217	2.1554750	-10.3938346	1.3325076	-291.1569176	-60.5189500
19	10	11.5762889	-2.1557025	-10.3938261	1.3295255	301.8633957	-62.4659705
19	11	-11.5762889	2.1557025	10.3938261	-1.3295255	291.1573105	-60.5278363

STRUCTURE BOSSLER COUPLING D8.0 STEEL (RIGID EARS, END SLIPPAGE)

LOADING 3

JOINT	X FORCE	Y FORCE	Z FORCE	X MOMENT	Y MOMENT	Z MOMENT
		SUPPORT REACTIONS				
11	-7.3171956	-21.5861552	-21.5862994	-0.	23.5756531	-23.5637589
12	-7.3167094	21.5857522	21.5857425	-0.0000038	-23.5622931	23.5750780
		APPLIED JOINT LOADS				
1	-0.0099242	-0.0000002	0.0000001	-0.0000000	-0.0000008	-0.0000029
2	0.0014759	-0.0000022	-0.0000031	0.0000001	0.0024574	0.0069945
3	7.3209408	0.0002443	0.0002810	-0.0002060	-0.0686994	0.0560865
4	7.3208923	0.0005943	-0.0000223	-0.0007286	0.0432248	-0.0553961
5	0.0003148	-0.0002539	0.0014228	0.0489787	0.0091581	-0.0104322
6	0.0002260	-0.0009688	-0.0010175	0.0081661	-0.0025749	0.0016463
7	0.0001220	0.0007578	-0.0000981	0.0443850	-0.0095720	-0.0087731
8	-0.0000014	-0.0003896	0.0002564	0.0063181	0.0015211	0.0013818
9	-0.0001424	0.0004621	-0.0002503	0.0180283	0.0042291	-0.0038657
10	0.0000016	-0.0000409	-0.0000121	-0.0004349	0.0001397	-0.0000396

STRUCTURE BOSSLER COUPLING D8.0 STEEL (RIGID EARS, END SLIPPAGE)

LOADING 3

MEMBER DISTORTIONS

MEMBER	DISTORTIONS			ROTATIONS		
	AXIAL	SHEAR Y	SHEAR Z	TORSIONAL	BENDING Y	BENDING Z
1	0.0000006	0.0000000	-0.	0.0000000	-0.0000000	0.0000000
2	0.0000452	-0.0000988	0.0000029	0.0000000	-0.0000001	-0.0000049
3	0.0000452	-0.0000990	0.0000000	-0.0000000	-0.0000000	-0.0000049
4	-0.0013852	0.2948482	-0.0373697	-0.0005031	-0.0000668	-0.0005149
5	-0.0013851	0.2948052	0.0373723	0.0005035	0.0000667	-0.0005160
6	-0.0013850	-0.2948053	0.0373696	-0.0005046	0.0000669	0.0005149
7	-0.0013850	-0.2948482	-0.0373722	0.0005035	-0.0000667	0.0005145
8	-0.0000103	-0.5135263	-0.0004123	-0.0005079	0.0000673	0.0005118
9	-0.0000103	-0.5135027	0.0004117	0.0005065	-0.0000672	0.0005112
10	-0.0000103	0.5135144	0.0004121	-0.0005070	-0.0000673	-0.0005113
11	-0.0000103	0.5134914	-0.0004114	0.0005070	0.0000672	-0.0005121
12	-0.0000102	0.5427387	-0.0034276	0.0005073	0.0000673	0.0005124
13	-0.0000103	0.5426860	0.0034272	-0.0005065	-0.0000673	0.0005114
14	-0.0000102	-0.5426704	0.0034274	0.0005067	-0.0000672	-0.0005106
15	-0.0000102	-0.5427538	-0.0034273	-0.0005083	0.0000672	-0.0005120
16	-0.0013859	-0.3239735	0.0412163	0.0005070	-0.0000673	-0.0005106
17	-0.0013859	-0.3239690	-0.0412159	-0.0005083	0.0000672	-0.0005117
18	-0.0013859	0.3240237	-0.0412161	0.0005073	0.0000672	0.0005127
19	-0.0013860	0.3240203	0.0412159	-0.0005062	-0.0000672	0.0005114

STRUCTURE BOSSLER COUPLING D8.0 STEEL (RIGID EARS, END SLIPPAGE)

LOADING 3

JOINT DISPLACEMENTS

JOINT	X DISPLACEMENT	Y DISPLACEMENT	Z DISPLACEMENT	X ROTATION	Y ROTATION	Z ROTATION
		SUPPORT DISPLACEMENTS				
11	0.	0.	0.	0.0000001	0.	0.
12	0.	0.	0.	-0.0000001	0.	0.
		FREE JOINT DISPLACEMENTS				
1	1.6609742	0.0001350	-0.0000845	0.0000000	-0.0000016	-0.0000022
2	1.6609742	0.0000457	-0.0000186	0.0000000	-0.0000016	-0.0000022
3	1.6610895	0.0000776	0.0000134	0.0000000	0.0000019	-0.0000057
4	1.6610568	0.0000137	-0.0000506	-0.0000001	-0.0000051	0.0000013
5	1.3683378	-0.0373448	0.0373675	0.0000000	0.0005109	0.0005092
6	1.3685121	0.0374086	-0.0373860	0.0000000	-0.0005127	-0.0005136
7	0.8304778	0.0339664	0.0339484	0.0000001	-0.0000006	-0.0000021
8	0.8303931	-0.0339370	-0.0339550	-0.0000001	-0.0000003	-0.0000018
9	0.2923959	-0.0373744	0.0373744	0.0000001	-0.0005117	-0.0005127
10	0.2924640	0.0373834	-0.0373834	-0.0000000	0.0005114	0.0005106

STRUCTURE BOSSLER COUPLING D8.0 STEEL (RIGID EARS, END SLIPPAGE)

LOADING 4

MEMBER FORCES

MEMBER	JOINT	FORCES			MOMENTS		
		AXIAL	SHEAR Y	SHEAR Z	TORSIONAL	BENDING Y	BENDING Z
1	1	0.0000000	-0.0000000	0.0000000	-0.0000093	-0.0000004	-0.0000000
1	2	-0.0000000	0.0000000	-0.0000000	0.0000093	-0.0000008	-0.0000001
2	4	-0.0002257	-0.0000023	25.0038054	-0.6289637	0.	-0.0001976
2	2	0.0002257	0.0000023	-25.0038054	0.6289637	-1000.0011749	0.0001037
3	2	-0.0001668	-0.0000023	25.0037894	-0.6289634	-1000.0005341	-0.0001035
3	3	0.0001668	0.0000023	-25.0037894	0.6289634	-0.	0.0000095
4	4	17.7322991	0.0135828	-0.1001961	0.1673537	0.0218422	0.2760508
4	6	-17.7322991	-0.0135828	0.1001961	-0.1673537	5.6948556	0.4989161
5	4	-17.7322659	-0.0135784	-0.1001765	0.1672974	0.0214800	-0.2759663
5	5	17.7322659	0.0135784	0.1001765	-0.1672974	5.6940978	-0.4987526
6	3	17.7322257	-0.0135775	0.1001919	0.1672732	-0.0220492	-0.2759224
6	5	-17.7322257	0.0135775	-0.1001919	-0.1672732	-5.6944082	-0.4987427
7	3	-17.7322395	0.0135814	0.1002084	0.1673292	-0.0223213	0.2759955
7	6	17.7322395	-0.0135814	-0.1002084	-0.1673292	-5.6950784	0.4988948
8	6	-17.6369193	0.0183899	-0.0062818	0.2432783	5.6848089	0.5900008
8	8	17.6369193	-0.0183899	0.0062818	-0.2432783	-5.3264028	0.4592364
9	5	17.6368666	-0.0183993	-0.0062791	0.2433732	5.6847762	-0.5903361
9	8	-17.6368666	0.0183993	0.0062791	-0.2433732	-5.3265214	-0.4594360
10	5	-17.6368318	-0.0183888	0.0062739	0.2432364	-5.6847029	-0.5901377
10	7	17.6368318	0.0183888	-0.0062739	-0.2432364	5.3267444	-0.4590374
11	6	17.6368792	0.0183808	0.0062756	0.2431385	-5.6847216	0.5898407
11	7	-17.6368792	-0.0183808	-0.0062756	-0.2431385	5.3266641	0.4588800
12	8	17.6368988	0.0183883	-0.0063015	0.2432536	-5.3264333	0.4590332
12	10	-17.6368988	-0.0183883	0.0063015	-0.2432536	5.6859660	0.5901156
13	8	-17.6368518	-0.0183658	-0.0062978	0.2429408	-5.3265846	-0.4586131
13	9	17.6368518	0.0183658	0.0062978	-0.2429408	5.6859039	-0.5892484
14	7	17.6368132	-0.0183758	0.0063005	0.2430536	5.3265283	-0.4589767
14	9	-17.6368132	0.0183758	-0.0063005	-0.2430536	-5.6860032	-0.5894549
15	7	-17.6368608	0.0183970	0.0063010	0.2433632	5.3264807	0.4593609
15	10	17.6368608	-0.0183970	-0.0063010	-0.2433632	-5.6859870	0.5902825
16	10	-17.7322853	0.0136042	-0.1002220	0.1676477	5.6959662	0.4989059
16	12	17.7322853	-0.0136042	0.1002220	-0.1676477	0.0222096	0.2772810
17	9	17.7322292	-0.0136277	-0.1002242	0.1679544	5.6960080	-0.4997977
17	12	-17.7322292	0.0136277	0.1002242	-0.1679544	0.0222915	-0.2777336
18	9	-17.7321985	-0.0136074	0.1002217	0.1676777	-5.6959764	-0.4994157
18	11	17.7321985	0.0136074	-0.1002217	-0.1676777	-0.0221828	-0.2769557
19	10	17.7322407	0.0135849	0.1002246	0.1673708	-5.6960808	0.4985556
19	11	-17.7322407	-0.0135849	-0.1002246	-0.1673708	-0.0222450	0.2765343

STRUCTURE BOSSLER COUPLING D8.0 STEEL (RIGID EARS, END SLIPPAGE)

LOADING 4

JOINT	X FORCE	Y FORCE	Z FORCE	X MOMENT	Y MOMENT	Z MOMENT
		SUPPORT REACTIONS				
11	-0.0000279	17.6803412	-17.6803775	-0.0000004	-0.4456730	-0.4457983
12	0.0000307	-17.6804264	17.6803718	-0.0000005	0.4468461	0.4467082
		APPLIED JOINT LOADS				
1	0.0000000	-0.0000000	-0.0000000	-0.0000093	0.0000000	-0.0000004
2	-0.0000000	0.0000527	0.0000308	2000.0016937	0.0000002	-0.0000005
3	-0.0000003	0.0001181	0.0001157	-0.0000014	0.0000220	0.0000172
4	0.0000024	-0.0001294	-0.0001761	0.0010442	0.0001342	-0.0001642
5	-0.0000015	0.0000358	0.0000196	0.0011242	0.0002304	-0.0002128
6	-0.0000028	0.0000127	0.0000125	-0.0002805	0.0000741	-0.0000735
7	0.0000006	-0.0000057	0.0000110	-0.0003904	0.0000817	0.0000818
8	-0.0000000	-0.0000016	-0.0000009	0.0000330	0.0000238	-0.0000074
9	-0.0000011	-0.0000046	-0.0000063	0.0001378	0.0000305	-0.0000264
10	-0.0000003	0.0000064	-0.0000005	-0.0000081	0.0000027	-0.0000030

STRUCTURE BOSSLER COUPLING D8.0 STEEL (RIGID EARS, END SLIPPAGE)

LOADING 4

MEMBER DISTORTIONS

MEMBER	DISTORTIONS			ROTATIONS		
	AXIAL	SHEAR Y	SHEAR Z	TORSIONAL	BENDING Y	BENDING Z
1	-0.0000000	-0.0000000	-0.	0.0000000	-0.0000000	-0.0000000
2	0.0000000	0.0000000	0.0010643	0.0000002	-0.0000784	0.0000000
3	0.0000000	0.0000000	-0.0020712	0.0000002	0.0000784	0.0000000
4	-0.0021230	-0.0002720	-0.0006377	-0.0000637	0.0000356	0.0000588
5	0.0021230	0.0002719	-0.0006377	-0.0000637	0.0000356	-0.0000588
6	-0.0021230	0.0002716	0.0006376	-0.0000637	-0.0000356	-0.0000588
7	0.0021230	-0.0002715	0.0006376	-0.0000637	-0.0000356	0.0000588
8	0.0021116	-0.0036241	0.0019968	-0.0000926	-0.0000692	-0.0000345
9	-0.0021116	0.0036264	0.0019969	-0.0000926	-0.0000692	0.0000345
10	0.0021116	0.0036264	-0.0019969	-0.0000926	0.0000692	0.0000346
11	-0.0021116	-0.0036242	-0.0019969	-0.0000926	0.0000692	-0.0000346
12	-0.0021116	-0.0016527	-0.0019495	-0.0000926	0.0000692	0.0000346
13	0.0021116	0.0016528	-0.0019495	-0.0000925	0.0000692	-0.0000345
14	-0.0021116	0.0016554	0.0019495	-0.0000925	-0.0000692	-0.0000344
15	0.0021116	-0.0016552	0.0019495	-0.0000926	-0.0000692	0.0000345
16	0.0021230	-0.0036211	0.0013956	-0.0000638	-0.0000356	-0.0000585
17	-0.0021230	0.0036278	0.0013956	-0.0000639	-0.0000356	0.0000586
18	0.0021230	0.0036279	-0.0013956	-0.0000638	0.0000356	0.0000587
19	-0.0021230	-0.0036213	-0.0013956	-0.0000637	0.0000356	-0.0000586

STRUCTURE BOSSLER COUPLING D8.0 STEEL (RIGID EARS, END SLIPPAGE)

LOADING 4

JOINT DISPLACEMENTS

JOINT	X DISPLACEMENT	Y DISPLACEMENT	Z DISPLACEMENT	X ROTATION	Y ROTATION	Z ROTATION
		SUPPORT DISPLACEMENTS				
11	0.	0.	0.	0.0000266	0.	0.
12	0.	0.	0.	0.0000266	0.	0.
		FREE JOINT DISPLACEMENTS				
1	-0.0000001	0.0000148	0.0000026	0.0003539	0.0000000	-0.0000002
2	-0.0000001	0.0000051	0.0000006	0.0003539	0.0000000	-0.0000002
3	0.0000081	-0.0085382	0.0085439	0.0002755	0.0000002	-0.0000001
4	-0.0000084	0.0085464	-0.0085427	0.0002755	-0.0000001	-0.0000004
5	-0.0000057	-0.0063985	-0.0064015	0.0002318	0.0000587	-0.0000589
6	0.0000054	0.0064049	0.0064019	0.0002318	-0.0000586	0.0000584
7	0.0000064	-0.0042700	0.0042717	0.0001510	-0.0000240	-0.0000243
8	-0.0000066	0.0042733	-0.0042715	0.0001510	0.0000241	0.0000239
9	-0.0000029	-0.0021412	-0.0021420	0.0000703	0.0000586	-0.0000587
10	0.0000028	0.0021420	0.0021412	0.0000703	-0.0000586	0.0000585

PROBLEM COMPLETED.

Conclusions.- Bossler couplings can be analyzed using STRESS. Results from tests reported in following sections show that STRESS is in reasonably good agreement with misalignment test results and in fair agreement with axial test results. The degree of agreement can be improved by using experimentally determined, non-uniform properties which take into account effective length lost in the clamp-up at the joints.

The use of STRESS for the analysis of non-symmetrical couplings is justified. This conclusion can be reached from the work herein because the STRESS program solved the present examples as if they were non-symmetrical structures.

TORQUE TESTS

Introduction.- This section presents and evaluates ultimate torque tests of Bossler couplings. Four topics are covered.

(1) description of tests and presentation of test results;

(2) prediction of critical buckling torques from pre-buckled deflection data;

(3) development of an empirical relationship, Equation (2), to predict torsional strength from coupling dimensions and material properties;

(4) comparison of observed torsional stiffness with theoretical stiffness, Equation (3).

Test Conditions.- A simple rig was made to apply pure torque to single coupling specimens. The rig is shown schematically in the following sketch.

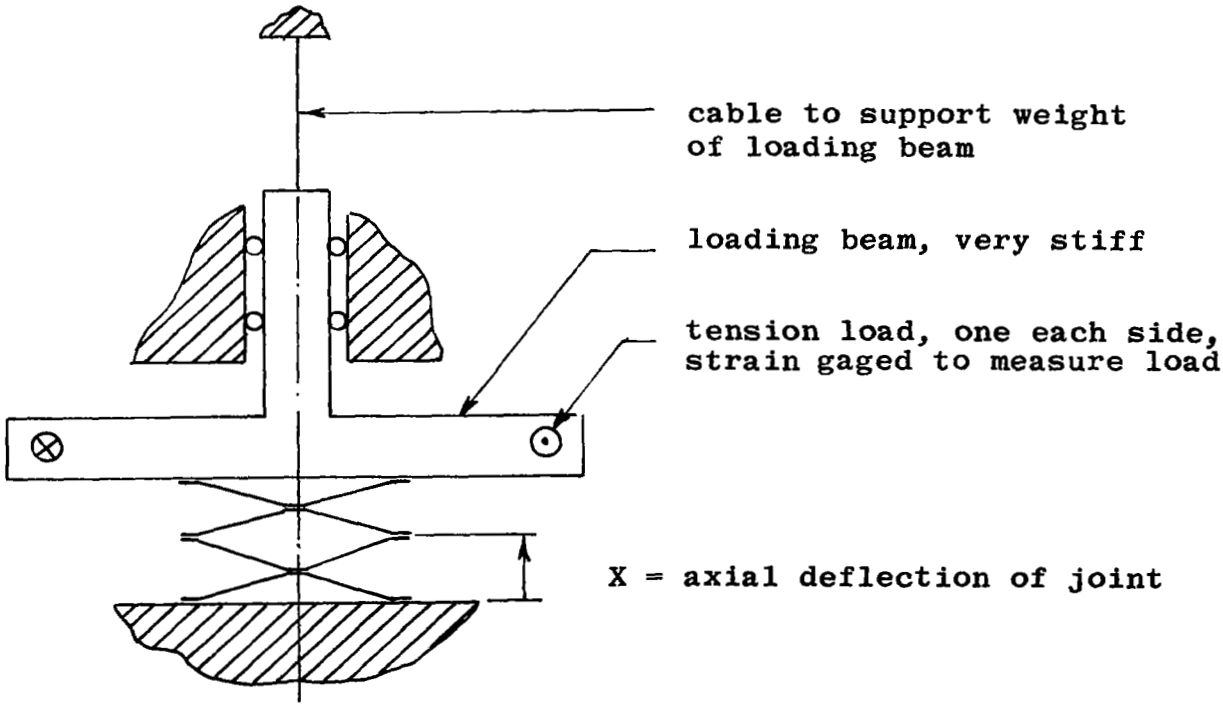

Rotation of the coupling was measured with dial indicators at a radius of 12.4 inches. The dial indicators had a least reading of .001 inches, thus providing a minimum reading of coupling rotation of .0046 degrees. Axial deflections X of joints were measured with dial indicators with a least reading of .0001 inches.

Test Specimens.- Two types of coupling were tested. They differed in size and material. The test variables for each type was the number of plates. The properties for each specimen type are shown below. A total of six couplings were tested.

	Type I	II	
Material	Steel*	Aluminum**	
E	27000	10500	ksi
σ yield	300	45	ksi
d	4.50	8.00	inches
S	.50	.75	inches
b	.56	1.06	inches
t	.084	.16	inches
n	4,6	2,4,4,6	

* nickel maraging steel, Grade 300, aged 3 hours at 900°F
** aluminum alloy 2024-T3, QQ-A-250/5.

Test Results.- Figure 8 shows curves of torque versus rotation for all tests. Table 1 lists axial deflection data for all three tests of Type II couplings. Instability limited the torque capacity of the couplings. The instability was characterized by axial motions of interior joints. The cusps in the curves shown in Figure 8 correspond to axial motions so large as to permit contact between bolt heads. It is apparent from the shape of the curves that stability was increased after the bolts contacted. The final mode of failure was an inelastic buckling of a compression element.

The curve for the test of a Type I coupling with n = 4 is particularly informative. In this test the torque was cycled twice before the final test to failure. The curve shows that the behavior was elastic for the first load cycle, and very nearly so for the second cycle. The slight permanent rotation which remained after the second load application is attributed to seating in the bolted connections or slight inelastic behavior. The cause for the hysteresis shown in the curves is not known definitely; it is attributed tentatively to friction in the joints.

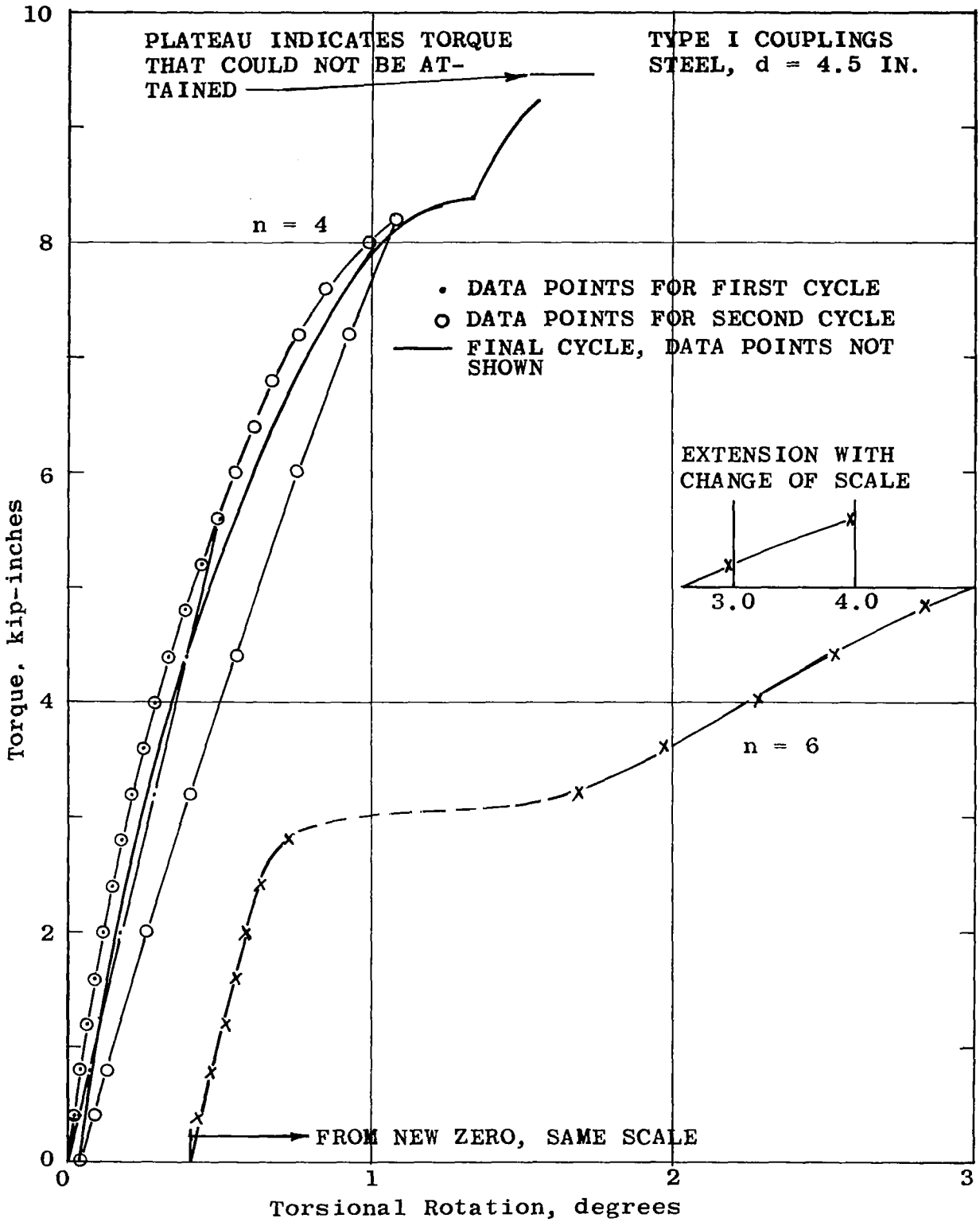

Figure 8. Torque-Rotation Curves (Pg. 1 of 2)

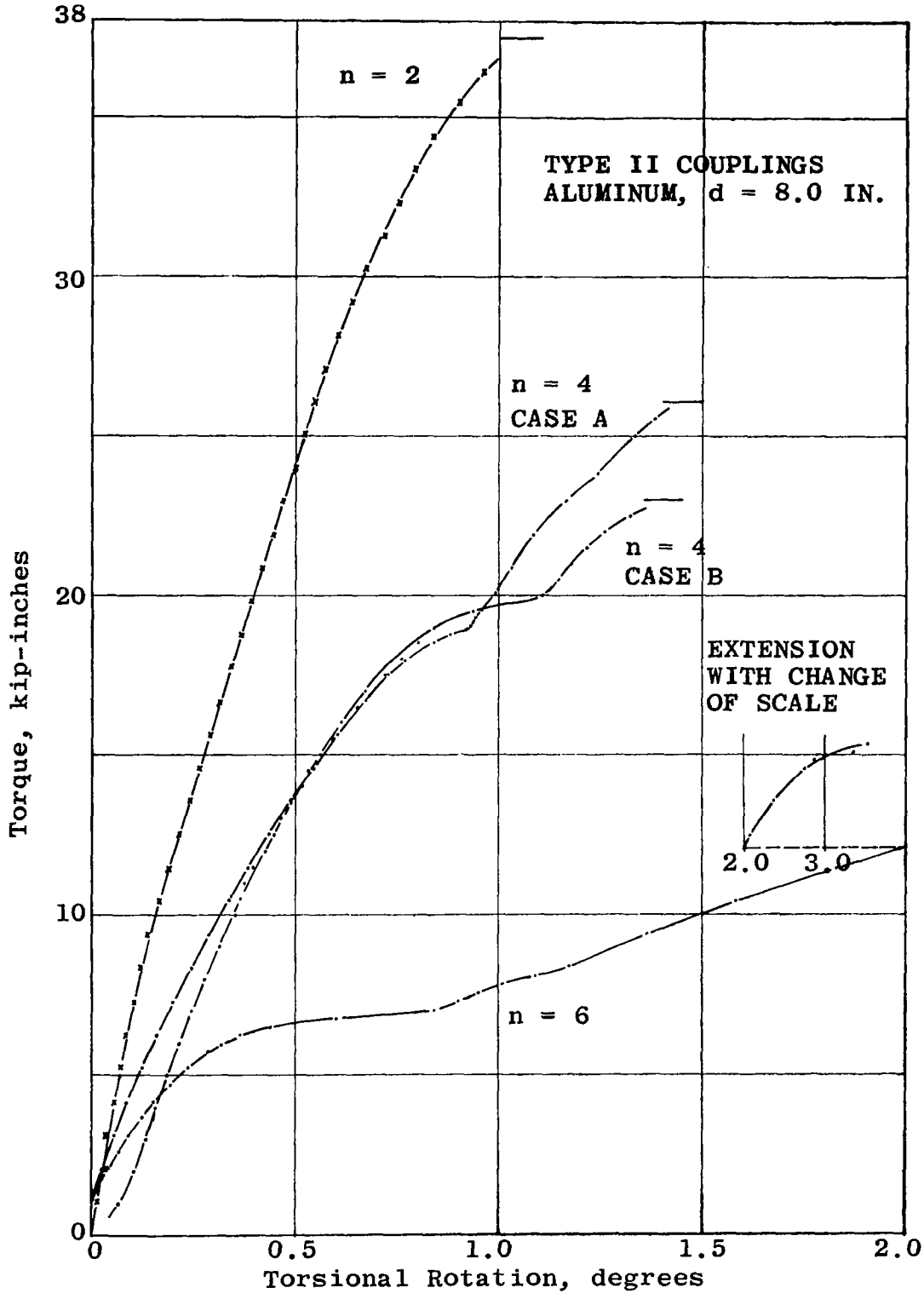

Figure 8. Torque-Rotation Curves (Pg. 2 of 2)

TABLE 1

TORQUE VERSUS AXIAL DEFLECTION

These data are simultaneous readings of torque and axial deflection at the interior joint which experienced the largest deflection during the tests of Type II couplings.

T = Torque, kip-inches
X = Axial Deflection, Inches^{-4}

For n = 2

.96T	X	.96T	X	.96T	X	.96T	X
1.	10	10.	22	19.	77	28.	198
2.	0	11.	26	20.	85	29.	228
3.	0	12.	40	21.	93	30.	285
4.	0	13.	49	22.	108	31.	318
5.	0	14.	52	23.	115	32.	358
6.	0	15.	52	24.	125	33.	407
7.	2	16.	52	25.	136	34.	471
8.	2	17.	64	26.	154	35.	616
9.	2	18.	74	27.	178		

For n = 4, Case A

.96T	X	.96T	X	.96T	X	.96T	X
1.00	0	9.00	91	13.50	438	16.25	1066
2.00	-5	10.00	126	14.00	627	16.40	1136
3.00	-12	10.50	147	14.50	706	16.75	1206
4.00	-10	11.00	186	15.00	786	17.00	1286
5.00	0	11.50	226	15.25	836	17.25	1392
6.00	9	12.00	277	15.50	887	17.50	1536
7.00	31	12.50	326	15.75	936	17.75	1646
8.00	61	13.00	386	16.00	997	18.00	1826

For n = 6

.96T	X	.96T	X	.96T	X	.96T	X
1.00	0	2.50	59	4.00	228	5.50	680
1.25	3	2.75	90	4.25	282	5.75	820
1.50	9	3.00	104	4.50	339	6.00	1008
1.75	17	3.25	128	4.75	416	6.25	1287
2.00	34	3.50	159	5.00	486	6.50	1834
2.25	39	3.75	194	5.25	568		

Southwell-Lundquist Plots.- Reference* 4 presents a method for determining the elastic stability load from simultaneous readings of load and deflection. The method has both theoretical and practical importance because it permits the critical load to be determined from non-destructive tests. Briefly summarized, the method consists of plotting $(X-X_1)$ versus $(X-X_1)/(T-T_1)$, where X and T are readings of deflection and load, respectively. X_1 and T_1 are initial readings which may correspond to any load less than the critical load. For columns the points so plotted will lie on a straight line**. The critical load is the slope of the line plus T_1.

The method was applied to the readings given in Table 1. The results are plotted in Figure 9. In general, the deflection readings at low torque levels were small and erratic making it necessary to use relatively large values for initial readings, X_1 and T_1. Results are shown for several choices for initial readings.

Lines connecting the points show a characteristic sharp bend which divides each line into two segments, each of which is nearly a straight line. The gradual bend in the line at large deflections is attributed to inelastic behavior. In the test with n = 2, inelastic behavior appears to have begun even in the first line segments.

The critical buckling torques deduced from the initial slopes of these lines are listed in Figure 9. It was found that the deduced buckling torques correspond approximately to the cusps in the torque rotation curves.

---

* Herein, the ordinates and abscissa are reversed from those in Reference 4 so that the slope of the line varies directly as the critical load.

** Reference 5 gives recent information regarding the effect of geometric nonlinearities on the shape of the line.

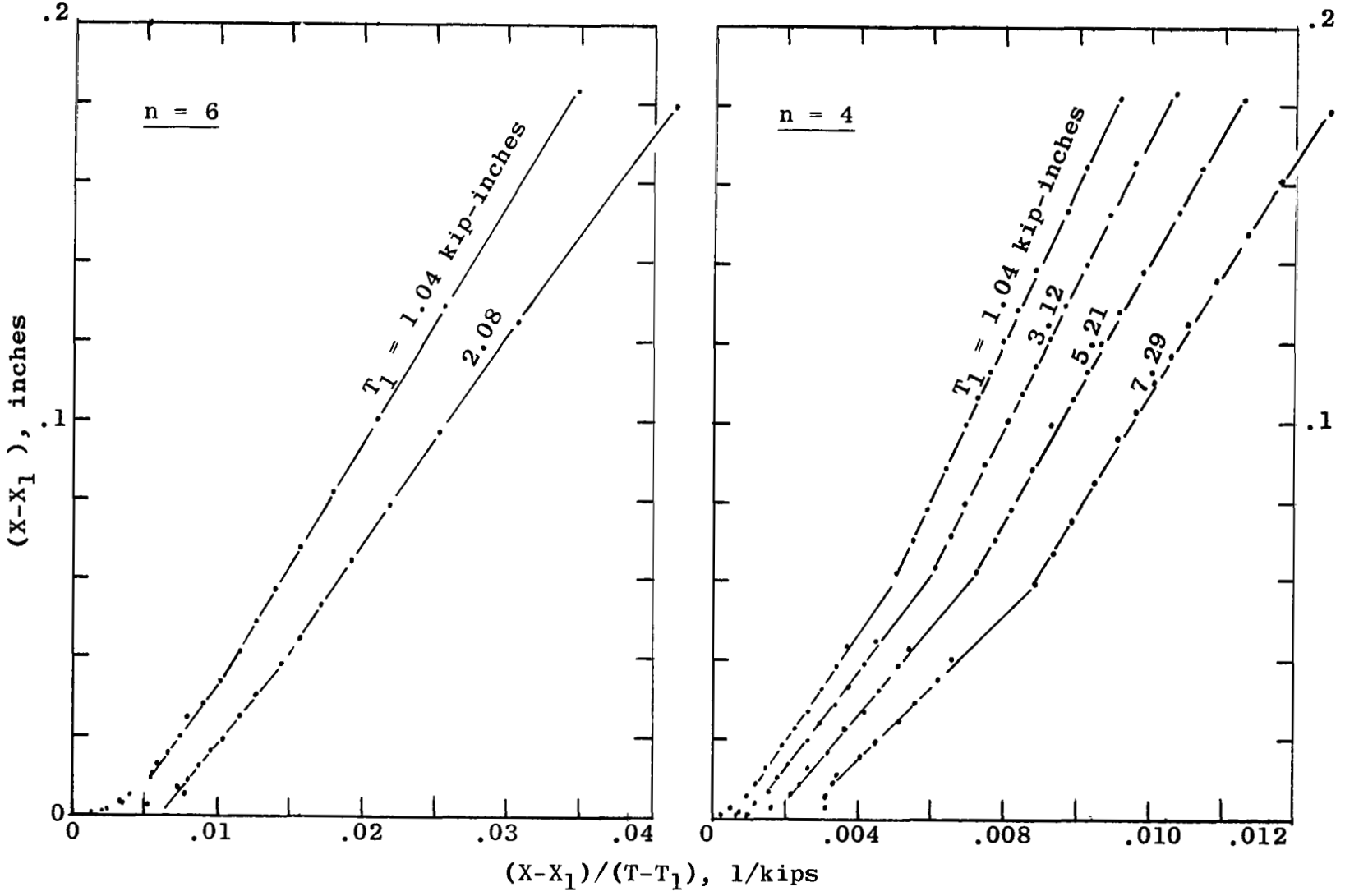

Figure 9. Southwell-Lundquist Plots (Pg. 1 of 2)

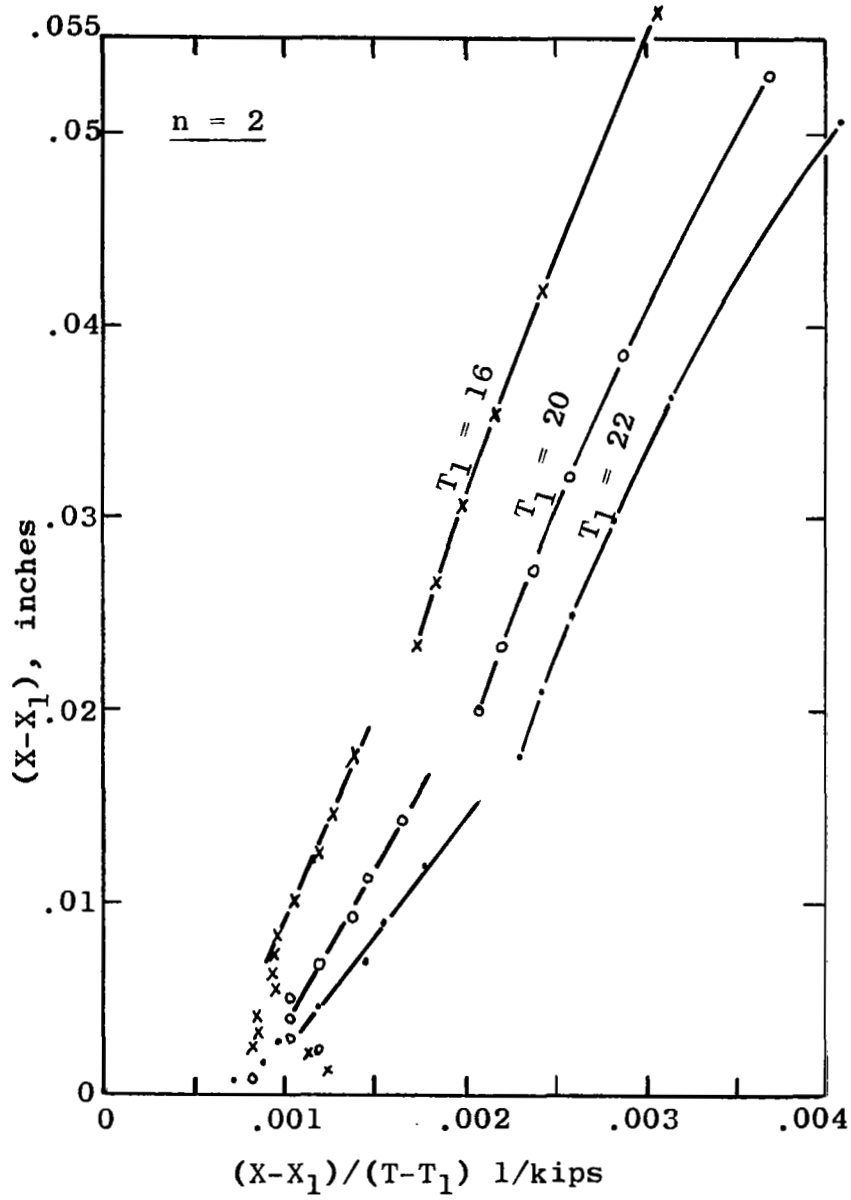

SUMMARY

n	T_1	Critical Torque From Plots, kip-inches	
		First	Second
6	1.04	6.6	7.8
	2.08	7.0	8.1
	*	7.0	8.2
4	1.04	15.8	22.9
	3.12	16.4	23.6
	5.21	17.3	23.4
	7.29	17.2	24.3
	*	19.0	25.5
2	16.7	37.5	50.5
	20.8	38.5	50.5
	22.9	35.9	53.1
	*	36.5	

* First cusp, Second cusp, or maximum torque from Figure 8. Included here to facilitate comparisons.

Figure 9. Southwell-Lundquist Plots (Pg. 2 of 2)

Equation for Torsional Strength.- An equation (Equation 2) for torsional strength of a coupling was developed from a consideration of a single element. The element was idealized as a simple strut with elastic constraints at each end, as shown in the following sketch.

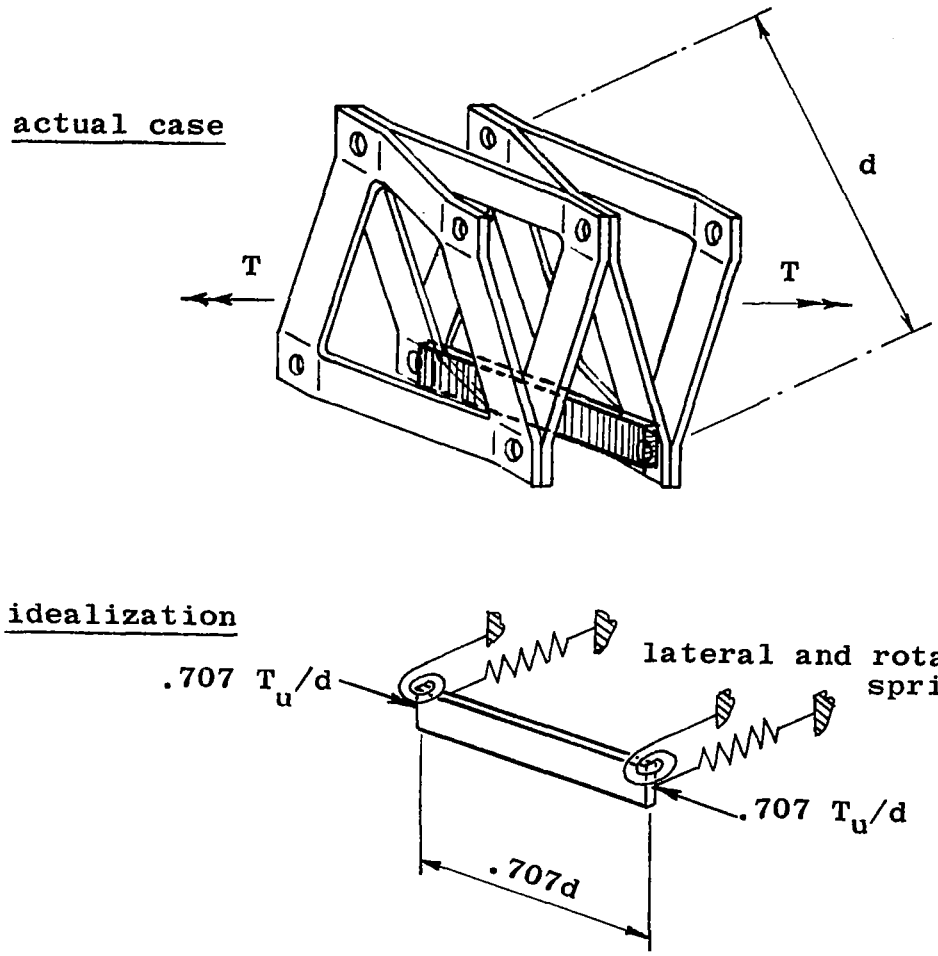

Typically, the elements are slender enough to fail by elastic instability. The Euler buckling load for the element limits the torque. Letting α = the fixity coefficient which accounts for end restraint, Euler's formula becomes, for the coupling:

$$.707\ T_u/d = \alpha\ \pi^2 EI/(.707\ d)^2$$

$$T_u = 2.3267\ \alpha\ bt^3E/d$$

The above equation could be used to calculate the torsional strength if α were known.

An empirical value for α was determined from the test data for Type II specimens, aluminum with d = 8 inches. The value $\alpha = 5.0\ n^{-.9}$ fits the test data reasonably well as shown by Figure 10.

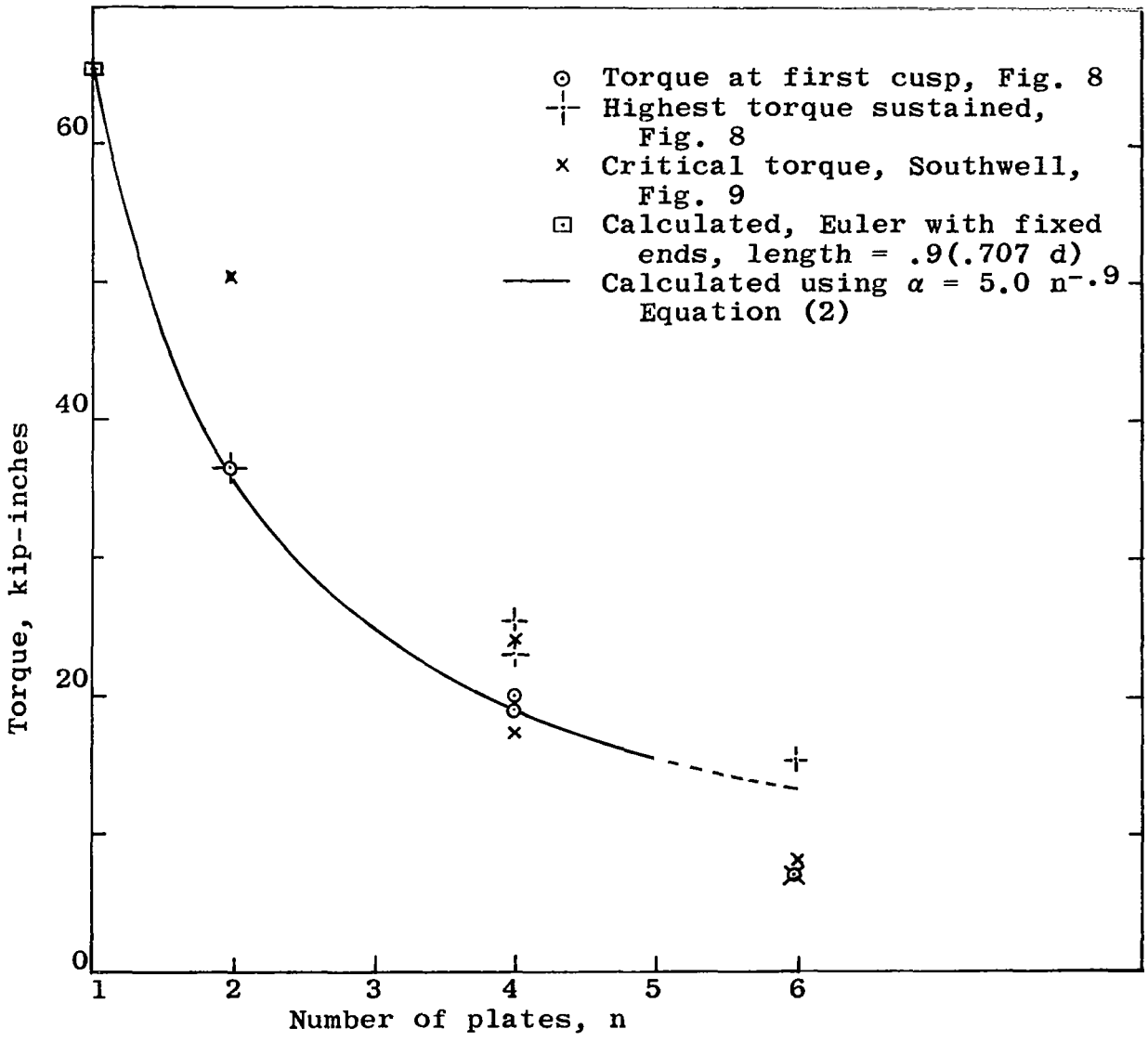

Figure 10. First and Terminal Buckling Torque versus Number of Plates

A check on the form of Equation (2) can be provided by a comparison of the results of Type I and Type II specimens. According to Equation (2), the ratio of critical torque between Type I and Type II specimens with the same n should be:

$$\frac{bt^3E/d,\ \text{Type I}}{bt^3E/d,\ \text{Type II}} = .349$$

The following comparison shows that .349 T_{crit} from Type II tests is in reasonable agreement with observed T_{crit}'s for Type I specimens.

	n = 4*		n = 6	
	$T_{first\ cusp}$	T_{max}	$T_{first\ cusp}$	T_{max}
Type II	19.5	24.0	7.0	15.3
.349 X Type II	6.8	8.4	2.4	5.3
Type I	8.4	9.2	3.0	5.6

* Average of two tests for Type II

Torsional Stiffness.- Experimental torsional stiffnesses were calculated from the slopes of tangents drawn to the curves shown in Figure 8, using the equation:

$$(JG)_c = \text{slope X } 57.3\ nS, \text{ experimental.}$$

Theoretical stiffnesses were calculated using the equation developed on Page 4.

$$(JG)_c = .707\ btdES, \text{ theoretical.}$$

The experimental and theoretical values are compared below. The units of $(JG)_c$ are kip inches/radian.

Specimen Type	I		II		
$(JG)_c$ theoretical	2020		7550		
n	4	6	2	4(A)	6

Zero Torque

$(JG)_c$ experimental	2090	1750	6880	6450	8200
experimental/theoretical	1.03	.87	.91	.85	1.09

Normal Operating Torque*

$(JG)_c$ experimental	1490	1750	3870	3990	5520
experimental/theoretical	.74	.86	.51	.53	.73

* It was assumed that the normal operating torque is one-third of the torque corresponding to the first cusp in the moment-rotation curve.

The comparison shows that at zero torque the experimental stiffness was approximately equal to the theoretical stiffness. At normal operating torque the experimental stiffness was roughly 40% lower. The recommended equation for torsional stiffness (Equation 3) assumes that the stiffness is 60% of the theoretical stiffness.

Conclusions.- The following conclusions can be drawn from the results of the ultimate torque tests.

(1) The coupling has high torque strength and stiffness, making it quite suitable for power transmission applications.

(2) Equations (2) and (3) provide reasonable estimates of the torque strength and stiffness, respectively.

(3) Torsional strength can be estimated from pre-buckled deflection data obtained in non-destructive tests.

(4) Additional tests are recommended to refine the torsional strength equation (Equation 2). The improved equation should be applicable to couplings with rectangular planform and should include the parameters (S/d) and (nS/length of the center shaft).

STIFFNESS TESTS, FLEXURAL AND AXIAL

Introduction.- The designer must know the stiffness of the couplings in order to calculate critical speeds and bearing loads induced by shaft misalignments or axial deformation. This section contains data from flexural and axial stiffness tests, and makes comparisons of the data to calculated results from Equations (10) and (20) and results from the computer program STRESS. Equations (10) and (20) are in good agreement with observed behavior.

Torsional stiffness data are not reported here; they are presented in the section on Torque Tests.

Test Apparatus.- In all stiffness tests, the coupling was bolted to a very stiff horizontal bench. A stiff cross made from steel channel sections was bolted to the free end of the coupling. Static loads were applied to the cross with dead weights. Angular rotations of the cross were detected using two dial indicators spaced 22 inches apart. The dial indicators have a least reading of .001 inches, giving a minimum reading of angular measurement of 0.000045 radians.

Test Specimens.- A 4-plate steel coupling with d = 8 inches was used for flexural stiffness and axial stiffness tests. The bolts that attached the coupling to the bench and to the cross were 7/16 inches in diameter. The bolts that fastened coupling plates together were 3/8 inches in diameter. In two tests reported herein, 3/4 inch diameter stand-off washers were used between the coupling and the bench and between the coupling and the cross. In one reported test, no washers were used.

Steel couplings with d = 4.5 inches were used for additional axial stiffness tests. All bolts were 1/4 inch in diameter. The number of plates varied from 1 to 6.

Other dimensions of the plates and couplings are given in the discussion parts of this section, where they are used in appropriate calculations.

Flexural Test Results.- Moment-Rotation curves are shown on Figure 11 for two tests. Both tests used washers between the coupling and the bench and between the coupling and the loading cross. A moment-rotation curve for the same coupling without washers is given on Figure 12. The curve with washers is also shown for comparison.

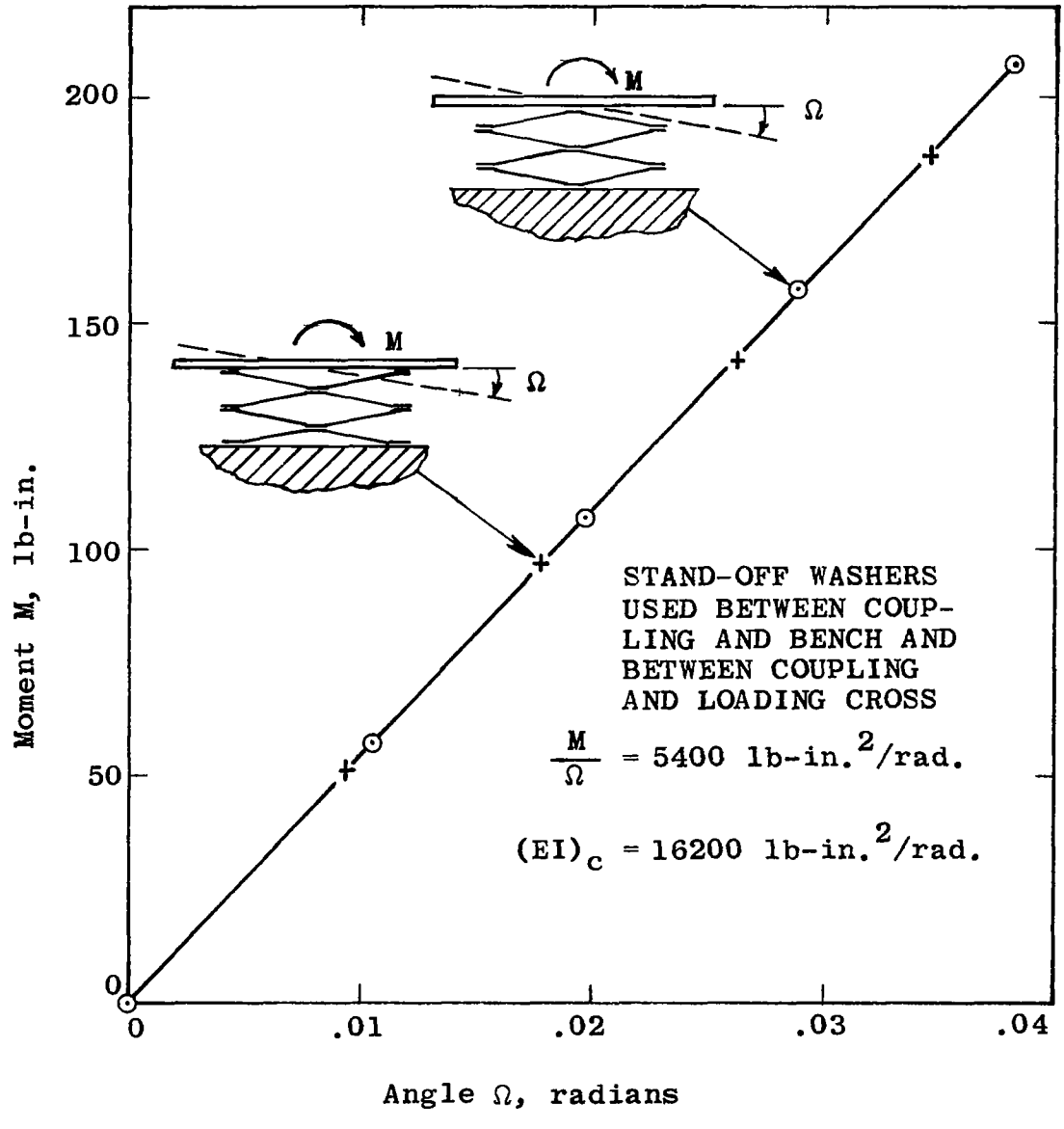

Figure 11. Experimental Moment-Rotation Curves

Flexural Test Discussion.- Consider the two tests shown in Figure 11. The moment in one test lies in the plane of the mounting bolts, and in the other test, in the plane of the non-mounting bolts. The planes are mutually perpendicular. The moment-angle curves coincide for both loading cases, producing a single moment-angle curve. The moment-angle curve is linear, therefore, the structure is elastic. Vector addition of moments and rotations may be used with rigor. A moment applied in any plane between the cases tested may be broken into components that lie in the planes tested. The component moments would cause proportional component rotations in the planes tested. The component rotations could be combined vectorially to find the resultant rotation in the plane of the applied moment. It will be seen that the resultant rotation is identical to the rotation that would occur if the applied moment were in either of the two test planes. It follows, therefore, that when the coupling is rotated while angularly misaligned, the applied moment will be constant in magnitude.

The computer program STRESS calculated deflections and rotations for moments in the planes shown in Figure 11. The program allowed free rotation of the plates about the axes of the mounting bolts, thus simulating free slippage of the stand-off washers. The computer results are shown in the Computer Analysis Section of this report. From these results, the flexural stiffnesses are calculated to be 15,610 and 15,355 pound-inches^2/radian. The stiffnesses differ by only 1.7%. STRESS confirms constant flexural stiffness for any direction of bending. The flexural stiffness from STRESS is different from the flexural stiffness from test because STRESS uses an element length, L = .707 d, which is the distance from bolt center to bolt center. The effective element length, L, is less than .707 d because of clamp-up at the joints.

The effective length of an element, L, can be determined from the flexural stiffness tests shown in Figure 11. From experiment, M/Ω = 5400 pound-inches^2/radian. For a four-plate coupling with a length of 4S, or 3 inches,

$$(EI)_c = (5400)(3) = 16,200 \text{ pound-inch}^2/\text{radian}$$

From Equation (10),

$$(EI)_c = .886 \frac{Ebt^3S}{L}$$

$$(L)(16,200) = (.886)(27\text{x}10^6)(1.0695)(.165)^3 \text{ x } .75$$

$$L = 5.321 \text{ inches}$$

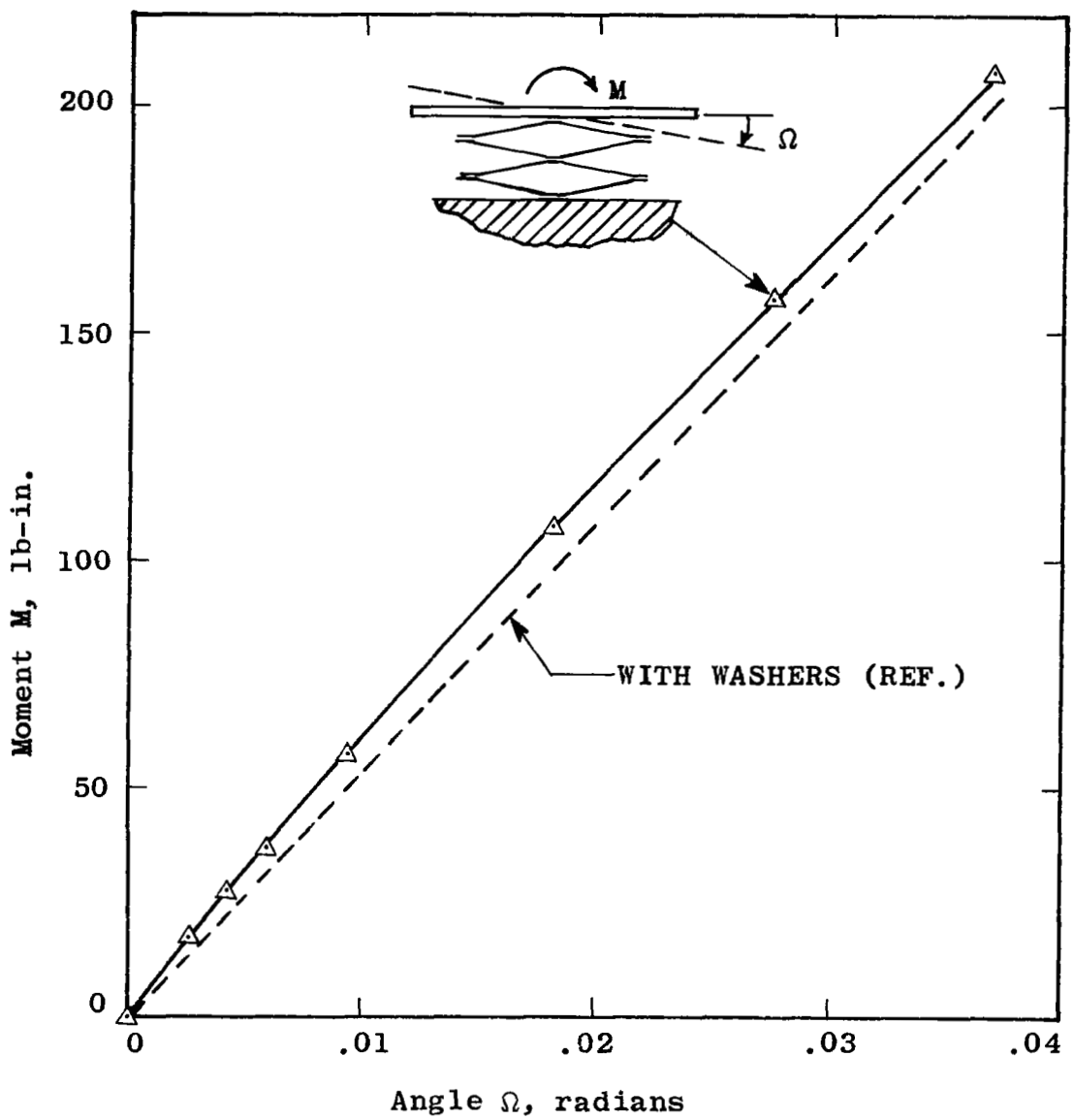

Figure 12. Experimental Moment-Rotation Curve, No Stand-Off Washers Used

It is noted that L is proportional to d. For the coupling tested, d = 8 inches. Therefore L = .665d. For convenience in design calculations, use

$$L = \frac{2}{3} d.$$

In a third test shown on Figure 12, stand-off washers were not used. For the direction of applied moment shown in Figure 12, the contact areas of the coupling end-plate attempt to rotate slightly about the axes of the mounting bolts. Friction over the broad contact area at the mounting bolts allows appreciable moments to be developed about the axes of the mounting bolts. These rotations do not occur when the direction of applied moment is perpendicular to the direction shown. The structure will have stiffness in the one plane that is different from the stiffness in a perpendicular plane. When the coupling is rotated while angularly misaligned, the applied moment will not be constant in magnitude.

It is important to note that a coupling with an odd number of plates has constant flexural stiffness for any direction of bending. The two directions of moment application shown in Figure 11 merely reverse the direction from which the structure is viewed. The rotations about the mounting bolts, although present, would be equal for each case, resulting in a structure that will always have constant stiffness.

The amplitude of the rotations about the mounting-bolts of the case shown in Figure 11 was examined by the computer program STRESS. The amplitude was found to be 2.32% of the angular misalignment of the 4-plate coupling, or 9.3% of the angular misalignment of each plate. The computer program STRESS then analyzed a different case using a single plate, finding that the amplitude of the in-plane rotation was 9.3% of the angular misalignment of the plate. The 9.3% amplitude was for a ratio of plate offset to plate diameter (S/d) of .0938. The computer program STRESS determined the amplitude of the in-plane rotation when S was cut in half and d remained constant, for an S/d ratio of .0469. The amplitude of the in-plane rotation was found to be 4.6% of the misalignment per plate. Thus, the amplitude is linearly inversely proportional to the ratio of plate offset to plate diameter, S/d.

Axial Test Results.- A force-deflection curve is shown in Figure 13 for a test of a steel four-plate coupling with d = 8 inches. Additional force-deflection curves are shown on Figure 14 for six tests of steel couplings with d = 4.5 inches.

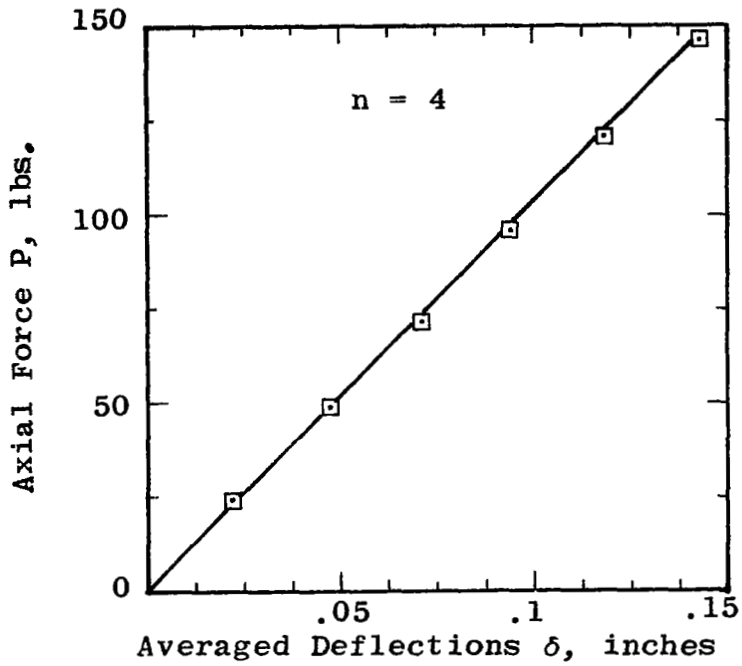

Figure 13. Experimental Axial Deflection Curve, d = 8

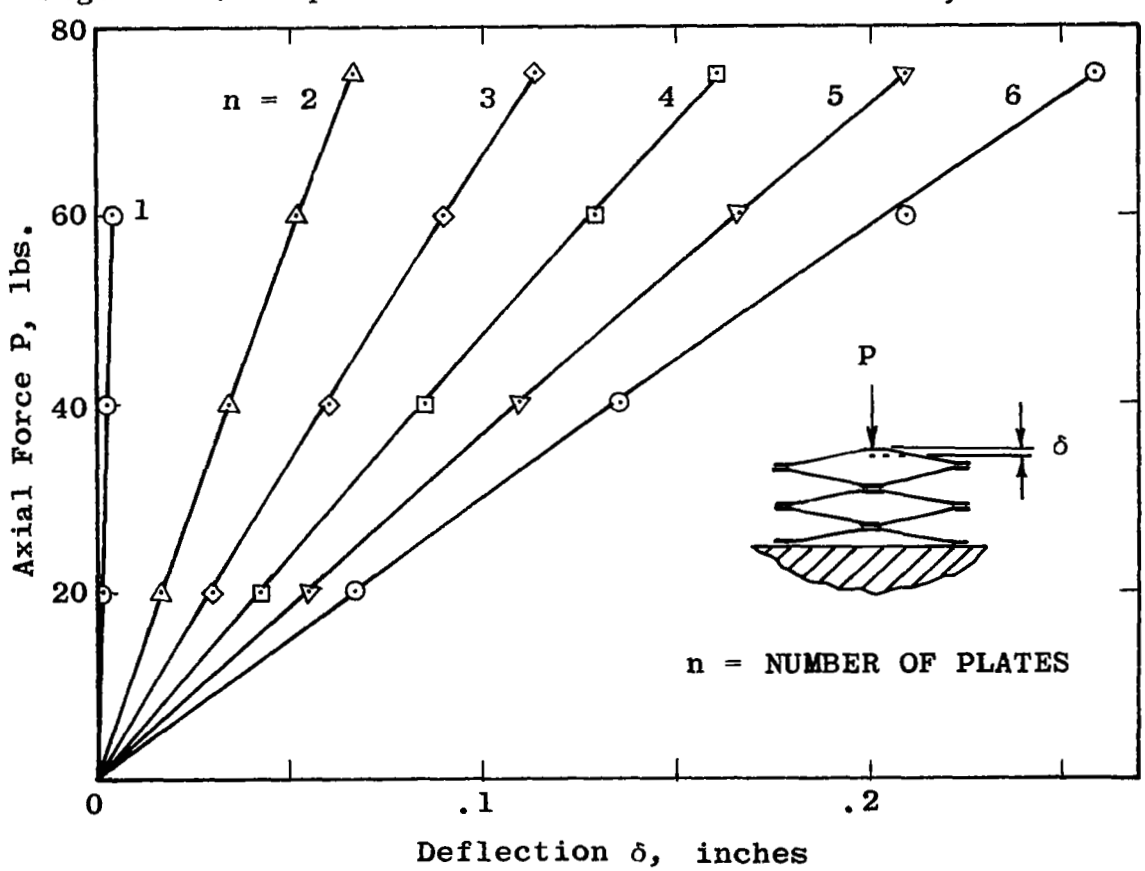

Figure 14. Experimental Axial Deflection Curves, d = 4.5

Axial Test Discussion.- The experimental axial deflection curve of Figure 13 shows a spring rate of 1025 pounds/inch. Equation (20) states:

$$(Ka)_c = \frac{48EI}{L^3} \quad \frac{1}{n-2 + \frac{2}{1.679(Sb/dt)^2 + 1}}$$

for this test specimen, $E = 27 \times 10^6$, $n = 4$, $S = .75$, $b = 1.0695$, $d = 8$, $t = .165$. Using $L = 2d/3$, $(Ka)_c = 1095$ pounds/inch by theory.

The agreement shown between theory and test (difference of 7%) is considered adequate confirmation of Equation (20) and of the approximation, $L = 2d/3$. The computer program STRESS calculated $(Ka)_c = 881$ pounds/inch using $L = .707\ d$. The error (16.3%) is large.

The experimental axial deflection curves of Figure 14 are slightly nonlinear, showing that compression changes the dimensions that affect spring rate. The initial spring-rates were selected for comparison with calculated spring-rates using Equation (20) and STRESS. The comparison is shown in Table 2.

Equation (20) was solved for the test cases of Figure 14, where $E = 27 \times 10^6$, $S = .5$, $b = .56$, $d = 4.5$, $t = .084$ and $n = 2,3,4,5,6$. The value of $L = 2d/3$ was used. The calculated values of $(Ka)_c$ are shown in Table 2.

The computer program STRESS calculated $(Ka)_c$ using $L = .707\ d$. The results are also shown in Table 2.

TABLE 2

AXIAL STIFFNESS SUMMARY, d = 4.5

n	Axial Stiffness $(Ka)_c$ Test	Eq. (20) $L = .667\ d$	STRESS $L = .707\ d$
1	20,000	-	-
2	1215	1275	1071
3	680	651	542
4	475	437	363
5	365	329	272
6	290	263	218

The difference in % error between test and calculated stiffness is given in Table 3.

TABLE 3

PERCENT ERROR IN STIFFNESS PREDICTION, d = 4.5

n	Test	Eq. (20) L = .667 d	STRESS L = .707 d
2	0%	4.9%	-11.9%
3	0	-4.3	-20.3
4	0	-8.0	-23.6
5	0	-9.9	-25.5
6	0	-9.3	-24.8

It is apparent that the test results and Equation (20) produce results that are in good agreement (error less than ±10%). The computer program STRESS predicts too soft spring-rates because the theoretical distance from bolt-center to bolt-center, L = .707 d, does not consider clamp-up at the joints. STRESS must use a modified L to produce more accurate results.

Conclusions.-

(1) Equations (10) and (20) are substantiated for calculating flexural and axial stiffness.

(2) The accuracy of the computer program STRESS can be improved by using an experimentally-determined effective element-length.

(3) Stand-off washers are needed between the coupling and its mounts to relieve frictional moments about the axes of the mounting bolts.

(4) The frictional moments about the axes of the mounting bolts can be controlled by changes in misalignment per plate, plate offset, plate diameter, and stand-off washer diameter.

(5) A coupling with an even number of plates has constant flexural stiffness for any direction of bending if stand-off washers are used between the coupling and its mounts. A coupling with an odd number of plates has constant flexural stiffness for any direction of bending whether stand-off washers are used or not.

STRAIN TESTS

Introduction.- In preceding sections, methods of analysis were presented and shown to be adequate for the prediction of stiffness. The question that remains is how well do the methods predict internal forces and moments (and thus, stresses). In this section, the analysis methods are evaluated by comparing theoretical internal forces and moments to experimental results obtained from strain gage measurements. This comparison shows good agreement between the analytical and experimental results, and therefore, substantiates the method of analysis.

Identification.- This section uses the same numbering conventions and coordinate systems that were established in the Computer Analysis Section. To understand the data in the present section, however, it is necessary only to remember the following definitions.

F_x = axial force
F_y = edgewise shear
F_z = flatwise shear
M_x = twisting moment
M_y = edgewise bending
M_z = flatwise bending.

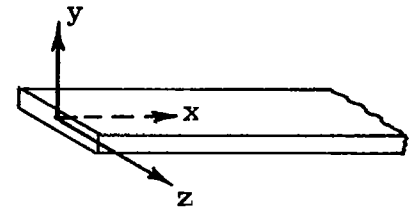

Test Specimens.- All strain gage tests were performed on a four-plate steel coupling with d = 8 inches. This same coupling design was the subject of the previously discussed STRESS examples and stiffness tests. Stand-off washers were used at the coupling mounting bolts. The function of these washers was discussed thoroughly in the Stiffness Test Section.

Instrumentation.- Uniaxial strain gages were applied to members 13 and 18 in the positions shown below. Ten gages were used on each member, five per side.

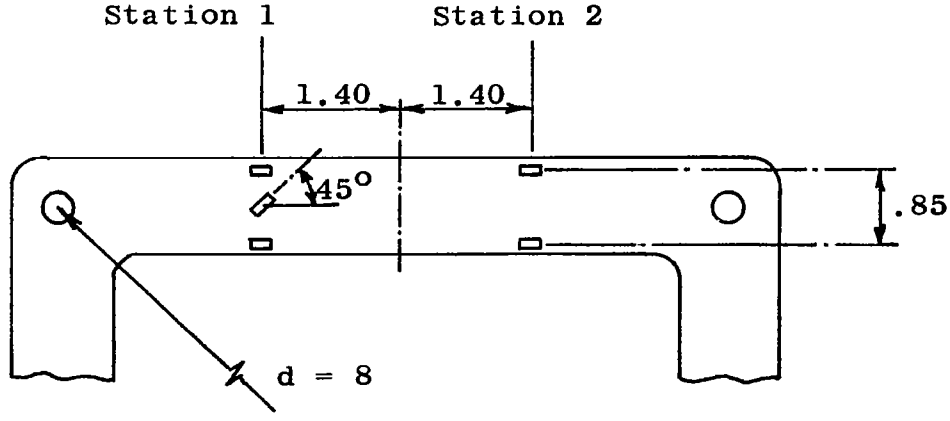

Internal moments and axial forces were calculated at stations 1 and 2 from the measured strains, modulus of elasticity, Poisson's ratio, and the section properties of the element. Transverse shears were then calculated from the moments at station 1 and 2 using the fact that the shear is constant between the stations. Moments at the ends of the member (element) were found using the fact that the moments vary linearly.

It is noted that the gage system contains more than the minimum number of gages required. Only three longitudinal gages are needed at each station, and only one 45^{o} gage is required at station 1. The extra gages provided insurance against gage loss through accidental damage or malfunction. Fortunately, all gages remained intact throughout the test series. The readings from the extra gages were used in the data reduction to reduce the effect of non-systematic observation errors. The internal forces and moments were determined for each combination of three gages at each station (4 combinations of 3 gages). Then results were averaged.

A large volume of data was produced in the strain tests. Its reduction by hand would have been costly and prone to error. Such errors were avoided by using a digital computer program to reduce the strain readings to the required final form (forces and moments at each end of members 13 and 18).

Single Coupling Tests.- Three different tests on a single coupling are reported. The test members and loading conditions are shown below.

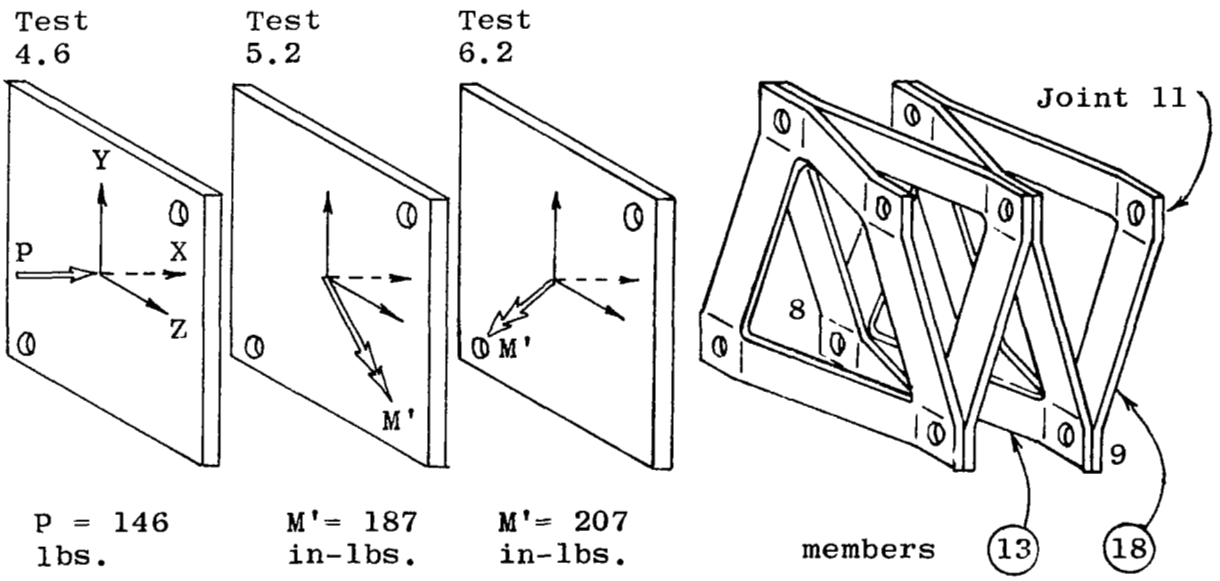

P = 146 lbs.

M'= 187 in-lbs.

M'= 207 in-lbs.

These tests correspond to fundamental conditions encountered in service. Test 4.6 corresponds to axial compression; Tests 5.2 and 6.2, to pure angular misalignment about axes of symmetry in bending.

Tables 4 , 5 , and 6 present the internal forces and moments for these tests. The tables show:

1. test values from measured strains.

2. theoretical values from the computer program STRESS.

3. theoretical values from the simplified analysis.

In general, all test and theoretical values show good agreements. The relative importance of the various forces and moments is apparent from the following values, which indicate the amount of each force or moment that is required to cause a stress = 1000 psi, in the test coupling (A stress concentration factor of 1.6 is included in M_y for the reasons discussed in the Simplified Analysis Section).

F_x	F_y	F_z lbs.	M_x	M_y	M_z in-lbs.
177	118	118	9	21	5

The results for Test 4.6 confirm the existence of a large edgewise bending moment in the end plate, member 18, when the coupling is subjected to an axial load. In an interior plate, member 13, the edgewise bending is very greatly reduced.

For the Tests 5.2 and 6.2 it is possible to evaluate the agreement of both the test results and theoretical values with the requirements of static equilibrium. From Equation (4), it is known that 2.828 ($|M_x| + |M_z|$) should equal the applied moment M'. From Tables 5 and 6 it is seen that the test results check static equilibrium within 12% even in the worse case (Test 6.2, member 13, joint 8). The theoretical values are in close agreement with static equilibrium.

In evaluating the results for Tests 5.2 and 6.2, importance should be given to the good agreement found for M_z because it is the primary cause of alternating stress during misalignment.

TABLE 4

INTERNAL FORCES AND MOMENTS FOR TEST NO. 4.6

Member, Joint	Source	Forces, lbs F_x	F_y	F_z	Moments, lbs-in M_x	M_y	M_z
	Test	8	-36	-10	8	50	-107
13, 8	STRESS	1	-37	- 4	1	17	-106
	Simplified		-37				- 98
	Test	-8	36	10	-8	6	-100
13, 9	STRESS	-1	37	4	-1	6	-104
	Simplified		37				- 98
	Test	119	-29	94	3	-271	- 85
18, 9	STRESS	116	-22	104	-1	-302	- 63
	Simplified		-23	99		-280	- 60
	Test	-119	29	- 94	-3	-262	- 80
18, 11	STRESS	-116	22	-104	1	-291	- 60
	Simplified		23	- 99		-280	- 60

TABLE 5

INTERNAL FORCES AND MOMENTS FOR TEST NO. 5.2

Member, Joint	Source	Forces, lbs F_x	F_y	F_z	Moments, lbs-in M_x	M_y	M_z	Check M'
	Test	10	-14	3	20	-11	-29	
13, 8	STRESS	3	-13	1	17	- 1	-24	
	Simplified				16		-25	
	Test	-10	14	-3	-20	- 4	-51	202
13, 9	STRESS	- 3	13	-1	-17	- 2	-48	182
	Simplified				-16		-50	187
	Test	-33	15	2	-17	- 4	53	196
18, 9	STRESS	- 2	12	1	-17	- 2	48	181
	Simplified				-16		50	187
	Test	33	-15	-2	17	- 5	30	
18, 11	STRESS	2	-12	-1	17	- 1	24	
	Simplified				16		25	

TABLE 6

INTERNAL FORCES AND MOMENTS FOR TEST NO. 6.2

Member, Joint	Source	Forces, lbs F_x	F_y	F_z	Moments, lbs-in M_x	M_y	M_z	Check M'
	Test	-28	16	- 1	-22	10	60	231
13, 8	STRESS	- 2	14	1	-19	- 3	54	207
	Simplified				-18		55	207
	Test	28	-16	1	22	- 6	34	
13, 9	STRESS	2	-14	- 1	19	- 1	27	
	Simplified				18		28	
	Test	-50	14	-14	-19	27	29	
18, 9	STRESS	- 2	14	- 1	-19	1	27	
	Simplified				-18		28	
	Test	50	-14	14	19	54	53	204
18, 11	STRESS	2	-14	1	19	3	54	206
	Simplified				18		55	207

Drive Train Assembly Tests.- A pair of 4 plate couplings and a center shaft were assembled in the drive train test rig used to qualify components for the UH2 helicopter. This rig is capable of applying torque and parallel offset misalignment to the coupling assembly. The test specimen installed in the rig is shown in Figure 15. Several tests were made in this rig under different combinations of torque and misalignment. In these tests, the strains in members 13 and 18 were measured at 15^{o} intervals as the coupling was rotated through 360^{o}.

Figure 16 presents typical results. It shows the internal moment M_Z versus position of rotation for four different test conditions. Joints 8 and 11 were chosen for presentation because they represent joints in a typical interior plate and a typical end plate. The following discussions are equally applicable to the curves for joint 8 or 11, except where noted.

Curve 1 shows the moments that occur when the input and output shafts were aligned as closely as possible. Theoretically, curve 1 should be a horizontal straight line, always zero. The moments shown by curve 1 are small, indicating that the initial alignment was quite good.

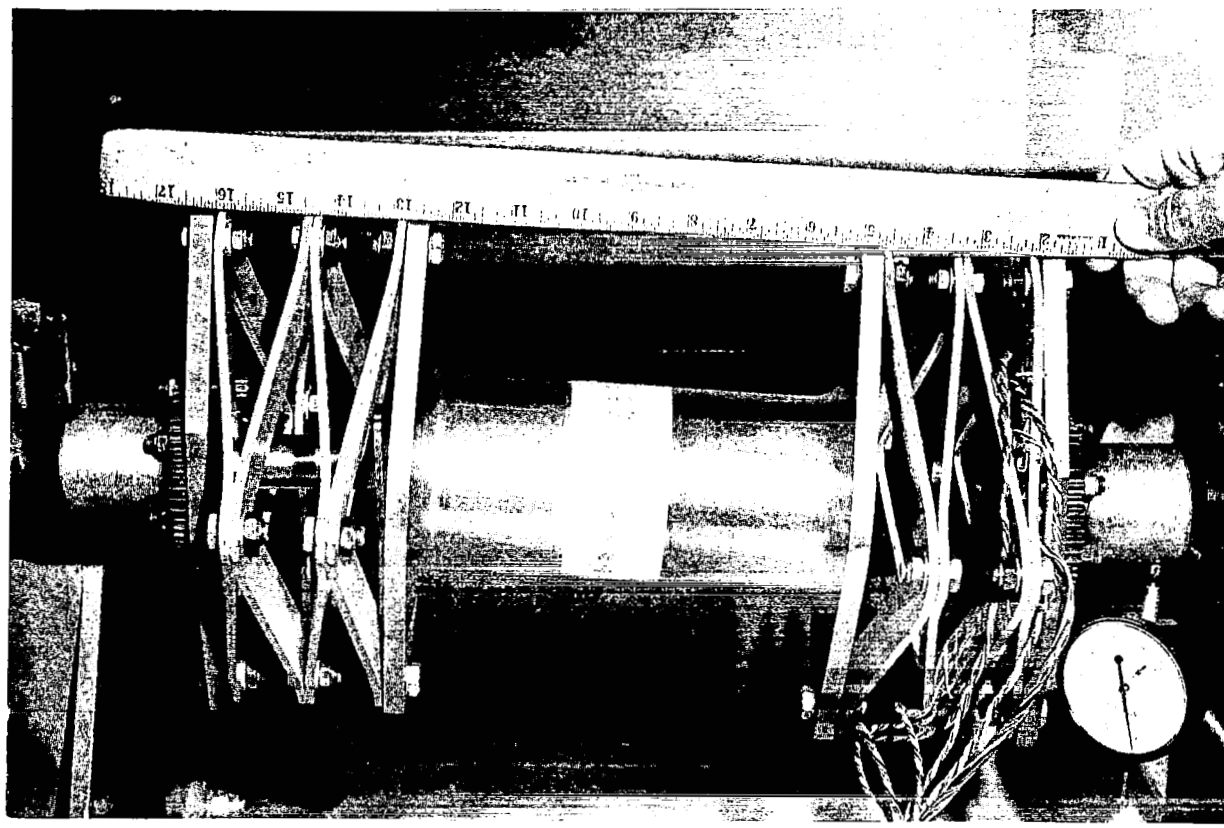

Figure 15. Strain Gage Test

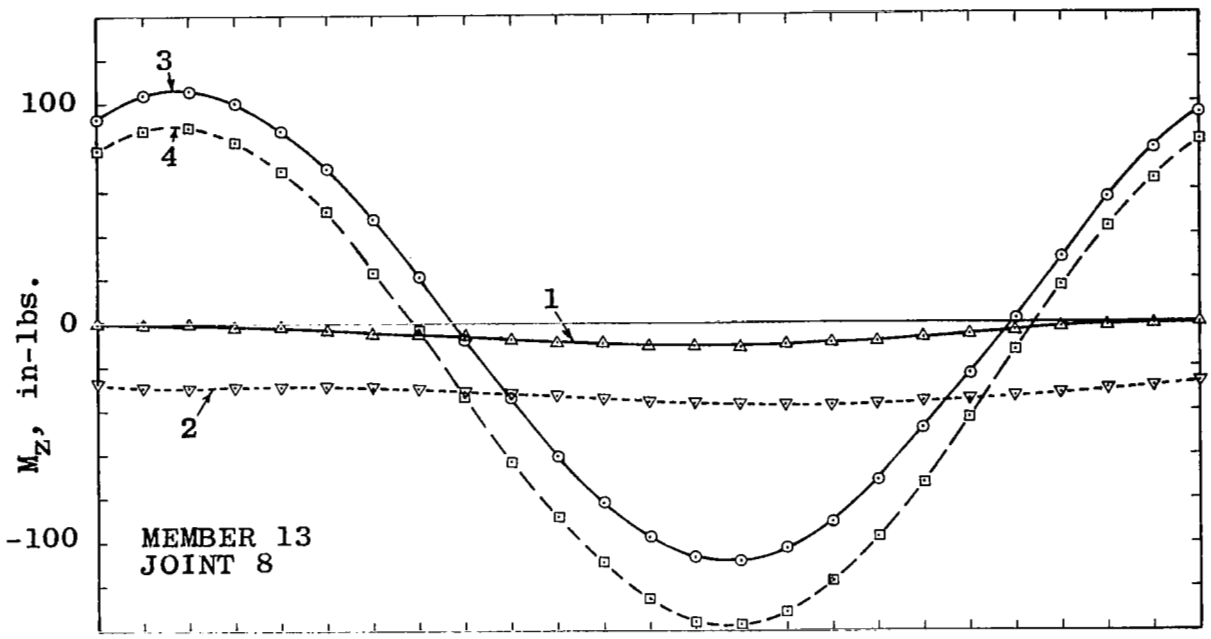

Curve No.	1	2	3	4
T, in-lbs.	0	16850	0	12800
offset, inches	0	0	.704	.744

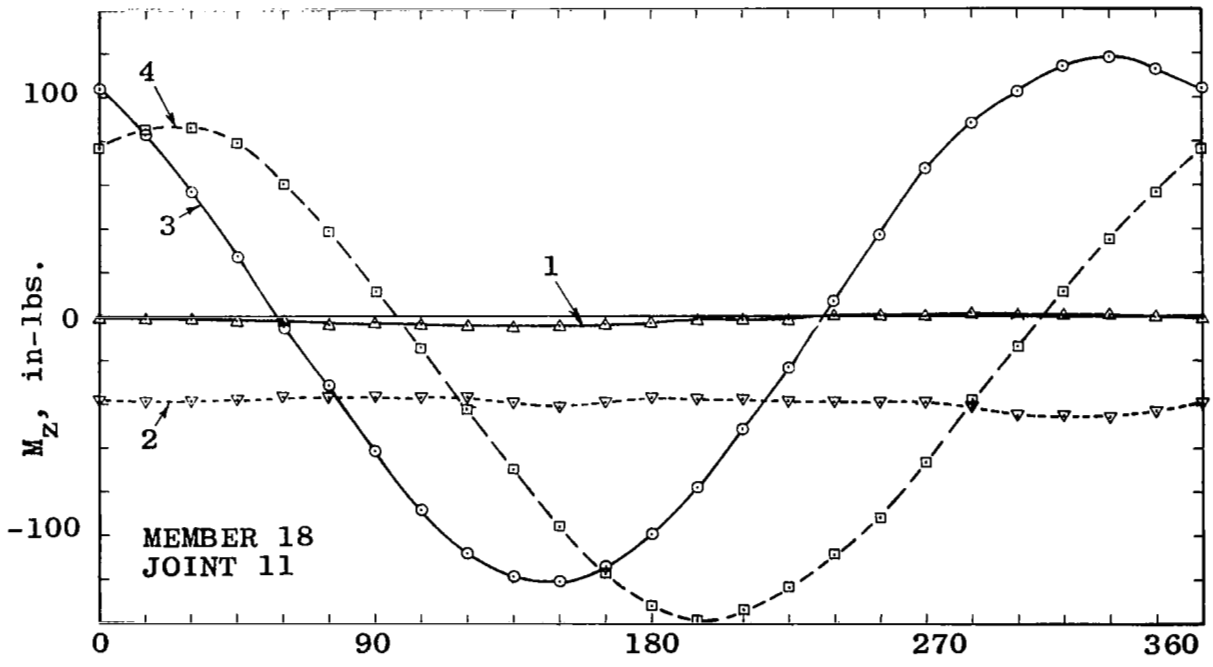

Figure 16. Test Flatwise Moments versus Angular Position

Curve 2 shows the results after a torque of 16,850 in-lbs. was applied to the assembly. Theoretically, no moment should occur from torque. However, curve 2 shows that a small steady moment was produced.

Curve 3 shows the moments that were produced when the coupling was rotated with the output shaft displaced .704 inches parallel to the input shaft. The results are compared to theory* in Figure 17 . Good agreement is seen in both amplitude and phase relationships.

Curve 4 in Figure 16 shows results for a test with combined torque and parallel offset misalignment. The torque was 12,800 in-lbs; the displacement, .744 inches. This torque was the maximum that could be applied in the extreme displacement condition without modification of the test rig. The test conditions of curve 4 are close to being a superposition of the test conditions for curves 2 and 3. Thus, curve 4 should be approximately the addition of curves 2 and 3, as it is for member 13. For member 18, curve 4 resembles the addition of curves 2 and 3 with a phase shift of 55 degrees. No reason is known for this phase shift. The phase shift is interesting, but not significant to the performance of the coupling. It is the peak-to-peak amplitudes that are important; they are the source of the alternating stress. The amplitudes are in agreement with theory.

Conclusions.- Good agreement was found between internal forces and moments measured in tests and corresponding values from both the simplified analysis and the computer program STRESS. The simplified analysis provided very close agreement. The STRESS results can be improved by using non-uniform member properties which account for stiffening at the bolted joints.

* See Appendix A

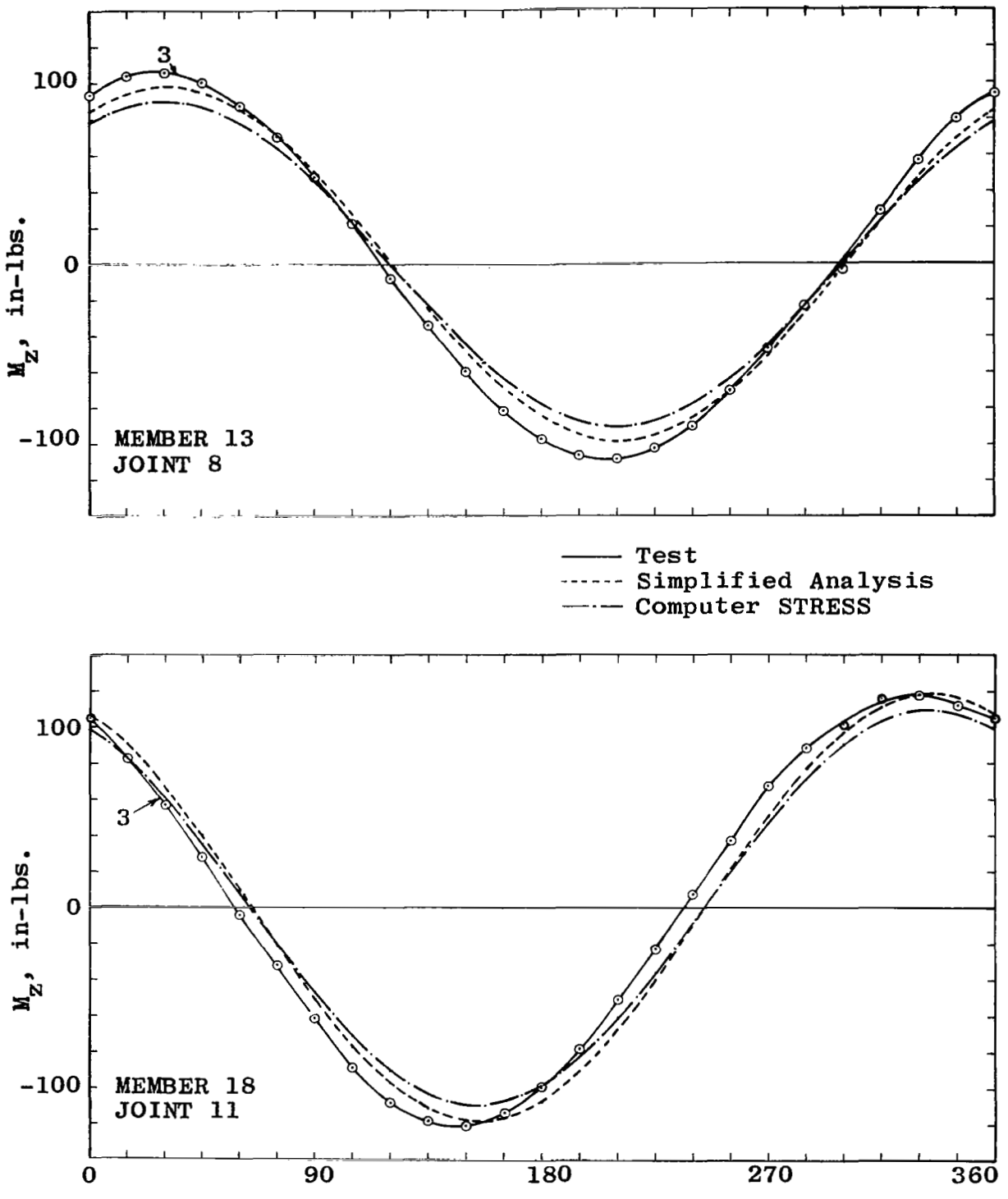

Figure 17. Comparison of Test and Theoretical Flatwise Moments

FATIGUE TESTS

Introduction.- Coupling misalignment causes the alternating stress which is the primary source of fatigue damage. The stress is believed predictable because of the agreement shown by the strain gauge survey, the computer program STRESS, and the simplified stress analysis. What is not known, however, is the stress at which failure occurs. Published fatigue test data provide guidance but are not considered adequate. Tests to failure were performed, one test at 9^{o} misalignment angle, one test at 5^{o} misalignment angle. One size of coupling was used for both tests. The tests were restricted to alternating stress alone by avoiding coupling extension or compression, by not transmitting torque, and by rotating at slow speed.

Specimen design and manufacture were kept simple deliberately, with the plan of adding refinements only after proof of need. The specimens for the fatigue tests were the first produced on prototype tools. Analysis of the test failures showed specimen imperfections that would be expected to reduce fatigue performance significantly. Nevertheless, they demonstrated impressive life at misalignment angles of 9^{o} and 5^{o}, indicating the excellent fatigue characteristics of the Bossler coupling. Because experience is limited to these two tests, additional testing is recommended.

Apparatus.- The test apparatus is shown in Figure 18. Each shaft has a removable centerline indicator in the form of a coaxial pointed rod. The points are located so that they meet at the center of the coupling. The shaft centerline indicators show that the shaft centerlines intersect at the center of the coupling, thus indicating uniform angular misalignment. They also indicate that no change of coupling length occurred, which would cause a steady stress. The angular misalignment was measured with an inclinometer to ± 0.1 degree and by calculation using measured shaft locations. The input shaft is driven by an electric motor at 1820 rpm. The coupling was inspected while turning with a stroboscope. An automatic power cutoff was provided by a vibration-sensitive switch.

Specimens.- The test specimens were four plate couplings with $d = 8$, $b = 1.069$, $t = .165$ inches. The material was 18% nickel maraging steel, grade 250, aged at $900^{o}F$ for three hours. A solution heat treatment after forming was not used. Plate manufacture was deficient, as discussed below under Results.

The first test at 9^{o} angular misalignment is shown on Figure 18. The calculated stress is ± 52 ksi, using Equation (14). No fretting protection was provided in order to reveal clearly the mode of first failure.

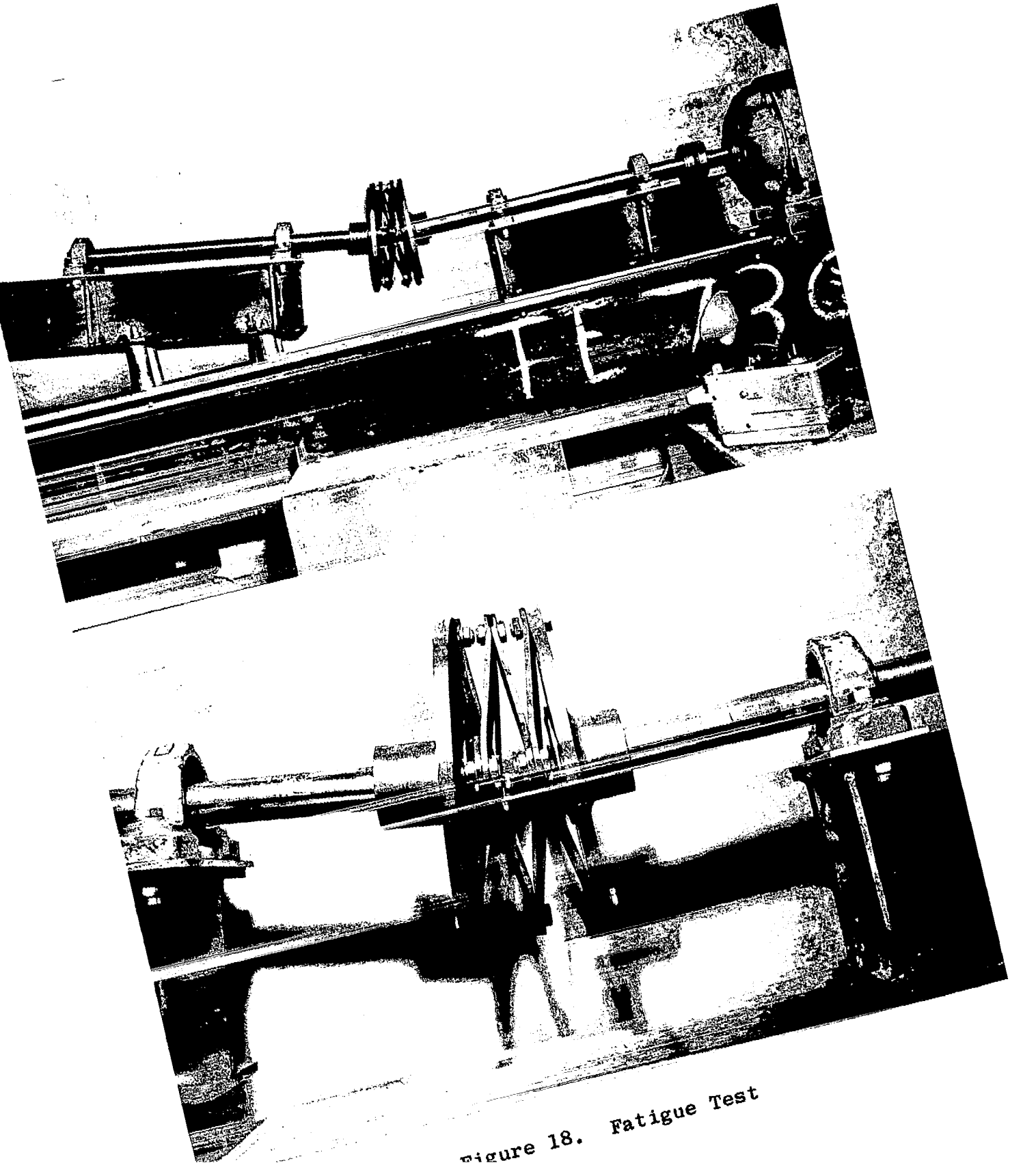

Figure 18. Fatigue Test

The second test at 5° angular misalignment induced a calculated stress of ± 29 ksi. In this test, a limited degree of fretting protection was provided. The individual coupling plates were electroplated with .002 inches of silver, and standoff washers were placed between the coupling and the shaft end-fittings.

Test Results.- The 9° test produced a fatigue failure at 3.3×10^5 cycles. The failure occurred in the end plate attached to the output shaft. The point of origin was .05 inches from the bolt hole on the side of the plate in contact with the output shaft end-fitting. The point of origin was in a fretting region as shown below.

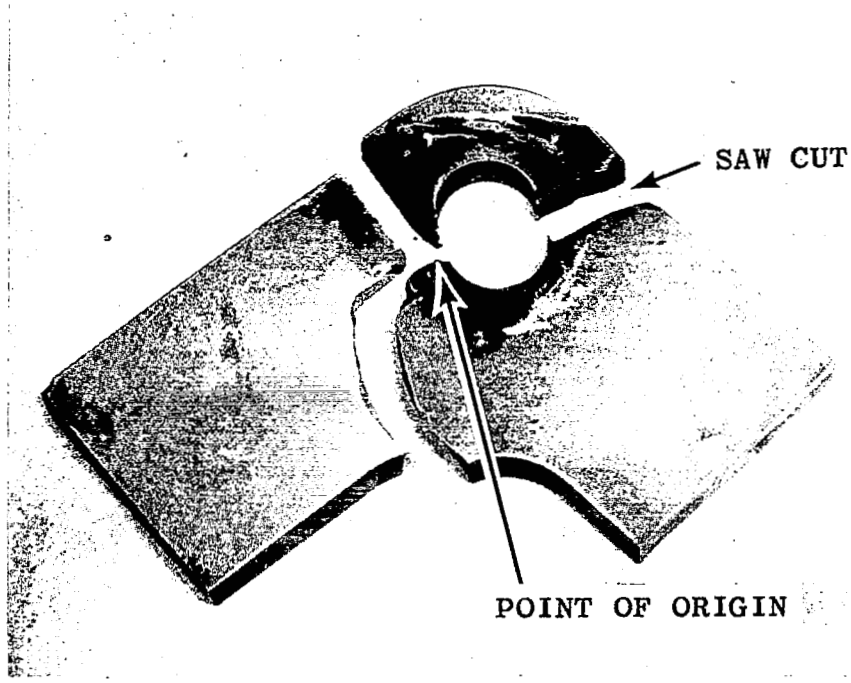

Figure 19. Specimen From 9° Test

The 5^{o} test produced a fatigue failure after 5.3×10^{6} cycles. The failure occurred on an interior plate. The point of origin was on the side opposite the contacting surface at the bend line in a die mark left by the forming process. The failure was not associated with fretting. The failure is shown below.

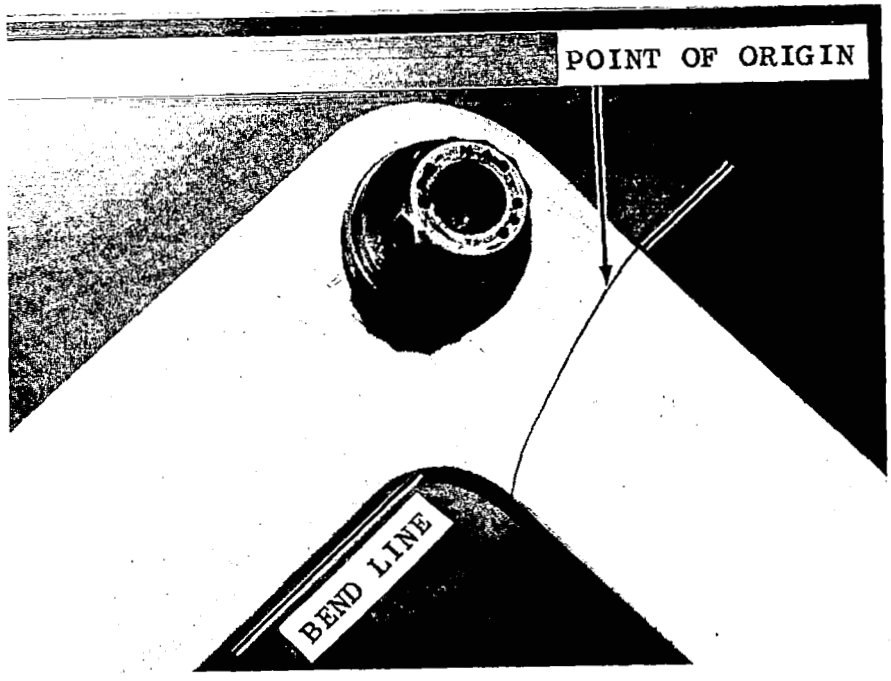

Figure 20. Specimen From 5^{o} Test

Discussion.- The die that produced the test specimens was found to have insufficient allowance for spring-back. As a result, the plates had joint contact faces that were tilted rather than perpendicular to the coupling centerline. A wedge-shaped gap could be seen between the plates in a joint when the bolts were loose. When the gaps were closed by tightening the bolts, the coupling shortened .250 inches. This produced a tension stress in the contacting surfaces. This locked in tension stress contributed to the fretting-induced failure at 9^{o}. The defective die also contributed to the failure at 5^{o} misalignment. The die had a bend radius which caused a slight

dent in the coupling plates. The failure originated in the dent. Subsequent changes to the die enabled plates of much better quality to be produced for other tests.

The 9° test showed a fretting-limited life that is not representative of the life that can be obtained with known surface treatments. The greatest improvement in endurance limit and reliability from treatments that induce surface compressive stress are described in the literature (References 6, 7). Reference 7 reported the effect of cold-rolling and shot-peening on the fretting-endurance limit of titanium and steel. Without surface treatment, fretting caused the mean endurance limit of titanium to drop from 79,030 psi to 44,060 psi. The corresponding standard deviations increased from 3280 psi to 19,870 psi. After severe cold-rolling or shot-peening, the endurance limits rise to above 85,000 psi with standard deviations less than 2820 psi, in spite of severe fretting. These results are shown graphically in Figure 21 taken from Reference 7. They also found that steel behaved in a similar manner.

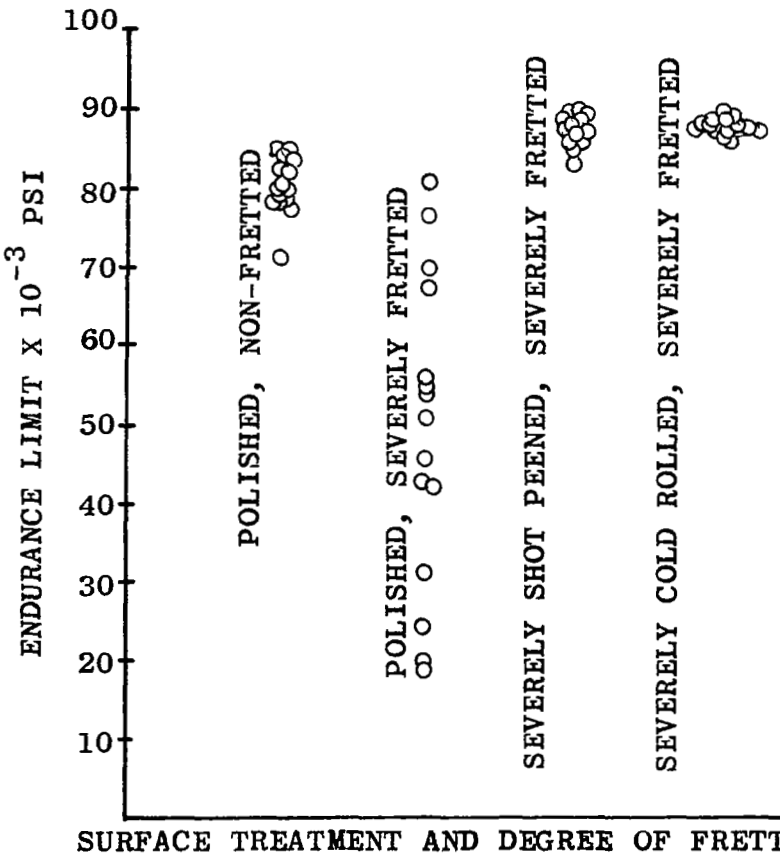

Figure 21. Comparison of Fretting Endurance Limits (From Figure 4-27, Reference 7)

The titanium data and comments on steel give rise to the expectation that maraging steel will derive similar benefits from surface compressive stress. Nitriding or shot peening are attractive methods of obtaining a surface compressive stress in a Bossler plate made of maraging steel.

In the case of the 5^{o} test, silver-plate and angle reduction were sufficient to impede fretting. A failure occurred in a non-fretted region. The failure was unexpected. It could not occur if the stresses were actually 5/9ths of the stresses endured for 3×10^{5} cycles in the 9^{o} test, according to the shape of published S-N curves for maraging steel (Reference 8). Other causes must have contributed to the failure. Four possible causes are known. A high tensile residual stress could have been left in the forming dent where the failure originated. A metallurgical notch could be present from the heat treatment because maraging would be affected by the residual stress. The dent would also contribute a geometric notch. A locked-in stress from clamping malformed parts was present.

For maraging steel, the residual stress and metallurgical notch will be avoided by adding a solution heat treatment after forming and before maraging. Other materials will require similar care. The geometric notch from forming will be removed by blending after forming or by developing a better forming process.

Other techniques are available to reduce stress locally, if required. For instance, stress can be lowered in the joint contact area by increasing plate thickness near the bolt holes.

Conclusions.- The potential performance of Bossler couplings at large misalignment angles is impressive. Fretting protection is necessary. Methods of protection can be used that are known to be effective.

CONSTANT VELOCITY TEST

Introduction.- Misalignment couplings may not be constant velocity devices. Output angular displacement may fluctuate with respect to input angular displacement. The fluctuation causes velocity change, (accelerations), which may be destructive during power transmission. Any assembly of even numbers of Hooke-type universal joints will transmit constant velocity if the yokes are aligned, if the misalignment angles are equal, and if all shafts are coplaner. One Bossler plate is kinematically analagous to a Hooke joint. Two plates are analagous to a pair of Hooke joints with yokes aligned. The shafts attached to a Bossler coupling are normally coplaner. Therefore, a Bossler coupling made up of any even number of plates with equal misalignment per plate will transmit constant velocity. For a Bossler coupling with an odd number of plates, n, all but one plate is paired with another. Because the overall misalignment will be shared among n plates, the resulting speed variation will be that of a single Hooke joint with a misalignment angle equal to total misalignment angle $\div n$. Typically, the resulting speed variation in a Bossler coupling with at least three plates will be one order of magnitude less than that in a conventional Hooke joint.

Constancy of velocity tests are reported in this section. Tests were made using the measurement apparatus alone, using a four-plate coupling with no misalignment and the same coupling with 9^{o} misalignment. Fluctuation in output displacement could not be observed directly. Statistical analysis of the test data* identified cyclic fluctuation on the order of 1/3 of the least reading of the measuring system. Based on the fact that the speed fluctuation was very small, if it existed at all, it is concluded that the Bossler coupling can be a constant velocity device.

Apparatus and Test.- The test arrangement was the same as the 9^{o} fatigue test, which is shown in Figure 18. Two shafts were each supported by two bearings. The bearings were mounted in pillow blocks that were attached to two I-Beams. The shafts were connected by a four-plate coupling. The instrumentation was a synchro transmitter on the input shaft coupled back-to-back with a synchro control transformer on the output shaft. The difference between the synchro signals was read on a phase angle voltmeter. The synchros had a specified accuracy of ± 5 minutes each. The two-synchro system specified accuracy was ± 8.5 minutes. Selection and careful matching reduced this error.

* By D. W. Robinson, Jr., Chief Research Engineer, Kaman Aircraft

The relationship of output angular displacement to input angular displacement was tested at 9°, the largest angle the particular test coupling could reach without internal interference. The 9° angle was sufficiently large to cause deformations that might affect displacement. A conventional Hooke-type universal joint at 9° misalignment has a geometric fluctuation of angular displacement of ±21.3 minutes. A fluctuation of this magnitude could be detected easily by the instrumentation used. The 9° angle is larger than the misalignment expected in most drive trains. Also, no output/input displacement error was observed during previous tests at smaller angles, leading to the belief that a large-angle test, such as 9°, would be required to uncover any fluctuation in output/input angular displacement.

Results and Discussion.- Three basic sets of data were taken:

1. Two synchros mechanically connected and hooked up to bridge circuit and instrumentation. Two calibration runs taken (Figure 22).

2. Same synchros and electronics but attached each side of Bossler coupling - shafts aligned. Three runs made (Figure 23).

3. Same as (2) but with coupling deflected 9°. Three runs made (Figure 24).

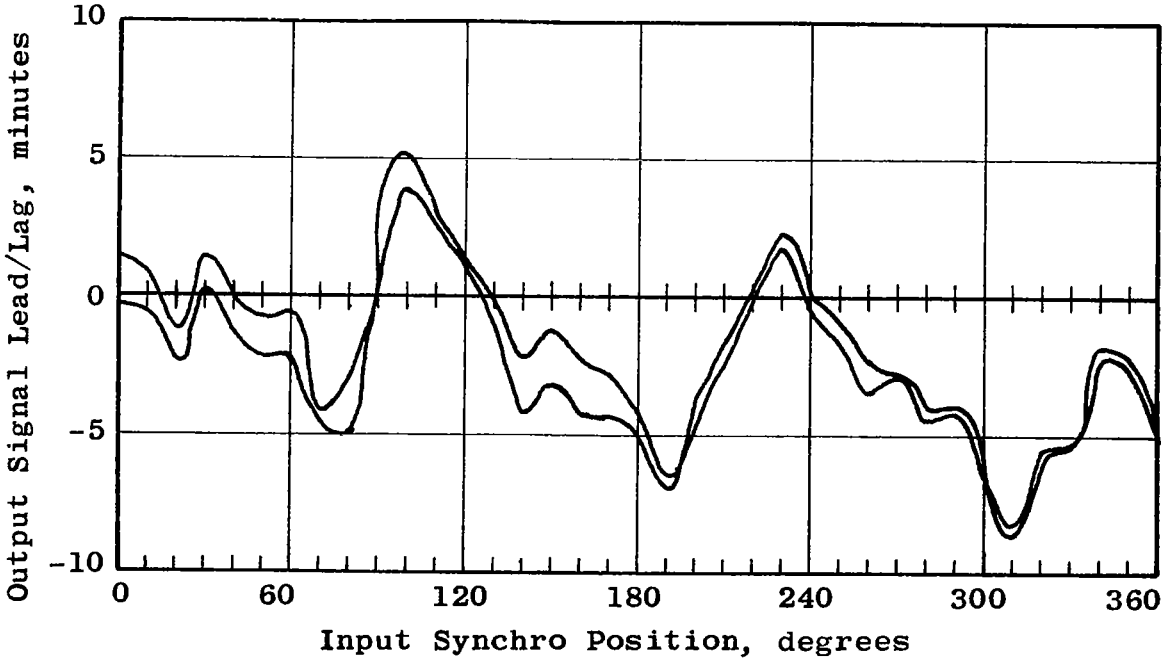

Figure 22. Measured Angular Difference, Synchros Aligned

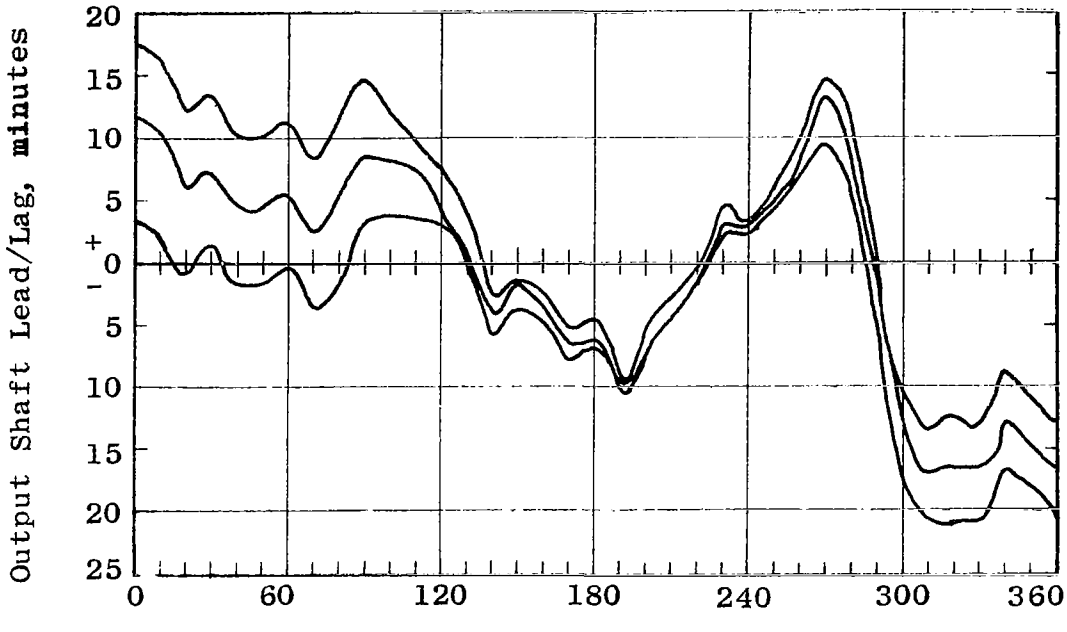

Figure 23. Measured Angular Difference, Shafts Aligned

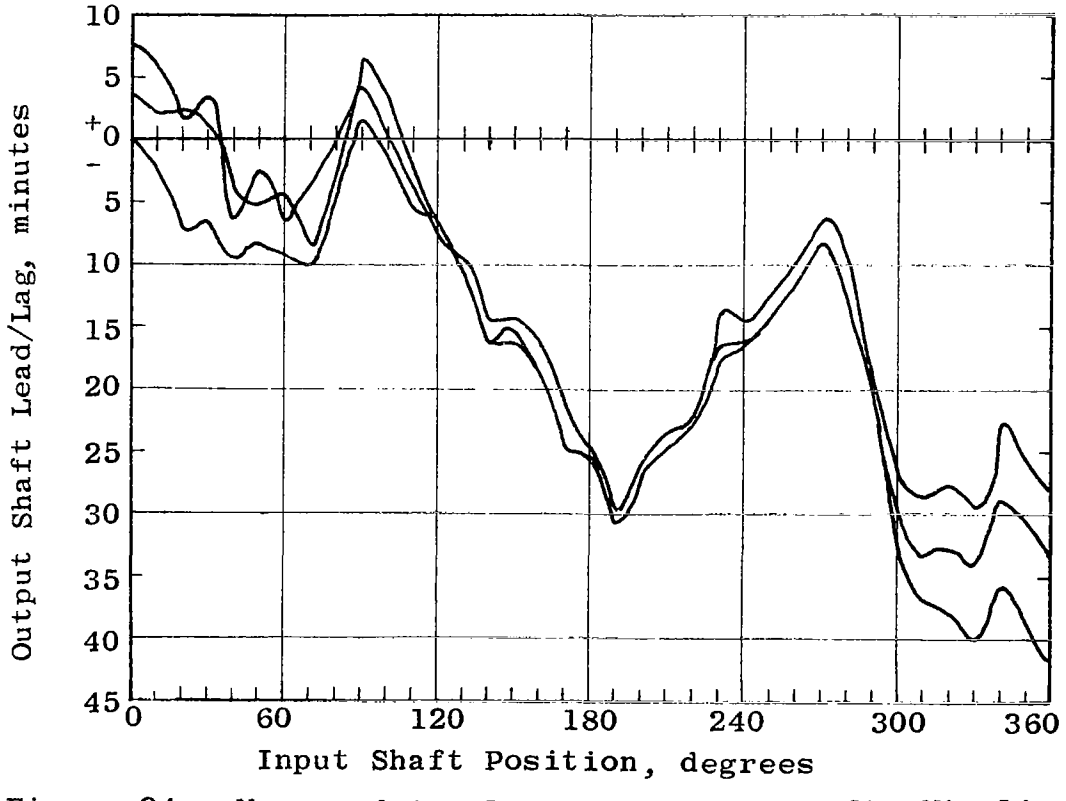

Figure 24. Measured Angular Difference, Shafts Misaligned 9°

Shapes of curves for all three set-ups showed variations which were followed quite closely by replicate runs. Much of the variation, therefore, appeared to be systematic, probably from several sources, with a superimposed random variation showing as difference between replications. One source of systematic variation was the angular difference across the coupling, and was the effect to be evaluated. This source was present only in set-up 3, Figure 24.

The Bossler coupling repeats geometric similarity every 180° of shaft rotation, as does the Hooke joint. Like the Hooke joint, therefore, any fluctuation in output displacement should be integral harmonics of twice shaft frequency. Thus any 180° of shaft rotation should produce one complete cycle of coupling fluctuation. By analyzing only the data lying between 110° and 290° shaft angle in set-ups 2 and 3, the effect of random variation between replications were minimized, seen by inspection of the data to be reasonably low between these limits and large elsewhere.

Variation between replications gave an indication of the consistency of the data between set-ups, and therefore the appropriateness of using differences between set-ups as a measure of the effect of the changes made deliberately - specifically, the effect of coupling deflection.

For each set-up, measured values for the replicated runs at each angle were averaged, and the variance (standard deviation squared) of the measured points about the average calculated by standard methods (Reference 9). A Fisher "F" test of the ratios of these variances indicated the probability that the data were directly comparable.

Set-Up	Variance	Degrees of Freedom	Variance Ratio, F	Critical Value of F $F_{.05}$	$F_{.01}$
1	.281	71			
			5.23	1.46	1.90
2	1.47	47			
			1.75	1.62	1.98
3	.837	47			

It was seen that the ratio of variances or Fisher "F" ratio between set-ups 1 and 2 greatly exceeded the critical value of F, even at the .01 level. Thus, there was considerably less than 1% probability that the set-ups were equivalent, with the differences in variation due entirely to chance. This would be expected, in that going from a bench calibration of the instrumentation alone to a calibration of the same instrumentation mounted on the actual test specimen introduces many new sources of variance in attachments, shaft alignment, bearings and test rig structure.

Therefore, the averages of the data from set-ups 1 and 2 were not compared directly.

Comparing set-ups 2 and 3, the F ratio again exceeded the critical value at the .05 level, although not at the .01 level. Also note that the variance was less in the deflected condition of set-up 3. This might be the result of the coupling bending stiffness introducing lateral preload on the bearings, removing a source of random variance. In any event, the comparability of data was only marginal, in that it was statistically probable that something other than just introduction of coupling error (a consistent bias - not a source of random variance) had changed going from set-up 2 to set-up 3. However, averages were compared looking for the harmonics of twice shaft angle characteristic of coupling error.

Differences between the averages of the three runs for set-up 2 and set-up 3 are presented on Table 7 and plotted on Figure 25 over the shaft angle range 110° to 290°.

TABLE 7

NET ANGULAR DIFFERENCE

Shaft Position Degrees	Output Lead/Lag - Minutes, Averaged 0°	9°	Net Difference - Minutes 0°-9°
110	7.0	-4.0	11.0
120	4.8	-7.2	12.0
130	1.9	-10.3	12.2
140	-4.1	-15.7	11.6
150	-2.4	-15.3	12.9
160	-3.6	-17.7	14.1
170	-6.5	-23.7	17.2
180	-5.8	-25.2	19.4
190	-9.7	-30.5	20.8
200	-6.5	-26.6	20.1
210	-3.8	-24.1	20.3
220	-1.0	-22.3	21.3
230	3.4	-15.9	19.3
240	2.8	-15.9	18.7
250	5.0	-13.8	18.8
270	12.7	-7.6	20.3
290	-3.9	-21.4	25.3

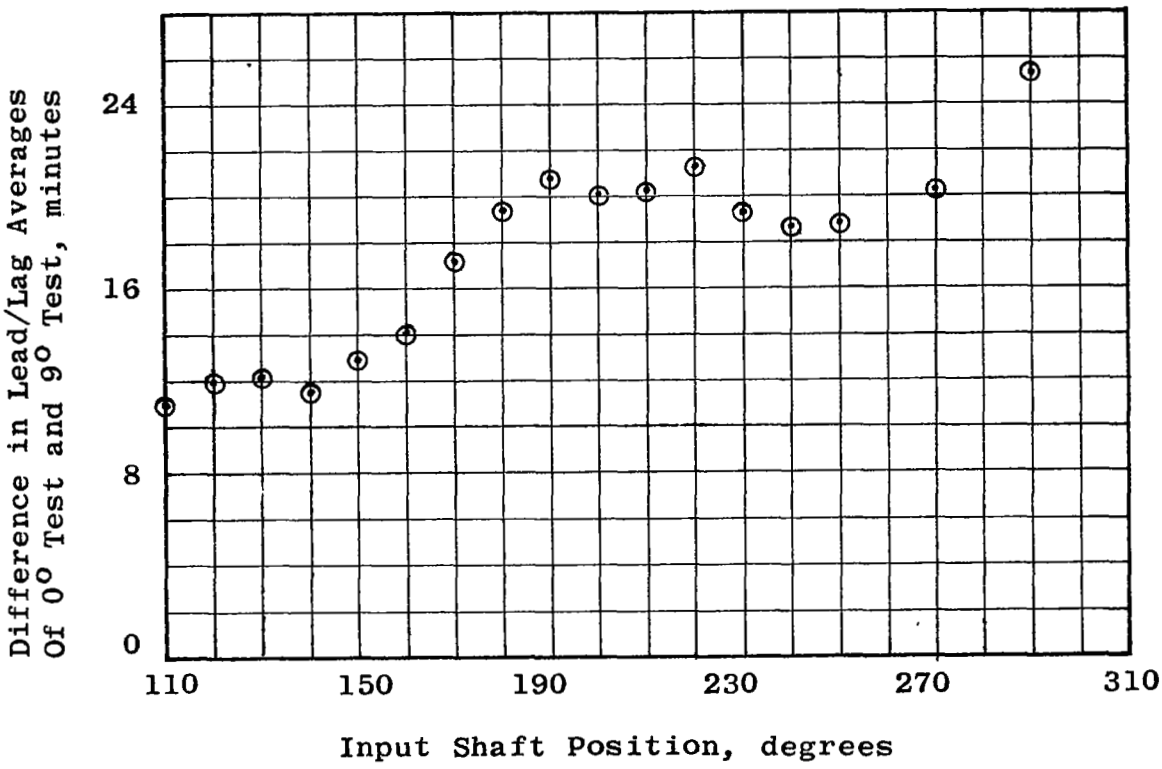

Figure 25. Net Angular Difference

It is expected that variation due to coupling error, together with other sources of systematic variation introduced or eliminated between set-ups 2 and 3, is included in the data plot of Figure 25 together with some of the random variation. Non-random sources of variation common to both set-ups, such as systematic instrument errors, are excluded.

Examination of the plot indicated the presence of at least two apparently non-random components: a linear slope, and a harmonic variation around that slope; together with the expected random variation or point scatter. The linear slope was obviously not a component of the coupling error, which, as has been shown, must be harmonic.

The linear trend was removed by linear regression. The regression was tested for significance and found to correlate as a real effect. The data with linear trend removed is shown in Figure 26.

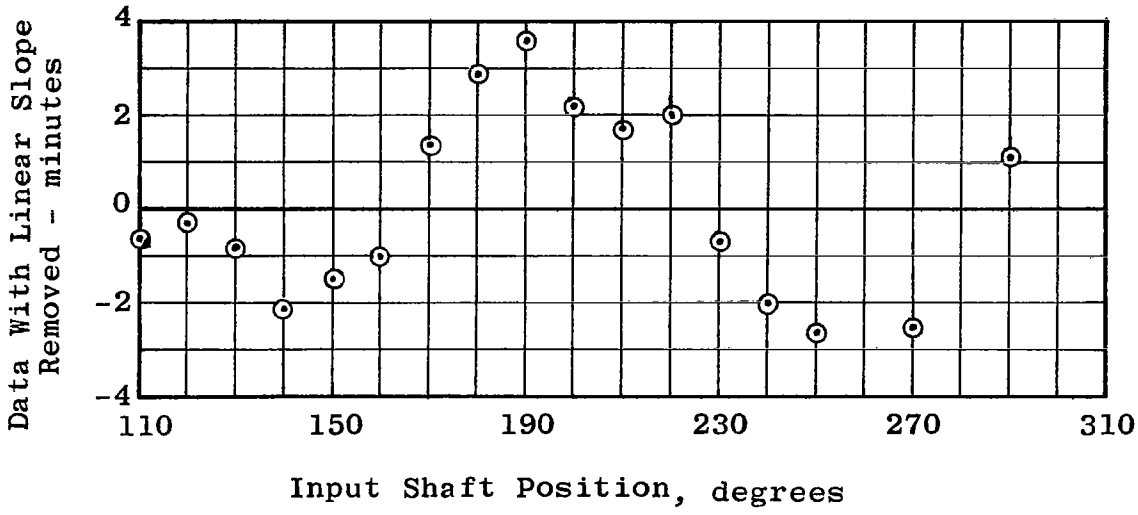

Figure 26. Harmonic and Random Angular Difference

A decided, although small, cyclic trend is seen. A harmonic analysis was performed to separate out harmonic components. The missing data points at 260° and 280° were obtained by interpolation. The second and fourth harmonic components were removed, to find the residual variance, and the resulting points are shown on Figure 27.

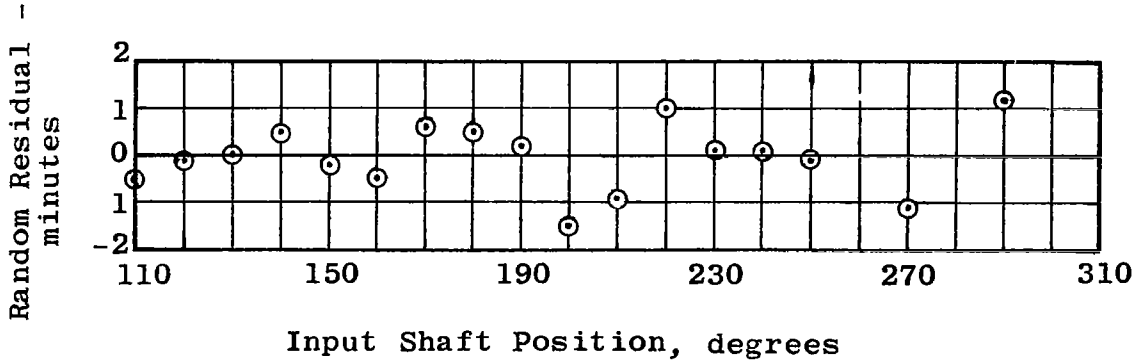

Figure 27. Random Angular Difference

The residual variance was compared to the variance of the averages of set-ups 2 and 3. No statistically significant difference was found, indicating that all important trends had been removed.

If the residual variance is used to establish 95% confidence limits on coupling error in terms of input shaft position θ,

$$\text{Error} = 1.95 \sin 2(\theta - 143^{\circ}35') - 1.74 \sin 4(\theta - 131^{\circ}5') \pm 1.4 \text{ minutes.}$$

Stated in words, the confidence level is 95% that the test system produced a cyclic fluctuation of output angular displacement with respect to input angular displacement that was larger than two minutes but smaller than five minutes. Two points are worth noting: the estimated error is less than the instrumentation can measure directly (8.5 minutes), and a conventional Hooke-type universal joint at the same 9° misalignment has a geometric fluctuation of ± 21.3 minutes.

Conclusions.- Based on the fact that the speed fluctuation tendency was very small, if it existed at all, it is concluded that the Bossler coupling can be a constant velocity coupling.

CRITICAL SPEED TEST

Introduction.- Bossler couplings have a great effect upon the critical speeds of shaft systems. For this reason, tests were made to demonstrate that conventional idealizations and analysis methods are adequate to predict the critical speeds of a system which includes Bossler couplings. The test rig was capable of a speed 12% higher than calculated first critical speed. Good agreement was found between the calculated and the observed first critical speed.

Test Rig.- The resonance test was performed in the test rig previously used to qualify drive train components for the UH2 helicopter. Figure 28 shows a sketch of this rig. The test rig operates at a constant 6210 rpm. Resonance was detected during start-up and shut-down using an MB pickup which sensed the velocity of motion at the center support. A CEC direct-writing oscillograph recorded the data.

Results.- During start-up and shut-down a resonance was detected at 5500 rpm. Figure 29 shows a tracing of the oscillograph record. No other resonances were observed in the speed range (0 rpm to 6210 rpm) of the test rig. The observed resonance is in good agreement with the calculated resonance of 5550 rpm for the first mode.

Analysis Method.- The analysis assumes that the critical speeds of the rotating system are identical to the natural frequencies of lateral vibration of the system when not rotating. The natural frequencies and mode shapes for lateral vibration were computed using the influence coefficient method with matrix iteration (Reference 10). In the analysis, the real structure was idealized as a weightless shaft which supports a finite number of lumped masses. Figure 28 shows the specific idealization used for the test rig and also shows the calculated shapes and frequencies for the first and second modes.

The couplings were treated the same as other segments of the shaft. The flexural stiffness (EI) for the couplings was computed using Equation (11). All data for the system is summarized in Table 8.

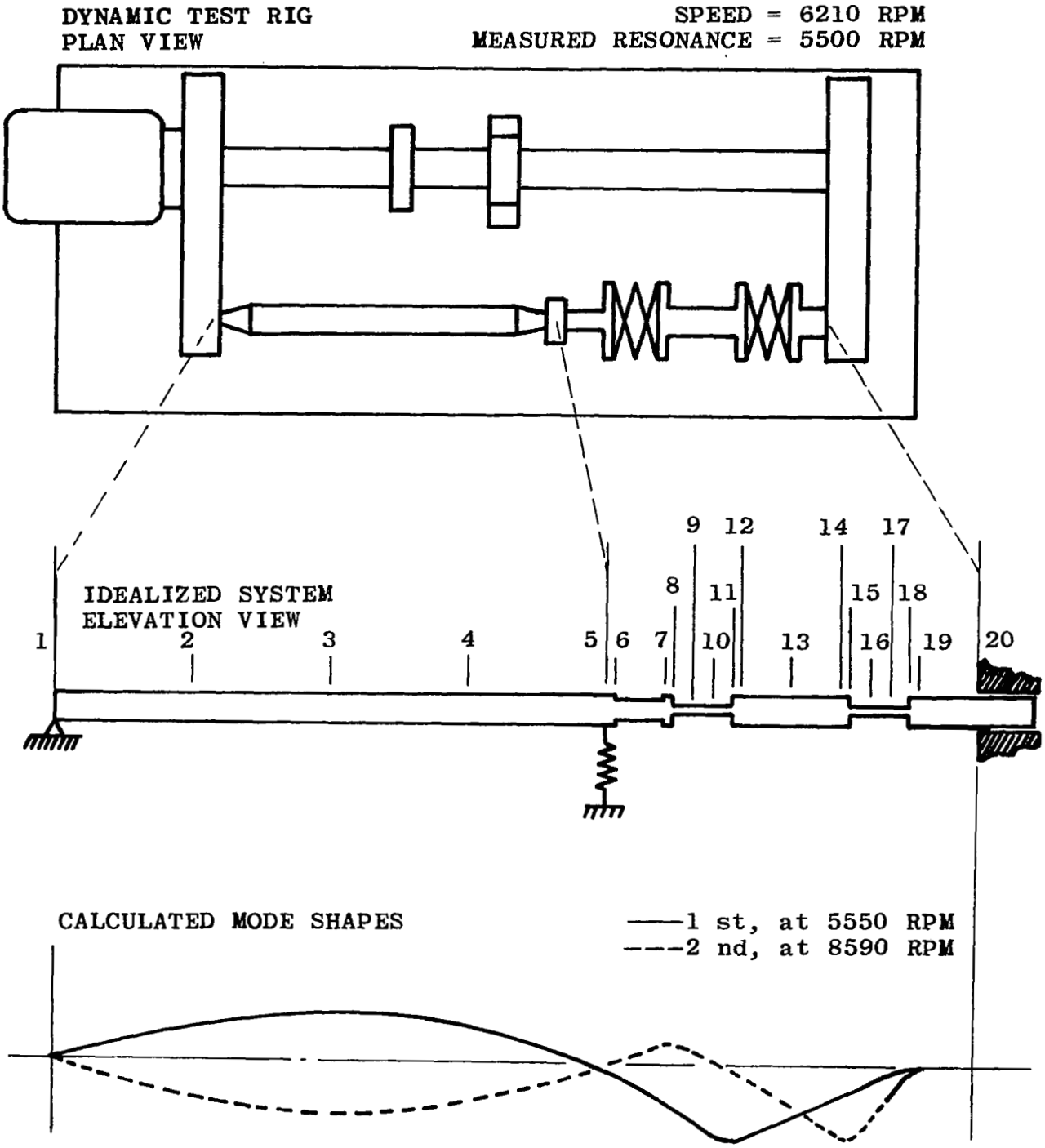

Figure 28. Dynamic Test Rig, Idealization, and Calculated Mode Shapes

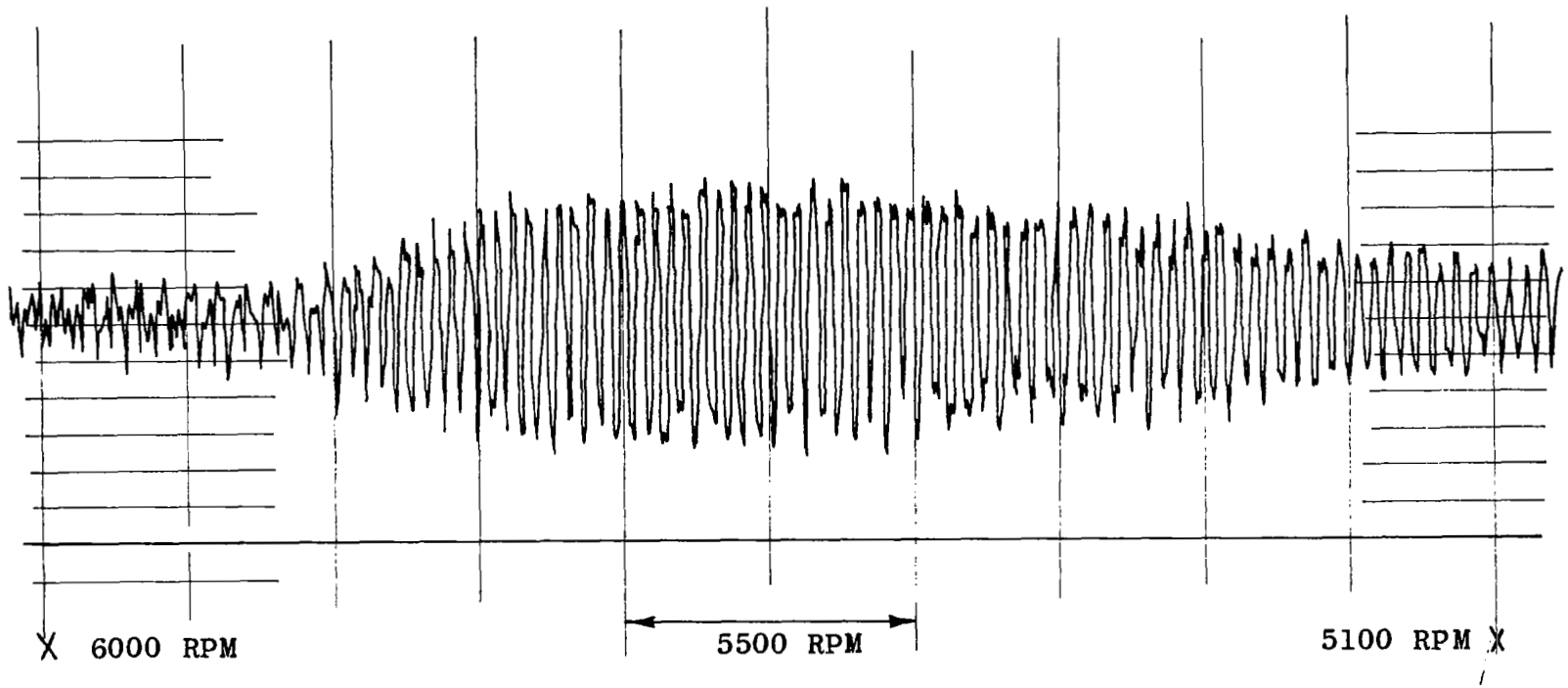

Figure 29. Trace of Oscillograph Record of Passage Through Resonance

TABLE 8

SUMMARY OF PROPERTIES OF IDEALIZED SYSTEM FOR THE DYNAMIC TEST RIG WITH BOSSLER COUPLINGS

INPUT				RESULTS		
No.	Position x in.	EI 10^6 lb.in.^{2}	Mass lb.sec^2/in.	Normalized Mode Shapes First	Second	Third
1	0.0	13.9	.00186	.000	.000	.000
2	11.75	13.9	.00372	-.419	.509	.731
3	23.50	13.9	.00372	-.631	.728	1.000
4	35.00	13.9	.00372	-.492	.536	.705
5	47.00	13.9	.00186	.087	.015	.193
6	47.00	8.2	.00113	.087	.015	.193
7	52.50	8.2	.01270	.511	-.261	.089
8	52.50	.0162	.00198	.511	-.261	.089
9	53.5	.0162	.00397	.702	-.211	.252
10	54.5	.0162	.00397	.935	-.034	.512
11	55.5	.0162	.00198	1.000	.130	.557
12	55.5	36.5	.00427	1.000	.130	.557
13	59.55	36.5	.00368	.712	.566	.018
14	63.6	36.5	.00427	.422	1.000	-.520
15	63.6	.0162	.00198	.422	1.000	-.520
16	64.6	.0162	.00397	.292	.844	-.486
17	65.6	.0162	.00397	.118	.393	-.244
18	66.6	.0162	.00198	.027	.108	-.075
19	66.6	13.9	.01090	.027	.108	-.075
20	73.72	13.9	.01090	.000	.000	.000

Stiffness of center spring = 80000 lbs/in

Frequency, rpm = 5550. 8590. 10600.

A Common Case.- In many applications the system could be simpler than the dynamic test rig. For example, a short center shaft with identical couplings at each end could be used in an engine-transmission system which provides nearly fixed lateral and moment restraint at the supports. Calculated mode shapes and frequencies for such an application are shown in Figure 30. Table 9 summarizes the input and results for this case. The couplings and center shaft in this example have the same stiffness and mass as those used in the previously discussed test rig.

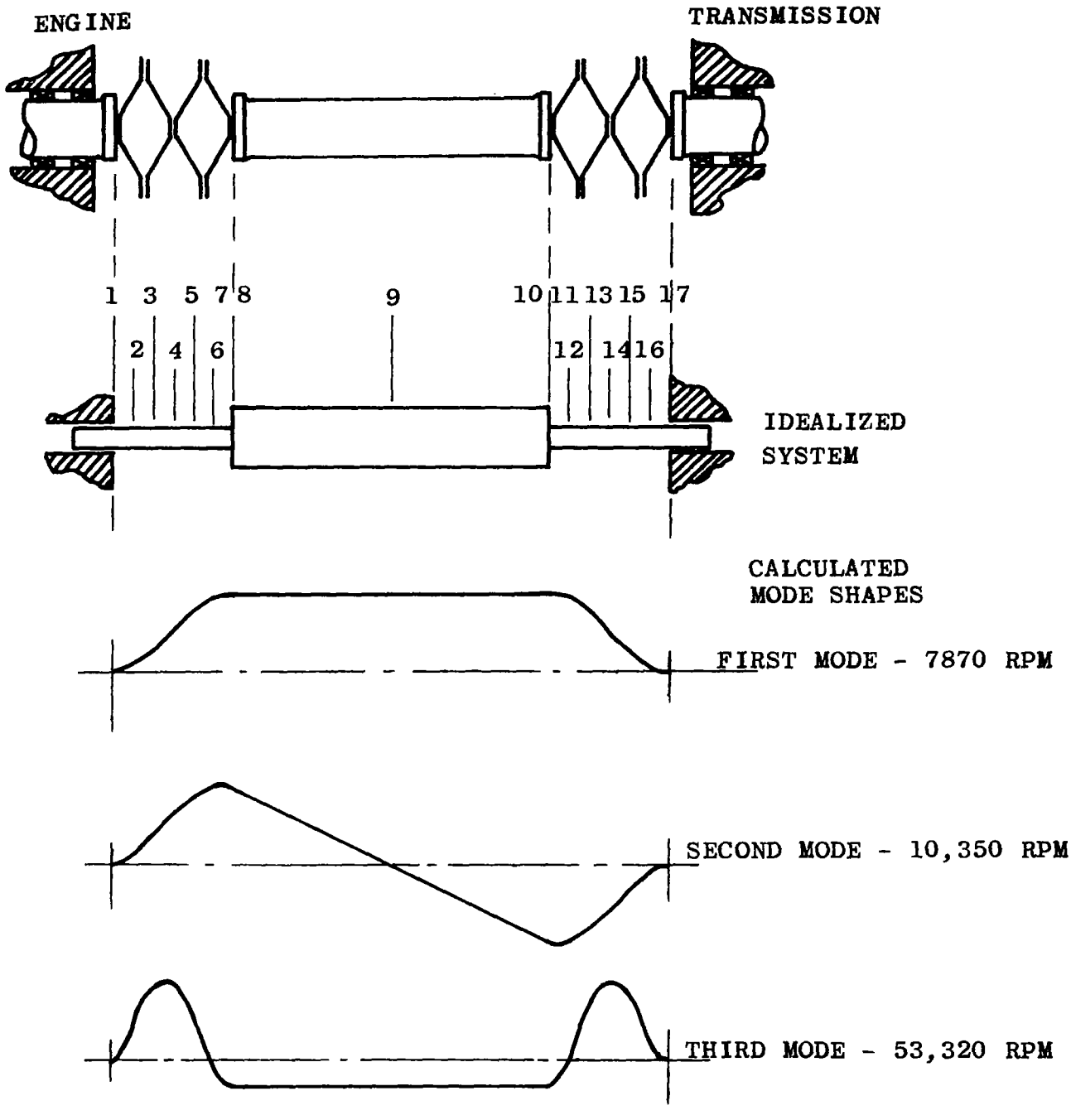

Figure 30. Bossler Assembly Between Firm Supports

TABLE 9

SUMMARY OF PROPERTIES OF IDEALIZED SYSTEM FOR BOSSLER ASSEMBLY BETWEEN FIRM SUPPORTS

INPUT				RESULTS		
No.	Position x in.	EI 10^6 lb.in.^{2}	Mass lb.sec^2/in.	Normalized Mode Shapes First	Second	Third
1	0	.0162	.00099	.000	.000	.000
2	.5	.0162	.00198	.078	.100	.327
3	1.0	.0162	.00198	.271	.337	.842
4	1.5	.0162	.00198	.516	.620	1.000
5	2.0	.0162	.00198	.753	.865	.632
6	2.5	.0162	.00198	.929	1.000	.003
7	3.0	.0162	.00099	.997	.973	-.343
8	3.0	36.5	.00427	.997	.973	-.343
9	7.05	36.5	.00368	1.000	.000	-.369
10	11.1	36.5	.00427	.997	-.973	-.343
11	11.1	.0162	.00099	.997	-.973	-.343
12	11.6	.0162	.00198	.929	-1.000	.003
13	12.1	.0162	.00198	.753	-.865	.632
14	12.6	.0162	.00198	.516	-.620	1.000
15	13.1	.0162	.00198	.270	-.337	.842
16	13.6	.0162	.00198	.078	-.100	.327
17	14.1	.0162	.00099	.000	.000	.000
			Frequency rpm =	7870.	10350.	53320.

A significant feature of the results for this example is the wide gap which exists between the second and third critical speeds. This gap may provide a suitable region for high speed, super-critical applications. Such operations could permit the Bossler couplings to be designed with more misalignment capability and with less weight. Supercritical operation also opens the possibility for very smoothly operating designs which employ dynamic self-balancing. However, it is important to note that a potential problem area also exists. The built-up nature of the Bossler coupling creates a possibility for a whirling instability involving non-synchronous precession (Reference 11) when operated above the first critical speed. The dynamic stability characteristics of supercritical systems employing Bossler couplings are unknown at present.

The example shown in Figure 30 also provides an opportunity for checking a simple single degree of freedom analysis using Equations (25) and (26) against the more complete analysis above which used 13 lumped masses. For this case:

$(EI)_c = 16200$

$nS = 3.0$

$M_S = (4.7 + 4.6)/386 = .02408$

From Eq. (25), $k = 14400$

From Eq. (26), $f_1 = 7370$ rpm

The value 7370 rpm obtained from the very simple analysis is in good agreement with 7870 rpm from the more complete analysis.

Conclusions.- It is concluded that conventional idealizations and analysis methods are adequate to predict the first critical speed of shaft systems using Bossler couplings. It is expected that the approach will be adequate for higher critical speeds as well.

It is also concluded that a single degree of freedom idealization is useful for the common case of two identical couplings supporting a stiff center shaft.

BALANCING TEST

Introduction.- The effect of unbalance in a rotating system is a static stress on a rotating member and a vibration in the stationary system. Generally, the vibration is more important, if for no other reason than annoyance (noise or shake).

It was anticipated that the Bossler coupling, assembled from many separate pieces, might have an inherent balance problem. The approach followed to investigate balance was to compare the effect of unbalance of a test drive-shaft using two Bossler couplings and a short center shaft to an equivalent drive-shaft using two gear couplings and a short center shaft (the UH2 helicopter drive-shaft). The UH2 drive-shaft has known behavior with respect to balance both in service and in the test rig used to develop it.

When balance of a UH2 drive-shaft is satisfactory, the vibratory displacement at the drive-shaft supports on the test rig is less than 8 mils at 6200 rpm. The test drive-shaft, however, had a first critical speed of 5500 rpm. Balance testing had to be performed at a speed below the first critical speed. The balance testing of the test drive-shaft was performed at 3100 rpm.

An unbalance causes a centrifugal force which produces a proportional displacement of the supports. The centrifugal force varies as the square of the speed of rotation. The force and displacement seen at 3100 rpm are therefore one-fourth of the forces and displacements that would be seen at 6200 rpm ($3100^2/6200^2 = 1/4$).

Displacements were measured at 3100 rpm in response to a very large unbalance, converted to an equivalent displacement at 6200 rpm, and found to be within the acceptable limit. An analytic investigation confirmed the small effect of unbalance and found that a balanced drive-shaft assembly using Bossler couplings will cause a much lower vibration than a balanced equivalent drive-shaft using gear couplings, because gear couplings require a radial internal clearance that allows a shaft location to change after balancing.

Apparatus and Tests.- The test drive-shaft and the test rig are shown on Figure 28. A probe was held at the bearing supports to pick up vibratory displacements. The displacements were given in mils by a vibration analyzer to which the probe was attached. The horizontal (H) and vertical (V) displacements were measured at the bearing supports on each end of the test drive-shaft.

The test drive-shaft was balanced by trial and error until the displacements were less than 3.5 mils. The 3.5 mils include displacements from test rig vibrations as well as from residual unbalance. The precision of initial balance is not critical, however, so long as it is low enough not to mask the increase in vibration caused by the addition of a known unbalance weight of practical size.

An unbalance of .33 ounces was attached at a radius of 4.75 inches, causing an unbalance of 1.57 ounce-inches. The 1.57 ounce-inches represents a gross error in balancing. Conventional drive-shaft manufacture includes balancing drive-shaft parts in a balancing machine to less than 0.1 ounce-inches of unbalance. The parts are then assembled without further balancing. Drive-shafts like the test drive-shaft can be balanced as a complete assembly in a balancing machine to less than 0.1 ounce-inches of unbalance.

The unbalance weight was wired to an outside corner of the plate attached to the right end of the short center shaft. This location has the lowest radial spring rate and the largest radius for an unbalance weight attached to a coupling plate. This location, therefore, will have the greatest effect for the type of unbalance most likely to occur. The H and V displacements were measured. The weight was moved to each of the other plate corners to insure that the phase angle of the original unbalance was accounted for.

Results and Discussion.- The results are given in Table 10 below.

TABLE 10

BALANCE TEST MEASUREMENTS

Test Condition	Displacement in Mils			
	Left End		Right End	
	H	V	H	V
Balanced	1.7	2.4	3.4	2.0
1.57 oz.-in. located at 3 o'clock	1.7	2.2	4.6	2.1
1.57 oz.-in. located at 6 o'clock	1.4	2.8	3.8	1.6
1.57 oz.-in. located at 9 o'clock	1.0	2.7	3.5	2.8
1.57 oz.-in. located at 12 o'clock	1.9	2.5	4.5	2.6

The effect of the known unbalance is the area of interest. The greatest change in displacement is approximately one mil. At 6200 rpm, the displacement would be four times as large as it is at the 3100 rpm used in the test, or roughly 4 mils. This is one-half the limit of 8 mils that is acceptable by definition. Because the relatively large unbalance produced the small effect shown, the Bossler coupling is found to be not particularly sensitive to unbalance.

Analytical Investigation.- Drive-train hardware can be balanced in a balancing machine to 0.1 ounce-inches. The 0.1 ounce-inch unbalance at 6210 rpm will have a rotating centrifugal force of 7 lbs. The plane of lowest radial spring rate is in the middle of the center shaft. The radial spring rate is 14,400 pounds/inch (see Critical Speed Test). The rotating centrifugal force of 7 pounds acting on this plane will produce a displacement of .0005 inches on the test drive-shaft.

The equivalent UH2 drive-shaft has two gear couplings and a short center shaft. The three parts are individually balanced to 0.1 ounce-inches. The gear couplings have an internal clearance of .003 inches maximum to allow the relative tooth motion resulting from misalignment. This internal clearance allows the 12 pound center shaft to change radial location, which results for the UH2 drive-shaft in a possible change of rotating centrifugal force of 40 lbs.

A comparison of shaft displacements (.0005 inches versus .003 inches) and centrifugal forces (7 lbs versus 40 lbs) shows that the Bossler coupling will cause a significantly lower vibration than a gear coupling in an equivalent drive-shaft. It is noteworthy that an equivalent Hooke-type universal joint has a larger radial clearance than a gear coupling.

Conclusions.- It is concluded that the Bossler coupling is not sensitive to unbalance. Also, a drive-shaft assembly using Bossler couplings will cause less vibration than an equivalent drive-shaft assembly using couplings with radial internal clearance, such as gear couplings or Hooke joints.

CONFIGURATION MODIFICATION TO IMPROVE PERFORMANCE

Introduction.- The investigations reported herein reveal that improved coupling performance can be obtained by reducing the plate offset, S. The improvements include higher operating speeds, greater parallel misalignment, lower thrust loads from axial extension and compression, reduced moment loads from angular misalignment, reduced size and weight, and greater margin of safety for fretting.

Design Constraints.- A coupling made of square plates will have a minimum-achievable offset that is the sum of an attachment allowance, plus the space required for axial compression, plus the space required for angular misalignment, plus a clearance allowance for tolerances on these dimensions. Design layout shows that approximately one-half the offset is required for the attachment allowance. A further constraint is that all plates should be alike for many reasons concerned with ease of design and manufacture.

Design Solution.- Bossler coupling plates need not be square. They can be rectangular. A coupling made of rectangular plates can have a smaller offset than a square plate coupling designed for the same job. Figure 31 shows an individual rectangular plate and a coupling made up of three of these plates. All plates are alike. The attachments miss each other. If the attachments were in line, the offset would be larger for the same useable gap. In one application study, S was reduced from .750 inches with square plates to .420 inches with rectangular plates.

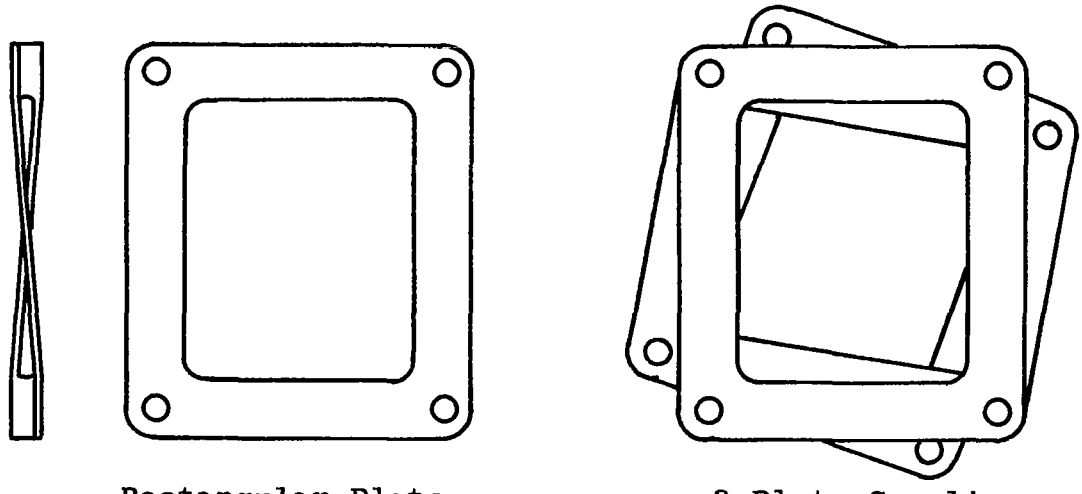

Rectangular Plate 3 Plate Coupling

Figure 31. Configuration Modification to Improve Performance

Because of the similarity of the rectangular-plate coupling to the square-plate coupling, it is probable that a simple adaptation can be made of the square-plate analysis and design procedure that are reported herein.

Conclusions.- The reduced plate offset allowed by rectangular plates should improve the performance of the Bossler coupling. Test and analysis are recommended to confirm this expectation and to adapt the existing analytical procedure to the new design.

FAIL-SAFE DESIGN

Introduction.- Couplings will be designed for infinite life. However, human error, accident, or other unforeseen events might cause extraordinary circumstances which the coupling could not survive indefinitely. In such an event, a fatigue failure will occur. A non-catastrophic mode of failure is very desirable. Also desirable is a warning signal that a failure has occurred. It is believed that a design solution has been found that will provide the desired behavior after a fatigue failure.

Description.- Figure 32 shows a typical fail-safe design. The center shaft is mechanically entrapped by concentric, overlapping shaft extensions. The radial clearance between the shaft extension is small. A non-contacting ring of low friction material is retained between the shaft extensions.

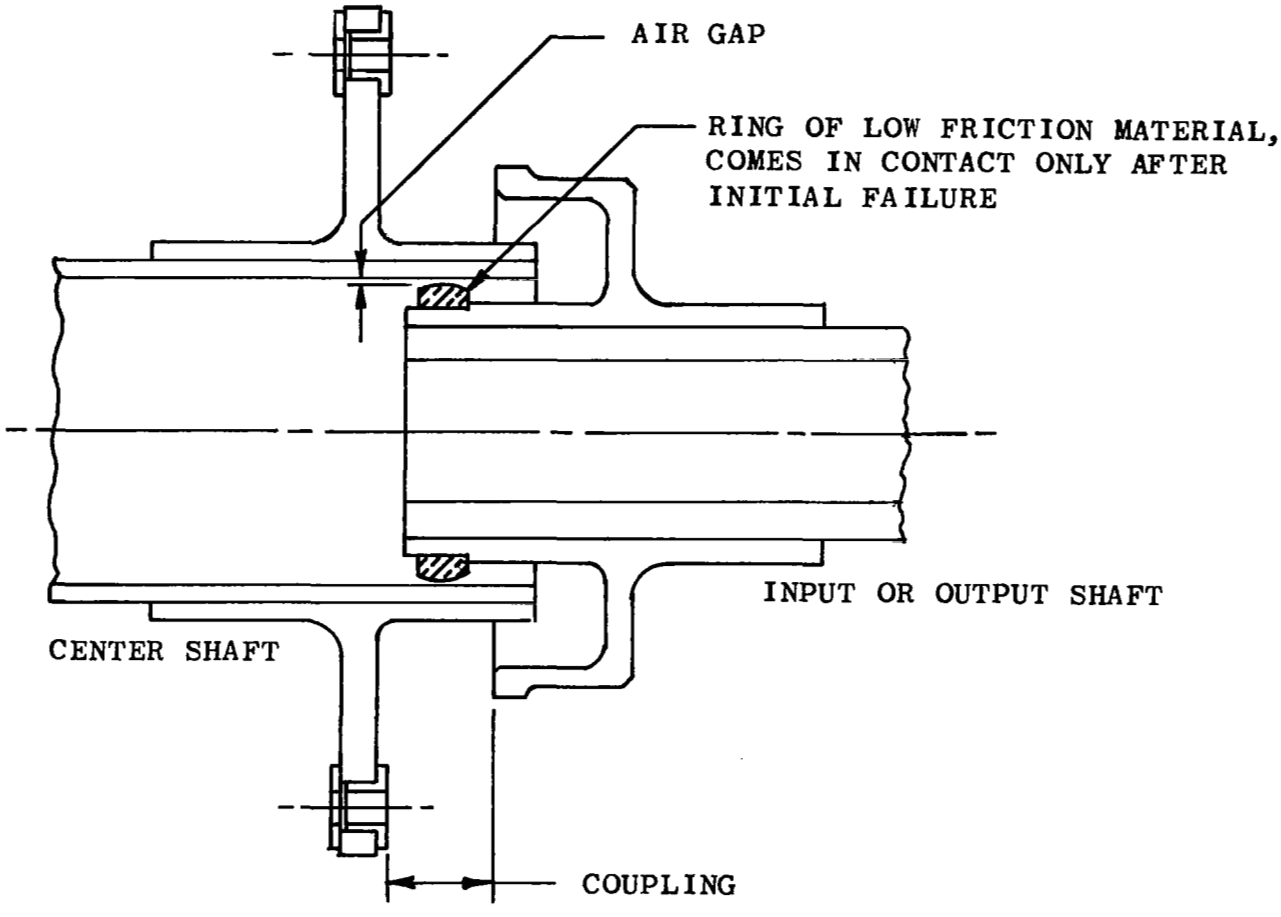

Figure 32. Fail-Safe Design

Operation.- It is expected that a fatigue failure will occur in one element of a plate, leaving three elements intact. Two of the surviving elements will be diametrically opposite each other. These two elements will act as drag links, if in tension, or as push links, if in compression. The remaining surviving link will help stabilize the coupling. The center shaft will move radially outward in response to centrifugal force. The radial movement will be limited by the small radial clearance between the shaft extensions. When the center shaft reaches the limit of radial movement, the two links which transmit the torque will be still in a well disposed arrangement. Torque transmission will continue. An axial force will be developed by the two links that transmit the torque. Axial movement is limited also by the mechanical entrappment. The wear material will reduce the erosion of the sliding parts, thus extending the life of the couplings in the failed condition.

Warning Signal.- The radial movement of the center shaft will cause an unbalance. It is believed the unbalance will cause a discernible vibration which can be interpreted as a warning that something is wrong. The amplitude of the vibration depends on the clearance, and can be controlled thereby.

Post-Failure Capacity and Lift.- After the initial failure, the capacity of the drive train will be reduced. However, the residual capacity could be sufficient to transmit normal operating torque if the initial coupling design provided sufficient torque capacity. An increase in torque capacity, however, requires accepting a reduction in misalignment capacity. The decision must be made for each application. The life of the coupling after a fatigue failure is limited and unknown. Tests can establish whether the post-failure life is satisfactory for a specific service requirement.

Conclusions.- A fail-safe arrangement for fatigue failure can be made. A failure warning will be provided by vibration after failure. After the initial failure, the ultimate torque capacity will be reduced, however, the coupling may be able to transmit normal operating torque for some time. These conclusions are based on considered opinion, not on test.

UNUSUAL CHARACTERISTICS AND POSSIBLE USES

Introduction.- The Bossler coupling has unusual characteristics based on its geometry, the freedom with which proportions can be varied and the freedom for selection of material. The potential usefulness of some of these characteristics is described below.

Unusual Characteristics Useful For Couplings.-

(1) The coupling has an empty center where other things can be located, such as hydraulic hoses, cooling fluid lines, electric power wires or even other drive-shafts.

(2) The coupling can accommodate large axial motions, which means that sliding splines or ball splines are not required as they are with some other couplings.

(3) The coupling can be biased for thermal growth by being stretched or compressed on installation, thus controlling the axial thrust on shaft bearings.

(4) The coupling can tolerate large transient angular excursions. Angular excursions can be over three times the design continuous operating angle. The excursion angle is set by static strength, not by fatigue strength.

(5) The coupling can have constant velocity even at large misalignment angles.

(6) The coupling can survive a large shock-torque in excess of its ultimate torque capacity without catastrophic failure. The coupling will be permanently deformed but can still function for a limited time.

(7) The coupling has a fail-safe for fatigue failure of any element. The unfailed members are sufficient to transmit torque and to accommodate misalignment for a limited time. Radial support of the coupling must be provided by special design features.

(8) The coupling can be designed for survival in high temperature, low temperature, hard vacuum, radioactivity and other hostile environments. The coupling needs no lubrication. Many materials can be used for coupling construction.

Unusual Applications For Unusual Characteristics.-

(1) The coupling can be made of material selected to conduct or insulate against electricity, heat, noise, vibration, or, as a radiating element with a high surface-area-to-weight ratio.

(2) The coupling can be made to mix or stir a fluid in which it is immersed, or to pump it. The pumping can be radially outward, radially inward, or longitudinally in either direction.

(3) The coupling can be a support mount which is a multiple-direction spring with high torque capacity.

(4) The coupling can be used in very light vehicles to transmit torque to the wheels and to provide spring suspension.

CONCLUSIONS

Introduction.- The section immediately before this one is entitled "Unusual Characteristics and Possible Uses". It lists conclusions that are not repeated here because of their close proximity.

General Conclusion for the Overall Program.- When the program began, the Bossler coupling promised superior performance but was unproven and unexplored. This program investigated many coupling-performance areas to find if any undesirable characteristics existed. None were found. The coupling is ready for application.

This program provided knowledge for designing Bossler couplings. However, if an application pushes the limits of coupling performance, tests should be made to optimize design details such as joint geometry and surface treatments. The development effort should establish confidence by proof testing of the whole coupling.

Conclusions from Each Section.- The following conclusions are abstracted from the conclusions in preceding sections. The conclusions are presented in the sequence in which they first appeared.

(1) Simplified formulas developed herein are adequate for the analysis of Bossler couplings. Tests show good agreement with formulas for torsional strength and stiffness, flexural and axial stiffness, steady and alternating stress, internal forces and moments, and critical speed. The formulas are applicable strictly only to couplings made of plates with square planform because the analyses used assumptions of symmetry and deflected position.

(2) The performance that can be obtained when the coupling is proportioned most efficiently can be found using design formulas and graphs presented herein.

(3) The computer program STRESS can analyze a Bossler coupling as a linear, redundant, elastic frame with no assumptions regarding symmetry or deflected position. STRESS predictions show good agreement with test results for flexural deformations of the coupling, and fair agreement for axial deformation. Agreement can be improved by using experimentally determined, non-uniform properties which take into account the stiffening effect of the bolted joints.

(4) The use of STRESS is justified for the analysis of non-symmetrical couplings.

(5) Typically, elastic instability limits torsional capacity of couplings. Torsional capacity can be provided for any level of power transmission.

(6) Torsional capacity can be predicted from prebuckled deflection data obtained in a non-destructive test.

(7) A coupling with an even number of plates has constant flexural stiffness for any direction of bending if stand-off washers are used between the coupling and its mounts. A coupling with an odd number of plates has constant flexural stiffness for any direction of bending whether stand-off washers are used or not.

(8) The potential performance of Bossler couplings at large misalignment angles is impressive.

(9) The Bossler coupling can be constant velocity.

(10) Conventional idealization and analysis methods are adequate to predict the first critical speed of shaft systems using Bossler couplings. It is expected that the approach will be adequate for higher critical speeds as well. A single degree of freedom idealization is useful for predicting the first critical speed of a system consisting of two identical couplings and a stiff center shaft.

(11) The Bossler coupling is not sensitive to unbalance. A drive-shaft assembly using Bossler couplings will cause less vibration than an equivalent drive-shaft assembly using couplings with radial internal clearance, such as gear couplings or Hooke joints.

(12) The reduced plate offset allowed by rectangular plates should improve the performance of the Bossler coupling. Compared to square plate design, the rectangular plate design is expected to increase critical speed and parallel misalignment, reduce thrust force, reduce bending stiffness, reduce size and weight, and increase the margin of safety for fretting.

(13) A fail-safe arrangement for fatigue failures can be made. A vibration after failure will give notice that a failure has occurred.

RECOMMENDATIONS

(1) Apply the Bossler coupling to a specific application that needs the unique capabilities of the coupling. Conduct testing to refine joint details and surface treatments. Establish confidence by proof testing of the whole coupling.

(2) Adapt the existing design equations for use with rectangular plates. The benefits of rectangular plates are listed in Conclusion (12).

(3) Test the fail-safe design.

(4) Investigate supercritical operation - specifically between the second and third critical speeds which are widely separated. Include dynamic self-balancing for very smooth operation in the supercritical regime.

(5) Investigate the effect on torsional strength of propertions substantially different from those tested in this program.

LIST OF REFERENCES

1. Seely and Smith, Advanced Mechanics of Materials, John Wiley and Sons, Inc., New York, New York, 1952.

2. Lipson, Noll and Clark, Stress and Strength of Manufacturing Parts, McGraw Hill Book Company, Inc., New York, New York, 1950.

3. Fenves, Logcher, March, Reinschmidt, STRESS: A User's Manual, M.I.T. Press, Massachusetts Institute of Technology, Cambridge, Massachusetts, 1964.

4. Lundquist, Generalized Analysis of Experimental Observations in Problems of Elastic Stability, NACA TN No. 658, 1938.

5. Roorda, "Some Thoughts on the Southwell Plot", Journal of the Engineering Mechanics Division, ASCE, Volume 93, No. EMG, Proc. Paper 5634, December 1967.

6. Comyn and Furlani, Fretting Corrosion - A Literature Survey, AD 430908, Defence Documentation Center, Alexandria, Virginia, 1963.

7. Starkey, Marco and Collins, An Investigation of the Mechanism of the Fretting-Corrosion-Fatigue Phenomenon, AD 218982, ASTIA, Arlington, Virginia, 1958.

8. Anonymous, VascoMax Maraging Steel Handbook, Vanadium-Alloys Steel Company, Latrobe, Pennsylvania, 1966.

9. Miller and Freund, Probability and Statistics for Engineers, Prentice-Hall, Inc., Englewood Cliffs, New Jersey, 1965.

10. Bisplinghoff, Ashley and Halfman, Aeroelasticity, Addison-Wesley Publishing Company, Inc., Reading, Massachusetts, 1957.

11. Gunter, Dynamic Stability of Rotor-Bearing Systems, NASA SP-113, Superintendent of Documents, Washington, D.C., 1966.

APPENDIX A

CALCULATION OF FLATWISE MOMENT VERSUS POSITION OF ROTATION FOR FIGURE 17

This Appendix shows the use of the simplified analysis formulas and moment-area principles for the calculation of two theoretical curves shown in Figure 17. The calculations herein are elementary and would not be presented, except for the fact that they illustrate:

(1) how to account for flexible ears on the pick-up flanges.

(2) how to account for moment gradient.

(3) how to vectorially add moments for any position of rotation.

It is appropriate to note here that the designer of a coupling for a specific application would not calculate stress as a function of angular position. It is sufficient for the designer to determine the peak-to-peak alternating stress from Equation (14). In this report, it was necessary to find the phasing of the stress because a detailed comparison with experimental data was sought.

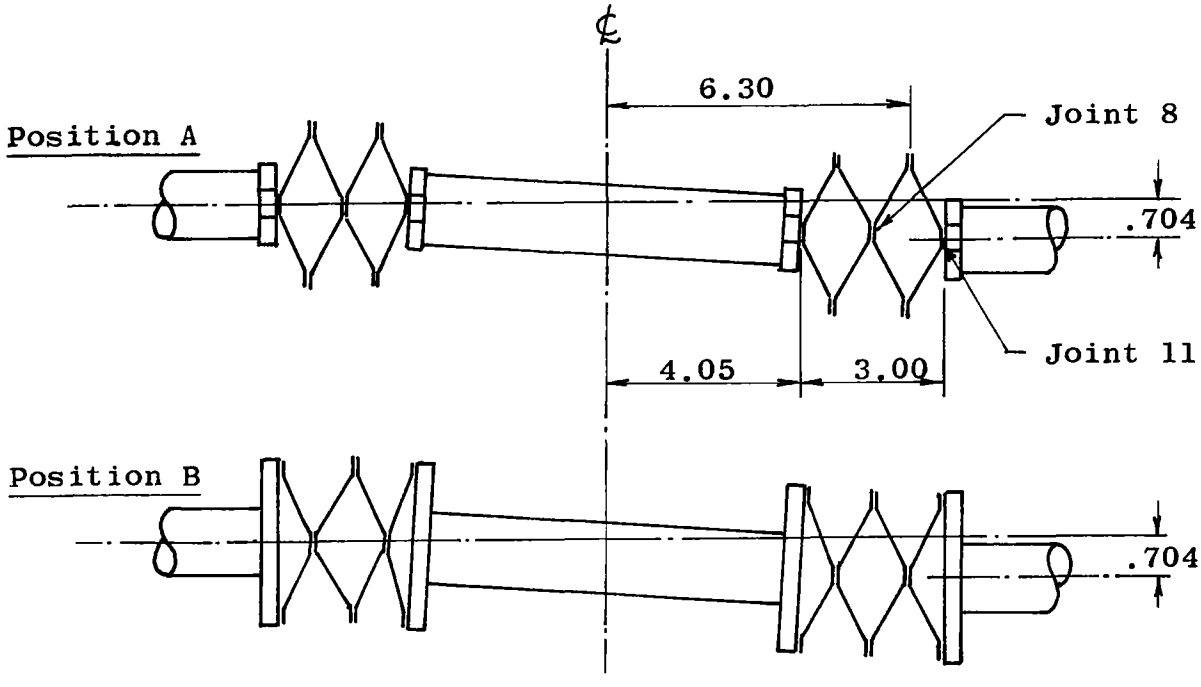

Moment Diagram.-

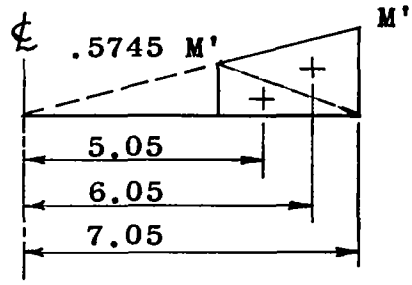

Stiffness, Determined by Test.-	Position A	Position B
ears on center-shaft, kip-in./rad.	246,000	large
ears on in(out)-shafts, kip-in./rad.	134,000	large
$(EI)_c$, (Eq. 10), kip-in.^{2}/rad.	16,200	16,200

Using Moment-Area Method,

In Position A		In Position B
$\frac{1.5\ M' \times 6.05}{16200}$ =	.0005602 M'	.0005602 M'
$\frac{1.5 \times .5745\ M' \times .505}{16200}$ =	.0002686 M'	.0002686 M'
$\frac{M' \times 7.05}{246000}$ =	.0000287 M'	
$\frac{.5745\ M' \times 4.05}{134000}$ =	.0000174 M'	
$\delta_{℄}$ = Σ =	.0008749 M'	$\delta_{℄}$ = .0008288 M'
.0008749 M' = .704/2		.0008288 M' = .352
M' = 402.3		M' = 424.7
(Eq. 9) at Joint 11, M = 107.0		Joint 11, M = 113.0
at Joint 8, M = 84.2		.5 M at 6.30 = 50.5

Rotation Angle	Member 18, Joint 11 (M = 107.0 cos θ-50.5 sin θ)*	Member 13, Joint 8 (M = 84.2 cos θ+50.5 sin θ)*
0	107.0	84.2
15	90.3	94.4
30	67.4	98.2
45	40.0	95.2
60	9.0	85.8
75	-21.1	70.6
90	-50.5	50.5
105	-76.5	27.0

etc. These values are plotted in Figure 17.

* The vectorial addition shown here is a consequence of the sign conventions given in the Computer Analysis Section 2 and the direction of rotation.

NASA-Langley, 1968 —— 15 CR-1241

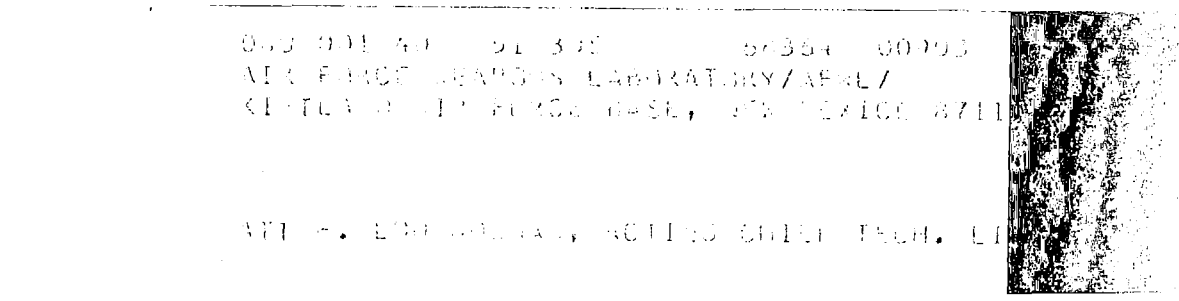

"The aeronautical and space activities of the United States shall be conducted so as to contribute . . . to the expansion of human knowledge of phenomena in the atmosphere and space. The Administration shall provide for the widest practicable and appropriate dissemination of information concerning its activities and the results thereof."

—NATIONAL AERONAUTICS AND SPACE ACT OF 1958

NASA SCIENTIFIC AND TECHNICAL PUBLICATIONS

TECHNICAL REPORTS: Scientific and technical information considered important, complete, and a lasting contribution to existing knowledge.

TECHNICAL NOTES: Information less broad in scope but nevertheless of importance as a contribution to existing knowledge.

TECHNICAL MEMORANDUMS: Information receiving limited distribution because of preliminary data, security classification, or other reasons.

CONTRACTOR REPORTS: Scientific and technical information generated under a NASA contract or grant and considered an important contribution to existing knowledge.

TECHNICAL TRANSLATIONS: Information published in a foreign language considered to merit NASA distribution in English.

SPECIAL PUBLICATIONS: Information derived from or of value to NASA activities. Publications include conference proceedings, monographs, data compilations, handbooks, sourcebooks, and special bibliographies.

TECHNOLOGY UTILIZATION PUBLICATIONS: Information on technology used by NASA that may be of particular interest in commercial and other non-aerospace applications. Publications include Tech Briefs, Technology Utilization Reports and Notes, and Technology Surveys.

Details on the availability of these publications may be obtained from:

SCIENTIFIC AND TECHNICAL INFORMATION DIVISION

NATIONAL AERONAUTICS AND SPACE ADMINISTRATION

Washington, D.C. 20546